

# Too Hot, Too Wet: Bayesian Spatial Modelling of Climate-Driven Salmonella Risk in New South Wales, Australia, 1991–2022

June 29, 2025

Oyelola A. Adegbeye<sup>1,2\*</sup>†, Tehan Amarasena<sup>2†</sup>, Mohammad Afzal Khan<sup>3†</sup>, Hassan Ajulo<sup>2</sup>, Anton Pak<sup>4</sup>, David Taniar<sup>3</sup> Theophilus I. Emeto<sup>2</sup>,

<sup>1</sup>Menzies School of Health Research, Darwin, Charles Darwin University, NT, Australia

<sup>2</sup> Public Health and Tropical Medicine, College of Medicine and Dentistry, James Cook University, Townsville, QLD 4811, Australia

<sup>3</sup>Faculty of Information Technology, Monash University, Melbourne, Australia

<sup>4</sup> Centre for the Business and Economics of Health, The University of Queensland, Brisbane, Queensland, Australia

## Abstract

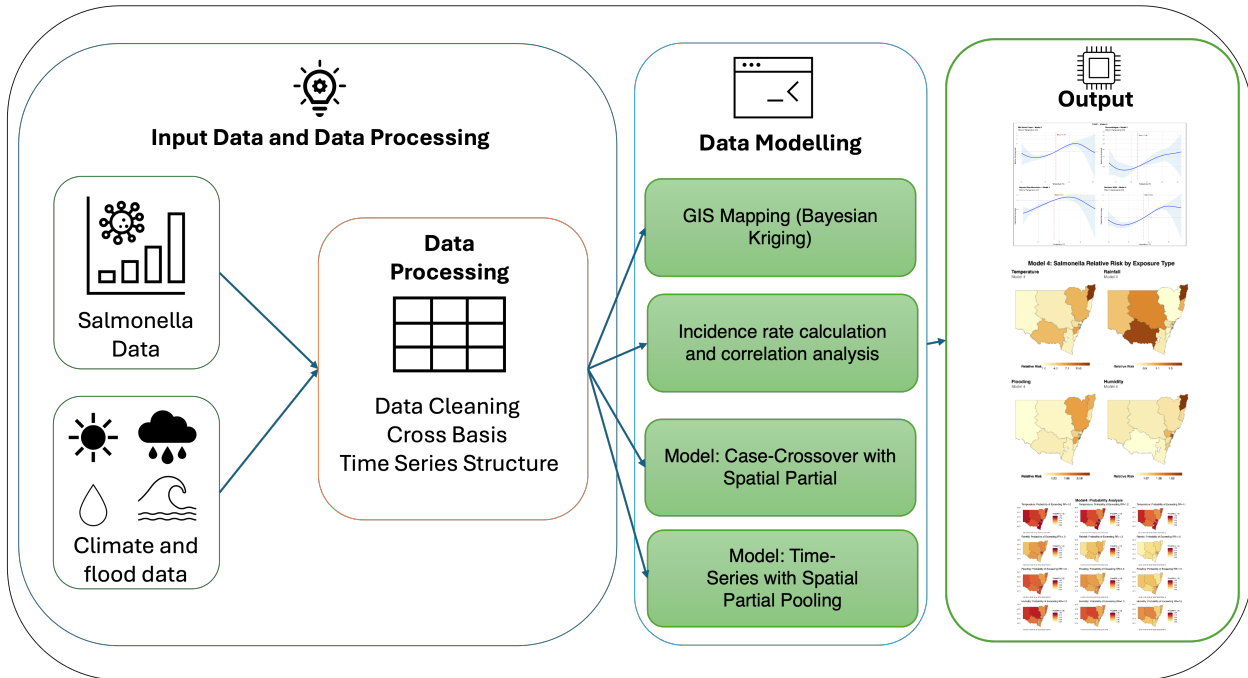
**Background:** Salmonella infections are responsible for a substantial number of hospitalisations due to bacterial gastrointestinal infections in Australia and contribute significantly to the global burden of infectious diseases. Evidence suggests a seasonal variation of salmonella worldwide, but there is limited literature on these relationships involving rainfall and temperature, particularly in Australia. **Objective:** This study investigated the trend of Salmonella cases and their relationship with climatic factors such as temperature, rainfall and flood events at the local health districts (LHDS) level across New South Wales (NSW), Australia. **Methods:** Monthly Salmonella cases and climate data (mean temperature, mean minimum temperature, mean maximum temperature and rainfall) were matched to their corresponding LHD in NSW. **Results:** Higher recordings of all the climate variables were positively associated with salmonella (all with  $p < 0.001$ ), and mean monthly minimum temperature was most strongly associated with salmonella ( $r = 0.404$ ). There is a greater association of mean monthly temperature and total daily rainfall with salmonella in metropolitan LHDs than in the rural/regional LHDs of NSW. **Conclusion:** Rising temperatures, increased rainfall, and flood events are likely to contribute to higher rates of salmonella in NSW. These findings have important public health implications that extend beyond NSW, highlighting the need

for broader national and global preparedness in the context of a changing climate.

**Keywords:** Salmonella, Foodborne disease, Climate variability, Environmental drivers, Climate change and health, Spatial Bayesian

† Equal contribution

\*Corresponding author: Oyelola Adegbeye, Menzies School of Health Research, Darwin, Charles Darwin University, NT, Australia



Graphical Abstract: Integrated Modelling Framework for Assessing Climate-Related Salmonella Risk in New South Wales, Australia. Environmental exposures (e.g., temperature, rainfall, flooding) and Salmonella case data are merged and pre-processed, followed by geospatial and statistical modelling. Techniques include Bayesian kriging for GIS mapping, incidence rate calculation with correlation analysis, and advanced modelling approaches such as case-crossover and time-series models with spatial partial pooling. The resulting outputs visualise relative risks and identify spatial clusters and environmental drivers of Salmonella across regions, supporting targeted public health interventions.

Geo: Geography and Environment Geographical Research

## 1 Background

Salmonellosis, the infection caused by *Salmonella* bacteria, contributes significantly to the global burden of disease, with an age-standardised mortality rate of 3 per 100,000 population [Ikuta et al., 2022]. Transmission occurs by consuming contaminated food (e.g., undercooked meat, eggs, dairy, raw fruits and vegetables), drinking contaminated water, coming into contact with infected person's faeces or infected animals (e.g. cattle, chickens, rodents, tropical fish and reptiles) [NSW Health, 2024, World Health Organization, 2018]. The incubation period can vary from 6 hours to 72 hours, and individuals are considered infectious while their stools test positive for Salmonella [NSW Health, 2024, World Health Organization, 2018]. A person can potentially be infectious from days to weeks post-acquiring the infection [NSW Health, 2024]. In developed countries such as Australia, it is usually less likely to be fatal, typically manifesting as an acute gastroenteritis [Darby and Sheorey, 2008]. However, it can spread rapidly and still cause severe illness, particularly in vulnerable populations with underlying health conditions. In 2015, salmonella was associated with an estimated 3013 hospitalisations and 13 deaths, resulting in a societal cost of over AU\$100 million [Akil

et al., 2014].

Salmonella, a leading cause of food-borne gastroenteritis and sepsis, has been associated with a rising incidence of foodborne illness in Australia [Ford et al., 2016, Ratnayake et al., 2024]. National Notifiable Diseases Surveillance System (NNDSS) data show that notifications almost doubled from 9,058 cases in 2009 to a peak of 18,044 in 2016, before falling sharply during the COVID-19 period to 10,129 in 2022 and rebounding modestly to 11,205 in 2023 [Australian Government Department of Health and Aged Care, 2024]. The pattern in New South Wales (NSW) mirrors the national trend: notifications climbed from 2,651 in 2009 to 4,519 in 2016 and have since declined by about one-third, stabilising at 3,031 cases in 2023 [Australian Government Department of Health and Aged Care, 2024]. Despite this recent decrease in notifications, current counts remain higher than a decade ago, underscoring the continuing burden.

A growing international literature demonstrates that Salmonella transmission is climate-sensitive, exhibiting seasonal variation [Tack et al., 2021, Thindwa et al., 2019, Morgado et al., 2021, Akil et al., 2014, Manchal et al., 2024]. Time-series studies in the Democratic Republic of Congo and Malawi have linked heavy rainfall and elevated ambient temperature, respectively, to surges in invasive non-typhoidal salmonella [Tack et al., 2021, Thindwa et al., 2019], while analyses from the United States show that warmer, wetter months are associated with faster bacterial replication and increased case counts, particularly in the southern states [Akil et al., 2014].

Australian evidence, though sparse, points in the same direction. In Adelaide, a 1°C increment in warm-season temperature increased notifications by 1–4 % [Milazzo et al., 2016], and a national study covering 1991–2019 found that a 1°C rise in mean monthly temperature anomaly was associated with a 3.4 % increase in cases, with El Niño periods elevating risk in NSW and Queensland [Davis et al., 2022]. However, the combined influence of rainfall, temperature and discrete flood events has not been examined at finer spatial scales, and no study has systematically assessed these drivers across NSW Local Health Districts (LHDs).

NSW is highly exposed to hydrometeorological hazards such as floods, bushfires, cyclones and hailstorms, which cost the state an estimated AU\$5.1 billion in 2020–21 and are projected to escalate under climate-change scenarios [Treasury, 2021]. Understanding how these hazards modulate enteric-disease risk is essential for targeted surveillance and preparedness can be used to strengthen early-warning systems, support climate-resilient food-safety policies and support a framework that can be applied in other Australian jurisdictions and comparable settings worldwide.

## 2 Materials and Methods

### 2.1 Study area and data sources

This study investigates the relationship between the incidence of salmonella and climatic factors—specifically rainfall, temperature, and flood events—across LHDs in NSW, Australia,

using data from 1991 to 2022. NSW is one of eight Australian states and territories, with LHDs categorised into six metropolitan and nine rural/regional districts (Figure 1).

### 2.1.1 Health data

Monthly non-identifiable notifications of salmonella cases were obtained from the NSW Health Notifiable Conditions Information Management System (NCIMS), via the Communicable Diseases Branch and the Centre for Epidemiology and Evidence. These data were aggregated by LHD and used to calculate monthly incidence rates. LHD population data were sourced from the NSW Department of Planning [NSW Department of Planning, Housing and Infrastructure, 2024]. For years before 2001, historical population estimates were retrospectively calculated using the department's earliest available annual growth rates (from 2002), applied separately for each LHD.

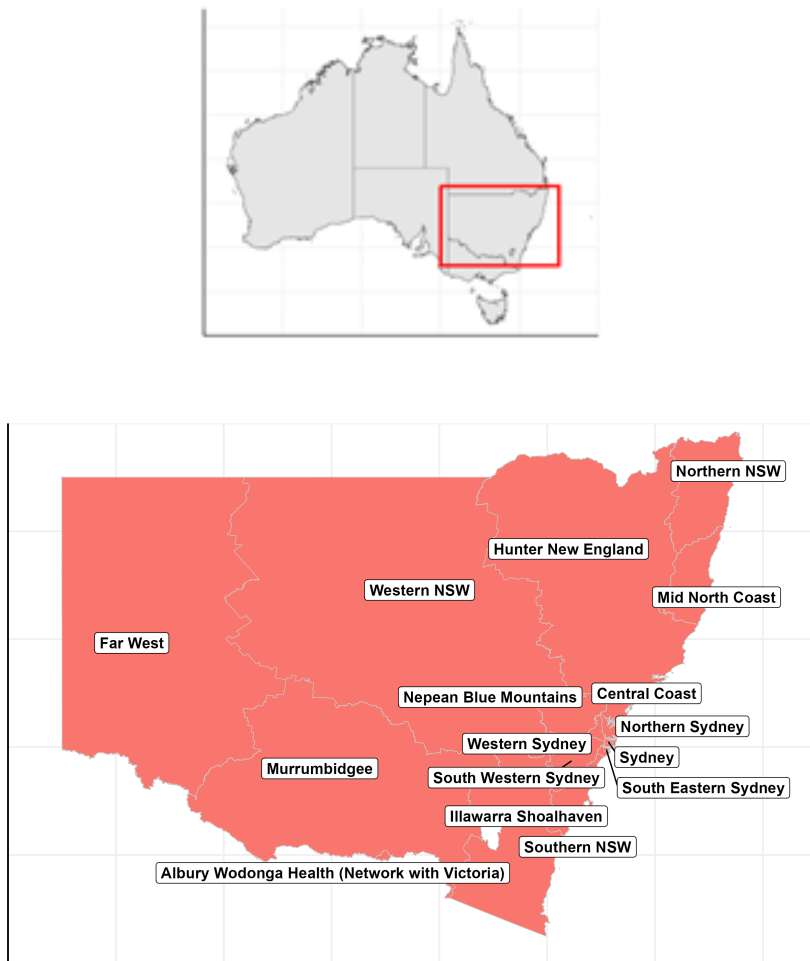


Figure 1: Map of Australia and the study area.

### 2.1.2 Meteorological data

Climate data were extracted from the Australian Bureau of Meteorology at the weather station level, including monthly total rainfall (mm), mean temperature ( $^{\circ}\text{C}$ ), mean maximum temperature ( $^{\circ}\text{C}$ ), and mean minimum temperature ( $^{\circ}\text{C}$ ) for the years 1991 to 2022 [Zippenfenig, 2024]. As the meteorological records are georeferenced but not labelled by LHD, each weather station's coordinates were manually assigned to the corresponding LHD using Google Maps. Where multiple stations existed within an LHD, values were averaged as appropriate.

## 2.2 Data analysis

Preliminary analysis includes yearly *Salmonella* incidence rates per 100,000 population calculated for each LHD. Pearson's correlation coefficients were used to assess the association between *Salmonella* incidence and climate variables, including mean, maximum, and minimum monthly temperatures, as well as flood wave events—defined as the number of days with river discharge exceeding the 95th percentile. To explore exposure-response relationships, we produced scatter plots with regression lines to visualise the association between *Salmonella* incidence and climate variables rainfall by LHD. Additionally, autocorrelation and partial autocorrelation functions (ACF and PACF) were computed to assess temporal dependence in *Salmonella* incidence.

### 2.2.1 Climate–salmonella associations

To investigate how climatic factors influence salmonella incidence across NSW, we applied spatial Bayesian distributed lag non-linear models (DLNMs), constructing distributed lag non-linear terms for each climate exposure to flexibly capture potentially non-linear and delayed associations [Quijal-Zamorano et al., 2024, Gasparrini et al., 2010]. Daily salmonella case counts for each LHD were linked with corresponding daily climate data, including mean temperature, total rainfall, a flooding index, and mean humidity. These data were structured into two formats to support complementary modelling strategies: a case-crossover dataset, where each day was nested within LHD–month strata (allowing within-stratum comparisons), and a time-series dataset, indexed by year and month per LHD (Figure 2).

For each climatic exposure, we defined a cross-basis using natural cubic splines to flexibly capture both the non-linear exposure–response relationships and lagged effects up to two days. Exposure splines used knots at the 10th, 50th, and 90th percentiles of observed values, while lag splines spanned lags 0 to 2 months. All exposures were mean-centred prior to basis construction, and the resulting basis matrices were appended to the datasets to model both immediate and delayed risk.

We modelled daily salmonella counts  $y_i$  using a Poisson likelihood, with the log of the expected count  $\log(\lambda_i)$  specified as the linear predictor [Maclure, 1991, Besag et al., 1991]. Two Bayesian models were fitted to estimate the association between climate variables and

salmonella risk, allowing for spatial and temporal variation in exposure-response relationships.

Firstly, a time-stratified case-crossover design [Maclure, 1991] was employed, using LHD-month strata as fixed intercepts, inherently controlling for time-varying confounders like seasonality and long-term trends:

$$\log(\lambda_i) = \alpha_{\text{stratum}(i)} + \sum_{\text{exposures}} f_{r(i)}(X_i) + \phi_{r(i)},$$

where  $\alpha_{\text{stratum}(i)}$  is the stratum-specific intercept for the LHD  $\times$  (month–year) stratum of observation  $i$ ,  $f_r(X_i)$  represents the DLNM basis contribution for each exposure  $X$  in region  $r$ , and  $\phi_{r(i)}$  is the spatial random effect for the region of observation  $i$ . The long-term trends and seasonality are handled implicitly via a time-stratified case-crossover design, where each LHD  $\times$  month–year combination is treated as a fixed-effect stratum  $\alpha_{\text{stratum}(i)}$ , absorbing time-varying confounders without requiring explicit temporal terms.

Secondly, a full Bayesian hierarchical time-series structure with random intercepts for LHD and calendar month, and included temporal random effects to capture region-specific long-term trends and anomalies. A spatially structured random effect ( $\phi_r$ ) was included using an intrinsic conditional autoregressive (iCAR) prior to account for spatial correlation between neighbouring LHDs[Besag et al., 1991]. Region-specific exposure–response curves were estimated using partial pooling around a global mean curve, with shrinkage determined by variance hyperparameters. This framework allowed estimation of both overall and LHD-specific climate–salmonella associations, accounting for spatial and temporal dependencies:

$$\log(\lambda_i) = \alpha_{r(i), m(i)} + \gamma_{r(i)}(\text{trend}_i) + \delta_{r(i), y(i), s(i)} + \sum_{\text{exposures}} f_{r(i)}(X_i) + \phi_{r(i)},$$

where  $\alpha_{r,m}$  is the intercept for region  $r$  in month  $m$  (capturing baseline seasonal variation),  $\gamma_r(\text{trend})$  is a region-specific long-term trend term (modeled with basis functions of time), and  $\delta_{r,y,s}$  is a region- and year-specific seasonal deviation (an adjustment for season  $s$  in year  $y$ ). These terms allow the model to account for secular trends and inter-annual variability in seasonal peaks.

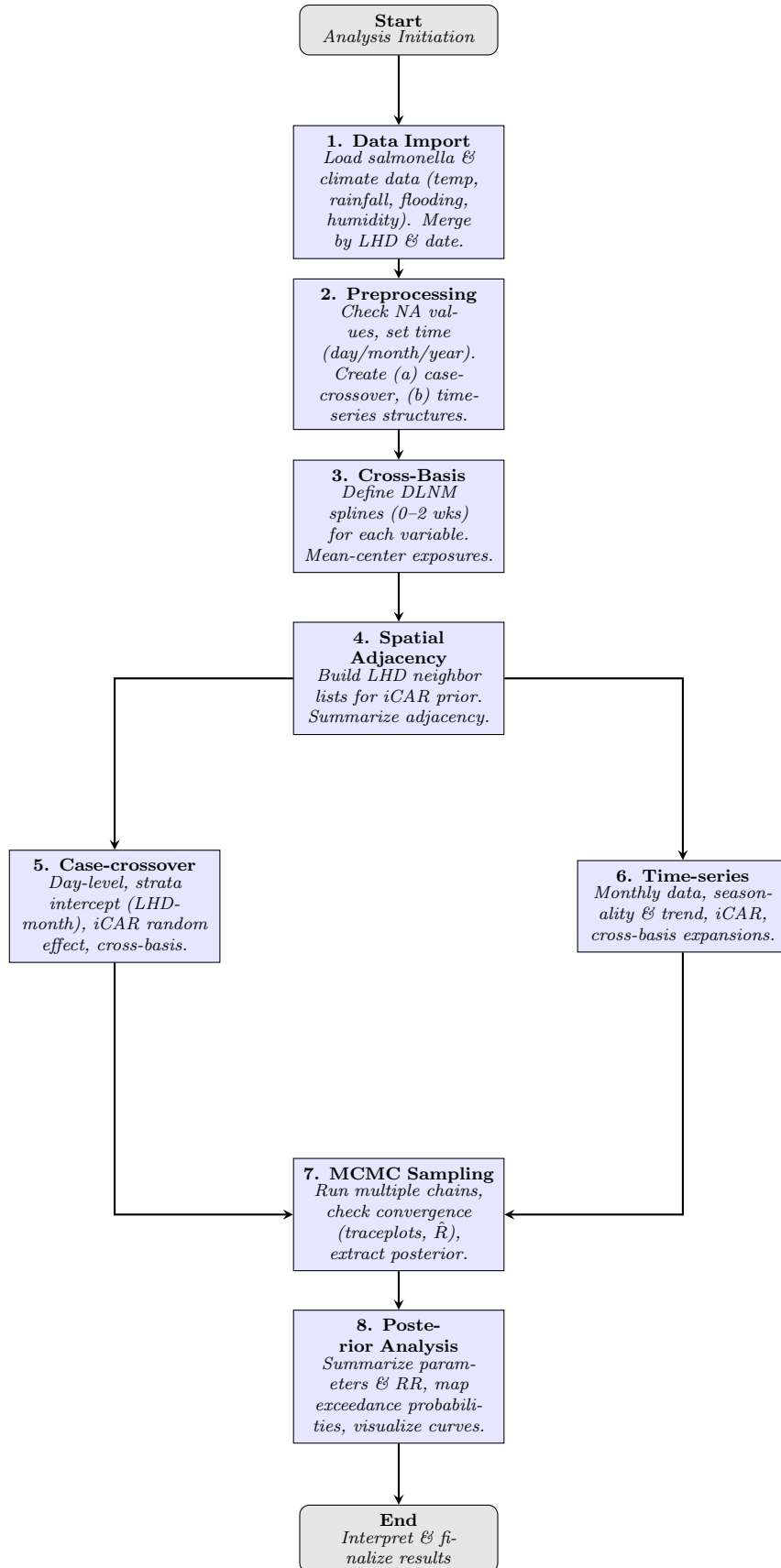


Figure 2: Methodological flowchart

## 2.3 Model priors

For both models, priors for all regression coefficients in the exposure cross-basis were given hierarchical normal distributions:

$$\beta_{r,j}^{(X)} = \mu_j^{(X)} + \sigma_j^{(X)} \theta_{r,j}^{(X)}, \quad \theta_{r,j}^{(X)} \sim N(0, \tau_X^{-1}),$$

with vague hyperpriors such as

$$\mu_j^{(X)} \sim N(0, 10^3), \quad \sigma_j^{(X)} \sim U(0, 10), \quad \tau_X \sim \text{Gamma}(0.1, 0.1).$$

Intercepts and other random effects were given diffuse priors (e.g.,  $\alpha \sim N(0, 10^3)$ ), and the iCAR precision  $\tau_\phi$  also had a  $\text{Gamma}(0.1, 0.1)$  prior. The models were fitted with three MCMC chains of 5,000 iterations each (after burn-in), and convergence was assessed by traceplots and  $\hat{R}$  statistics. Posterior samples of all key parameters (including derived quantities such as relative risks) were extracted for inference.

All models were fitted in a Bayesian framework using the NIMBLE package [de Valpine et al., 2017] in R version 4.3.3.

## 2.4 Ethics

No specific ethics approval was required for this study as data analysis was based on publicly available data. salmonella data were obtained from de-identified notifiable disease data, whilst the climate data were obtained from the Australian Bureau of Meteorology.

# 3 Results

## 3.1 Exploratory Spatial Data Analysis

Between 1991 and 2022, the mean monthly number of Salmonella cases was 13.3 ( $SD = 13.3$ ), with a median of 9 cases. The maximum monthly count was 190 cases, recorded in South Eastern Sydney in January 2016, while none were recorded in NSW during the 1990s (Table 1). Figure 3 shows peaks of salmonella cases recorded during the years 2007-08, 2010-12, 2014-16 and 2020-21. Increased flood wave events were recorded over 2007, 2011-13, 2016-17 and 2020-22. These are in keeping with recorded major flooding events in NSW such as the Hunter Valley and Central Coast floods in 2007, Wollongong floods in 2011, Northern NSW floods in 2012-13, Central West and Riverina floods in 2016, ‘Cyclone Debbie’ in 2017 and NSW North Coast floods in 2020-21. The figure also illustrates numerous flood wave events recorded during the 1990s, which coincide with increased salmonella case recordings, but these rises are not as obvious as those seen from the 2000s.

Table 1: Summary salmonella cases and climatic variables

Variable	Mean	SD	Min	25th	Median	75th	99th	Max
1. Max. temp	21.51	5.34	7.15	17.5	21.46	25.1	34.5	40.2
2. Mean Temp	16.75	5.09	2.75	12.9	16.92	20.7	28.1	34.1
3. Min. Temp	12.53	5.08	-0.6	8.52	12.7	16.7	21.9	27.9
4. Rainfall (mm)	60.66	55.7	0	0	0	2	275.8	493
5. Flood Events	1.25	2.53	0	0	0	2	12	19
6. Elevation (m)	254.27	300	0	44	140	415	1125	1125
7. Salmonella Cases	13.33	13.3	0	4	9	18	60	190

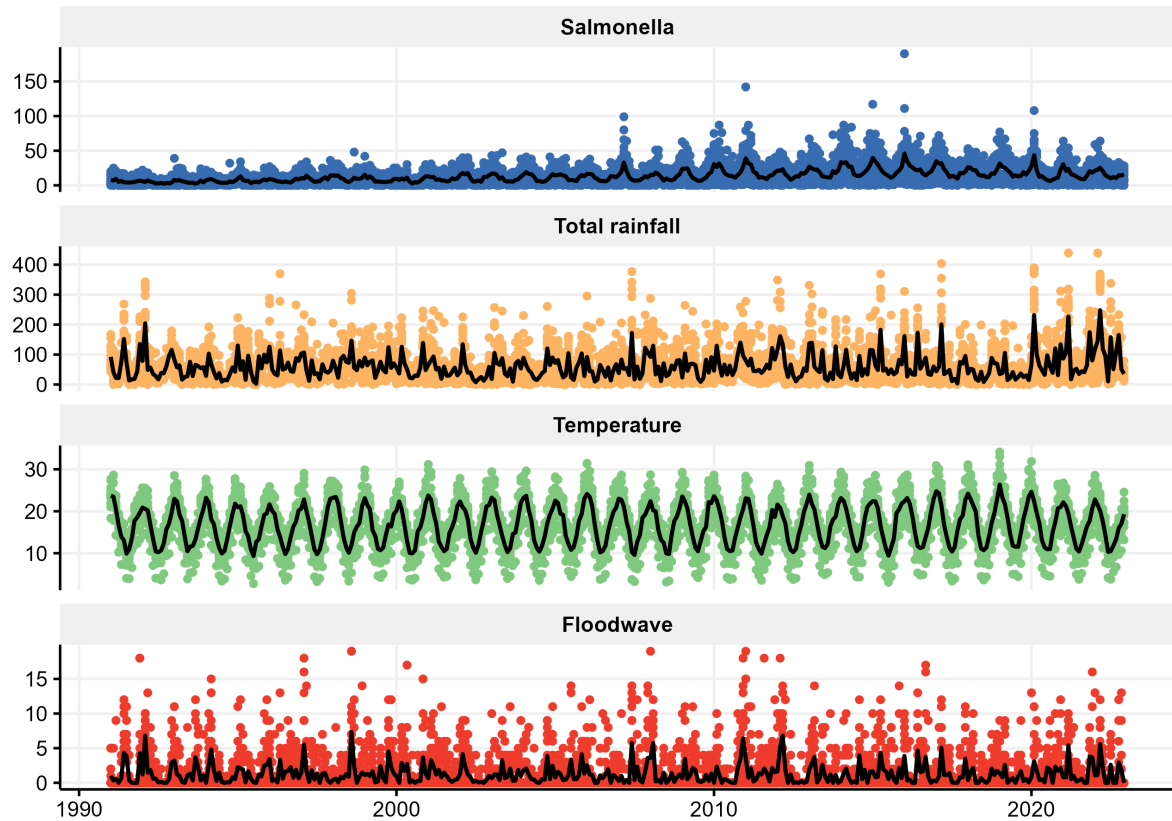


Figure 3: Time series plot of salmonella cases, total rainfall, mean temperature and floodwaves over the study period, 1991-2022

. Thick lines represent monthly averages.

Time series decomposition of monthly Salmonella cases in NSW reveals a gradual upward trend, particularly between 2000 and 2015, and a consistent seasonal pattern with annual

peaks (Figure S6). Irregular spikes in the residual component suggest sporadic outbreaks. Associations between monthly mean temperature and Salmonella cases across 15 LHDs (Figure S7), and total daily rainfall (Figure S8), indicate that temperature has the strongest association.

Positive correlations were observed between the number of Salmonella cases and all the climatic variables (Table 2). The variable with strongest correlation with Salmonella cases was mean minimum temperature (0.404,  $p<0.001$ ), followed by mean temperature (0.331,  $p<0.001$ ), then mean maximum temperature (0.242,  $p<0.001$ ), then rainfall (0.176,  $p<0.001$ ) and finally flood wave events (0.113,  $p<0.001$ ). The LHDs with higher recordings of mean minimum temperatures are more likely to have reached the minimum temperature threshold for favourable salmonella reproduction and also likely to have had less intra-LHD temperature variability as mean minimum temperature is strongly positively correlated with mean temperature 0.841 ( $p<0.001$ ) and with mean monthly maximum temperature 0.956 ( $p<0.001$ ).

Table 2: Inter-correlation analysis of Salmonella cases and climatic variables

Variable	<b>2</b>	<b>3</b>	<b>4</b>	<b>5</b>	<b>6</b>	<b>7</b>
<b>1.</b> Max. temp	0.961 (.001)	0.841 (.001)	0.047 (.001)	0.003 (0.812)	-0.289 (.001)	0.242 (.001)
<b>2.</b> Mean Temp	0.956 (.001)	0.139 (.001)	0.065 (.001)	-0.402 (.001)	0.331 (.001)	
<b>3.</b> Min. Temp	0.245 (.001)	0.128 (.001)	-0.465 (.001)	0.404 (.001)		
<b>4.</b> Rainfall (mm)	0.538 (.001)	0.020 (0.132)	0.176 (.001)			
<b>5.</b> Flood Events	-0.019 (0.153)	0.113 (.001)				
<b>6.</b> Elevation (m)	-0.207 (.001)					
<b>7.</b> Salmonella Cases						

### 3.2 Spatial temporal association

The full Bayesian spatiotemporal model (BSM) provided a better fit and predictive performance than case-crossover model (CCM) according to most evaluation metrics. **Table 3** summarizes the comparison. BSM achieved a lower root mean squared error (RMSE) and mean absolute error (MAE) in predicting daily case counts than case-crossover, and explained a greater proportion of variance in cases (pseudo- $R^2 = 0.854$  vs. 0.827). Information criteria also favoured BSM: the deviance information criterion (DIC) was substantially lower for BSM (998003) than CCM (1217211), and BSM had lower AIC and BIC values, despite its greater complexity. One metric, a quasi-AIC (QAIC) based on overdispersion-adjusted likelihood, was slightly lower for CCM, suggesting CCM model may have fit the marginal overdispersion a bit more parsimoniously. However, the QAIC calculated from the Bayesian posterior deviance (QAIC<sub>MCMC</sub>) favoured BSM. Overall, BSM's ability to explicitly model seasonality and trend yielded improved fit, so subsequent results focus on BSM. BSM shows improved fit in most criteria (lower error and information criteria, higher  $R^2$ ).

Figure 4 shows the posterior median RR in each LHD for an extreme value of the exposure (approximately the 95th percentile) relative to a low reference value (approximately the 5th

percentile) for BSM. There is substantial spatial heterogeneity in the strength of associations. All regions show RRs above 1, confirming a positive association between high ambient temperature and salmonella risk. However, the magnitude varies: coastal and metropolitan LHDs generally have moderate increases, whereas some inland areas see very large effects. High rainfall exhibits an inverse association in many coastal LHDs (median RR < 1), whereas some inland areas show slightly positive effects. Flood events are associated with modestly higher Salmonella risk in most LHDs, although confidence intervals often include 1, indicating some uncertainty. High humidity is consistently associated with elevated risk, particularly in arid inland areas.

We also mapped the posterior probability that  $RR$  exceeds thresholds such as 1.0, 1.2, and 1.5 (Figure 5). This approach highlights where climate effects on salmonella are most credibly high. For temperature, nearly the entire state shows  $P(RR > 1.0) \approx 1.0$ . Rainfall probability maps confirm that many coastal LHDs are quite likely to have  $RR < 1.0$  under heavy rainfall, while a few inland LHDs might experience  $RR > 1$ . Similar patterns appear for flooding and humidity, though with generally smaller effect sizes than temperature.

Table 3: Model fit and predictive performance metrics for case-crossover vs BSM.

Metric	CCM	BSM
RMSE (Root Mean Squared Error)	5.55	5.10
NRMSE (normalized)	0.416	0.382
$R^2$ (pseudo)	0.827	0.854
MAE (Mean Absolute Error)	3.46	3.01
Symmetric Mean Absolute Percentage Error (SMAPE) (% error)	33.28	29.43
AIC (Akaike Information Criterion)	32395	31335
BIC (Bayesian Information Criterion)	32422	31361
DIC	$1.217 \times 10^6$	$9.980 \times 10^5$
QAIC (quasi-likelihood AIC)	<b>1058.7</b>	1212.3
QAIC <sub>MCMC</sub> (Bayesian)	$2.401 \times 10^6$	$1.963 \times 10^6$
Overdispersion $\phi$	30.825	26.012

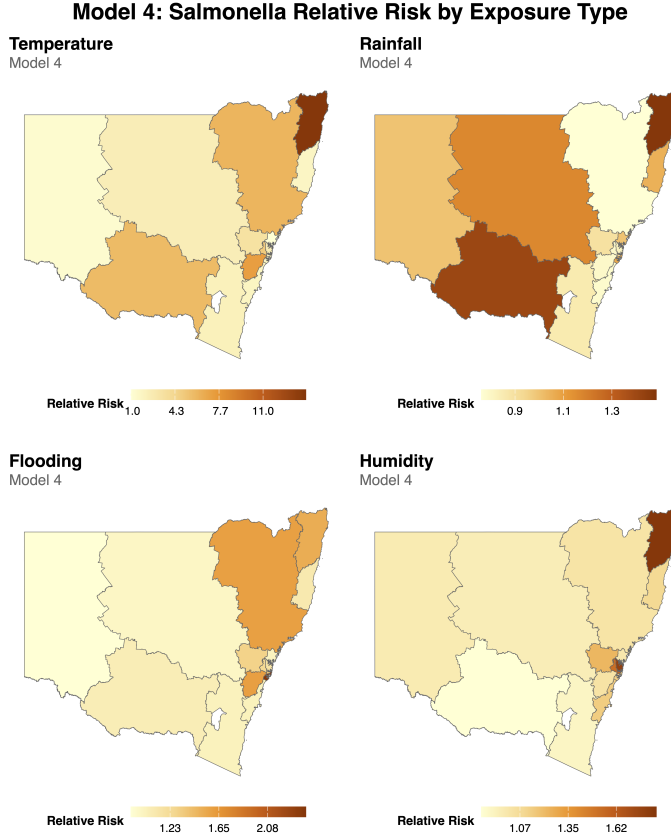


Figure 4: Spatial distribution of the estimated relative risk (RR) of salmonella associated with extreme values of each climate variable under BSM. Panels show posterior median RR by Local Health District for: **Temperature** (hot vs. cool conditions), **Rainfall** (wet vs. dry conditions), **Flooding** (occurrence of a flood-wave vs. none), and **Humidity** (high vs. low). Darker colours indicate higher risk. Temperature and humidity display positive associations across most of NSW, while rainfall shows mostly neutral or negative associations (coastal areas in lighter shades). Flooding has a modest positive effect in a few regions.

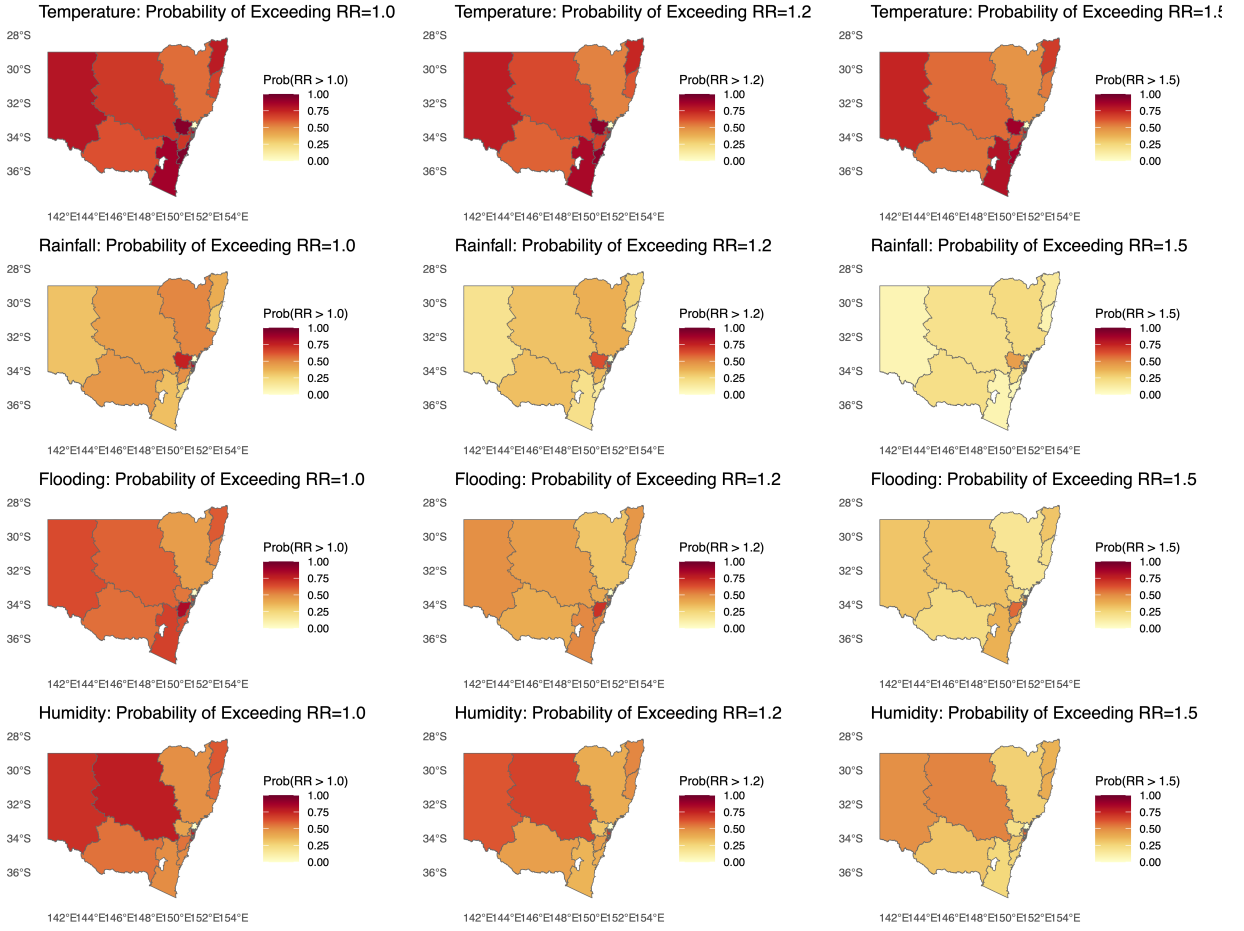


Figure 5: Posterior probability that the relative risk (RR) exceeds thresholds (1.0, 1.2, 1.5) for each exposure in BSM. Shading indicates the probability level in each Local Health District.

Table 4: Percentile-based Relative Risk (RR) of salmonella by LHD Region and Climate Variable (Model 4).

LHD_Region	Exposure_Variable	Percentile_01	Percentile_05	Percentile_95	Percentile_99
Central Coast	Temperature	1	1	1	1
Central Coast	Rainfall	1	1	1	1
Central Coast	Flooding	1	1	1	1
Central Coast	Humidity	1	1	1	1
Far West	Temperature	0.080740247	0.213869738	73.92587627	267.5275332
Far West	Rainfall	0.227374665	0.330998601	1.631278554	2.264071579
Far West	Flooding	0.377428106	0.519176818	3.877306934	8.002540058
Far West	Humidity	0.287753087	0.502740148	5.410657971	8.523476745
Hunter New England	Temperature	0.03033711	0.100901856	16.8634952	44.85844703
Hunter New England	Rainfall	0.203074302	0.377763598	2.519106964	3.813781419
Hunter New England	Flooding	0.098171759	0.261742841	2.271246373	4.460884407
Hunter New England	Humidity	0.171026528	0.281433009	3.302778582	5.565653225
Illawarra Shoalhaven	Temperature	0.643402352	1.019594741	46.12321426	160.7950954
Illawarra Shoalhaven	Rainfall	0.302289456	0.386281074	1.605198127	2.370698459
Illawarra Shoalhaven	Flooding	0.415502136	0.550500746	10.86629813	22.26608337
Illawarra Shoalhaven	Humidity	0.278373583	0.412745757	2.546343158	3.793110538
Mid North Coast	Temperature	0.098521501	0.262574241	20.2161786	46.9733247
Mid North Coast	Rainfall	0.23673706	0.361101287	1.710759609	2.434160836
Mid North Coast	Flooding	0.197816838	0.365067095	2.726093689	6.250608931
Mid North Coast	Humidity	0.149182284	0.288176961	3.983171666	6.433422467
Murrumbidgee	Temperature	0.023763315	0.069304815	38.15712152	120.7928287
Murrumbidgee	Rainfall	0.289426304	0.413480595	4.882190966	10.7634129
Murrumbidgee	Flooding	0.282133841	0.493404488	2.657055536	5.374489626
Murrumbidgee	Humidity	0.188931236	0.34853429	3.294671745	5.587532122
Nepean Blue Mountains	Temperature	0.315851562	0.882181465	44.3036658	90.16564765
Nepean Blue Mountains	Rainfall	0.416893032	0.599639638	3.525085745	5.299521964
Nepean Blue Mountains	Flooding	0.235944143	0.397158474	2.624836898	4.222444075
Nepean Blue Mountains	Humidity	0.151259655	0.276979153	2.566727432	3.761174773
Northern NSW	Temperature	0.22121113	0.409528201	33.44315662	91.58140086
Northern NSW	Rainfall	0.264868629	0.389389324	2.309775422	3.966416505
Northern NSW	Flooding	0.336585347	0.512982579	5.389524257	9.818119108
Northern NSW	Humidity	0.208278286	0.34834911	4.611972332	9.571959437
Northern Sydney	Temperature	0.12599555	0.346443153	891.4571558	3404.400668
Northern Sydney	Rainfall	0.621601061	0.790162824	2.972036724	3.798855896
Northern Sydney	Flooding	0.451059459	0.61170126	6.163795345	12.52898845
Northern Sydney	Humidity	0.333048386	0.532727048	7.499738399	13.79705764
South Eastern Sydney	Temperature	0.053521242	0.162855909	31.1228754	57.80442161
South Eastern Sydney	Rainfall	0.27842577	0.349062495	2.412597544	5.261274991
South Eastern Sydney	Flooding	0.267229956	0.402586802	4.652618287	9.175042015
South Eastern Sydney	Humidity	0.440062896	0.620736132	6.543920917	14.36005064
South Western Sydney	Temperature	0.024575492	0.098193843	15.86903793	32.30960631
South Western Sydney	Rainfall	0.437995076	0.547331306	2.802175672	5.226756282
South Western Sydney	Flooding	0.596886913	0.761621925	13.51941605	20.92376091
South Western Sydney	Humidity	0.280664455	0.424163053	3.308795352	5.665223401
Southern NSW	Temperature	0.238697486	0.501107708	101.28808	232.3867248
Southern NSW	Rainfall	0.1536923	0.322386448	1.627983743	2.054482292
Southern NSW	Flooding	0.519866814	0.643882674	11.08511662	17.65861612
Southern NSW	Humidity	0.321417194	0.42789131	2.939859061	4.148360631
Sydney	Temperature	0.027505564	0.100586095	30.60874568	63.63161618
Sydney	Rainfall	0.218098699	0.345065848	1.994229216	2.888172441
Sydney	Flooding	0.183150005	0.364979686	2.662465535	4.894075438
Sydney	Humidity	0.162806343	0.261833175	2.874748963	4.460311856
Western NSW	Temperature	0.118288764	0.239469219	19.95883272	54.94712745
Western NSW	Rainfall	0.324914482	0.409099243	2.249879104	3.140185113
Western NSW	Flooding	0.409120231	0.546634878	7.248039241	15.94616073
Western NSW	Humidity	0.311572966	0.531862647	4.86110417	10.36105379
Western Sydney	Temperature	0.131082001	0.245080708	19.96270452	37.63261572
Western Sydney	Rainfall	0.32848966	0.489568254	3.308062881	6.000357652
Western Sydney	Flooding	0.199159743	0.337267458	2.620118257	6.916105653
Western Sydney	Humidity	0.159390838	0.261623816	3.150951123	5.701835681

Table 4 illustrates how *salmonella* risk varies non-linearly with climate extremes across different LHDs. Generally, we observe a J-shaped pattern for each climate variable: at the low extreme (1<sup>st</sup> and 5<sup>th</sup> percentiles), the relative risk (RR) of salmonella is often below 1.0 (indicating lower risk than under typical conditions), whereas at the high extreme (95<sup>th</sup> and 99<sup>th</sup> percentiles) the RR is above 1.0, in many cases dramatically so.

High ambient temperature shows the most pronounced effect on salmonella risk. Nearly every LHD exhibits a steep rise in RR at the 95<sup>th</sup> and especially 99<sup>th</sup> percentile of temperature. For example, in the Far West LHD (an arid inland region), the RR for salmonella jumps from about 0.08 at the 1<sup>st</sup> percentile (extremely cool days) to 267.5 at the 99<sup>th</sup> percentile (extreme heat). Likewise, Sydney (urban central) rises from  $\approx$  0.03 at the coldest end to 63.6 at the hottest end. Several rural or southern districts (e.g., Southern NSW, Nepean Blue Mountains) also reach very high RRs (well above 50) under extreme heat. An extreme case is Northern Sydney, with an estimated RR exceeding 3400 at the 99<sup>th</sup> percentile of temperature—although this value is likely an outlier with wide uncertainty, it underscores the potential for exponential increases in risk at the furthest temperature extremes. At the opposite end, extremely low temperatures are associated with RRs near 0 (e.g., Murrumbidgee  $\approx$  0.02, Sydney  $\approx$  0.03 at the 1<sup>st</sup> percentile), indicating minimal risk during cold conditions.

In other words, very cool or dry conditions tend to suppress salmonella incidence, while very hot or wet conditions greatly increase the risk. This non-linear behaviour suggests that salmonella rates remain relatively stable around moderate climate conditions (baseline  $\approx$  1.0 RR), but decrease at one end and surge at the other end of the climate spectrum.

Extreme precipitation events also show a clear impact on salmonella risk, though generally the magnitude is less extreme than for temperature. In most LHDs, drought-like conditions (very low rainfall, 1<sup>st</sup> percentile) correspond with RR below 1 (often in the 0.2–0.5 range), whereas heavy rainfall (95<sup>th</sup>–99<sup>th</sup> percentiles) pushes RR above 1. For example, in the Murrumbidgee LHD (a rural agricultural region), the RR rises from 0.29 at the 1<sup>st</sup> percentile of rainfall to 10.76 at the 99<sup>th</sup> percentile—indicating more than a tenfold higher risk during periods of extreme rainfall. Several other districts see roughly 2- to 6-fold increases in risk at high rainfall extremes (e.g., Western Sydney RR  $\approx$  6.0 at the 99<sup>th</sup> percentile rainfall, vs. 0.33 at the 1<sup>th</sup>).

Notably, when heavy rain leads to flooding, the risks can spike further: e.g., Illawarra Shoalhaven (coastal) shows RR  $\approx$  22.3 at the 99<sup>th</sup> percentile of flooding, and South Western Sydney has RR  $\approx$  20.9 at 99<sup>th</sup> percentile flooding. In contrast, at the 1<sup>st</sup> percentile of flooding (essentially no flooding), RRs are  $< 0.5$  in those same areas, indicating much lower baseline risk when significant flooding is absent.

High relative humidity emerges as another factor amplifying salmonella risk, though its effects are somewhat intertwined with temperature (hot periods are often humid). Still, the data show that at the 99<sup>th</sup> percentile of humidity, RRs are elevated in many LHDs, while at very low humidity (dry air) RRs are below 1. For instance, South Eastern Sydney has RR  $\approx$  14.4 at the most humid extreme, compared to 0.44 at the 1<sup>st</sup> percentile. Even the arid Far West LHD exhibits an increase from RR  $\approx$  0.29 at minimal humidity to  $\approx$  8.5 at

the highest humidity percentile, suggesting that occasional surges in moisture (e.g., storms in desert regions) can facilitate outbreaks.

The relative impact of these climate extremes varies considerably between LHDs, highlighting specific regional vulnerabilities. Some districts exhibit far greater sensitivity to certain climate variables than others. The Far West stands out for its extreme temperature effect, an unsurprising finding given its desert-like climate. Meanwhile, the Central Coast shows minimal change in risk across all percentiles ( $RR \approx 1.0$ ), indicating that climate factors had lesser influence in this region's mild environment. Most other regions fall between these extremes. Generally, rural and inland LHDs (Far West, Western NSW, Southern NSW, Murrumbidgee) face more dramatic swings in climate and thus exhibit more pronounced climate-related RRs. In Murrumbidgee, for instance, aside from its temperature effect, it also had one of the highest rainfall-related risks. On the other hand, urban/metropolitan LHDs like Sydney and Western Sydney also show significant increases with climate extremes, but typically not as steep. Notably, Illawarra Shoalhaven and South Western Sydney show very high RRs for flooding (over 20-fold increase), suggesting specific local vulnerabilities (e.g., low-lying areas or stormwater overflow).

## 4 Discussion

Our analyses highlight the significant influence of meteorological factors, specifically temperature, humidity, and under certain conditions, rainfall and flooding, on the incidence of salmonella in NSW. By employing two complementary Bayesian modelling approaches, a case-crossover design and a spatiotemporal time-series framework, this dual approach allowed for robust validation of climate-disease associations and underscored the importance of accounting for seasonality, long-term trends, and localised spatial heterogeneity in epidemiological modelling.

### Non-linear relationships and extreme percentiles

A principal finding of this study is the markedly non-linear relationship characterising the association between climatic variables and the risk of salmonella. The summary of RR at the 1<sup>st</sup>, 5<sup>th</sup>, 95<sup>th</sup>, and 99<sup>th</sup> percentiles of each exposure reveals a pronounced "U" or "J" shape, across most LHDs. Specifically, at the lower percentiles (cooler or drier conditions), RRs frequently fall below unity, suggesting a potential reduction in risk. Conversely, at higher percentiles, particularly above the 95<sup>th</sup>, RRs increase substantially, indicating a disproportionate rise in risk under extreme conditions. Notably, several LHDs exhibited substantial increases; for instance, the Far West LHD showed a significantly high RR at extreme heat percentiles, while Illawarra Shoalhaven demonstrated 20-fold or greater increases at the highest flood index percentile. These dramatic increase underscore the potential for rapid escalation of salmonella risk under intense climatic conditions, such as heatwaves, extreme rainfall, or periods of unusually high humidity. These non-linear patterns align with prior research demonstrating exponential increases in Salmonella growth rates above specific temperature thresholds and the mobilisation of environmental pathogens by precipitation events [D'Souza et al., 2004, Baker et al., 2019]. Such a pattern aligns with known seasonality and environ-

mental survival of *Salmonella*—for instance, infections tend to drop during cold spells and spike during hot weather [D’Souza et al., 2004]. These findings reinforce that hot weather is a major driver of salmonella outbreaks [Scallan et al., 2011]. Each degree of warming has been shown to elevate *Salmonella* infection rates by roughly 5% per 1 °C in pooled analyses [Williams et al., 2020], and here we see that at very high percentiles those increases compound into enormous relative risks. Even short-term heatwaves can significantly boost cases; for instance, one Australian study found a 34% increase in salmonella risk when temperatures exceeded 41 °C [Bennett et al., 2014]. Thus, the relationship between temperature and salmonella is highly non-linear—beyond a certain threshold, the risk appears to accelerate sharply with each additional degree of heat.

### Probability of exceeding thresholds

Complementing the point estimates, the probability maps for exceeding specific risk thresholds provide valuable insights into the spatial distribution and certainty of these climate effects. These maps illustrate that extensive areas across NSW have a high probability ( $P > 0.7$ ) of increased salmonella risk associated with extreme heat or humidity. Coastal LHDs generally appear less susceptible to rainfall-associated risk (with  $P(RR > 1)$  often below 0.5 for heavy rain), whereas inland or semi-rural districts demonstrate higher vulnerability. Overlaying these exceedance probabilities onto specific regions allows for the identification of potential local hotspots. For example, while western Sydney might face a moderate probability of a flood-induced surge, the probability of a temperature-driven increase in the Far West LHD above a certain heat threshold is markedly higher. These probability-based findings add a crucial dimension to the RR estimates by quantifying the confidence with which we can assert that extreme climatic conditions will elevate *Salmonella* risk above defined thresholds (e.g.,  $RR \geq 1.5$ ). Consequently, these findings can inform targeted public health strategies, enabling authorities to prioritise interventions, such as enhanced food safety inspections or public health advisories, when meteorological forecasts indicate a high probability of exceeding relevant climatic thresholds.

### Comparisons between CCM and BSM models

Comparison of the findings from the two modelling approaches revealed broad agreement, particularly regarding temperature as a primary driver of short-term salmonella risk. The case-crossover design was well-suited for capturing acute fluctuations in risk (e.g., comparing incidence during a heatwave to control periods), and sometimes yielded slightly higher effect estimates for extreme exposures, reflecting its focus on day-to-day contrasts less subject to seasonal confounding [Maclure, 1991]. Spatiotemporal time-series framework on the other hand provided a more comprehensive perspective, accounting for both baseline incidence differences (via spatial random effects) and overarching temporal trends in climate and disease. The superior model fit performance of the model was evidenced by lower DIC and improved RMSE, suggests that explicitly incorporating seasonality and a spatiotemporal structure provides more stable and robust overall estimates.

### Climate specifics

Consistently across all LHDs, elevated ambient temperatures were associated with significantly increased salmonella risk, which aligns with the known temperature-dependent growth and survival characteristics of *Salmonella* bacteria. The disproportionate effect at the upper

extreme is exemplified by the dozens-fold increase in RR observed in many districts at the 99<sup>th</sup>-percentile of heat. The relationship with rainfall was more complex. While moderate precipitation sometimes showed minimal or potentially protective associations in some coastal areas, likely related to dilution or flushing effects, extreme rainfall events have the potential to mobilise pathogens in the environment, contaminate water sources, and contribute to localised flooding, thereby increasing case counts. The observed vulnerability of certain inland or semi-rural LHDs (e.g., Murrumbidgee, Western Sydney) to extreme rainfall echoes prior findings linking rainfall-runoff, sewage overflow, and infrastructure failures during flood events, which can contaminate water and food supplies [Ebi et al., 2006, Hall et al., 2012].

Flood-linked risks demonstrated marked spatial heterogeneity, with specific LHDs (e.g., Illawarra, South Western Sydney) showing substantial surges in risk at the highest flood index percentiles. This is likely attributable to flood-induced disruption of critical infrastructure, such as sewage and water treatment systems, leading to widespread environmental contamination. However, the negligible flood impacts observed in some areas may reflect more resilient infrastructure or lower frequency of significant flood events. Elevated humidity was also positively associated with increased risk, albeit generally to a lesser degree than extreme temperature or flooding in most LHDs. Nonetheless, a subset of inland districts (Far West, Western NSW) exhibited notable increases in RR with high humidity, suggesting that atmospheric moisture can exacerbate bacterial persistence, particularly when coupled with elevated temperatures [Baker et al., 2019].

Mechanistically, high humidity can prolong the survival of *Salmonella* on surfaces and foods by preventing desiccation, further exacerbating the effect of heat [Baker et al., 2019]. Similarly, very dry periods tend to suppress *salmonella*, while intense rainfall elevates it, consistent with the “concentration–dilution” hypothesis in environmental microbiology [Curriero et al., 2001]. During extended dry spells, pathogen levels in the environment may drop, leading to lower disease risk; however, heavy rainfall can wash pathogens from soil or animal waste into water sources and food-production areas [Hall et al., 2012].

### **Spatial heterogeneity and local vulnerabilities**

A key insight from this study is the substantial spatial heterogeneity in climate sensitivity observed across the 15 LHDs. Regions such as the Far West exhibited exceptional sensitivity to extreme heat and humidity, whereas others, like the Central Coast, showed comparatively minimal changes in risk across temperature or humidity extremes. Importantly, densely populated urban LHDs (e.g., Sydney, Western Sydney) were not immune to the impacts of climate stressors, particularly concerning acute heatwaves and flooding events. These findings reinforce the understanding that the impact of broader climate signals on local health outcomes is mediated by the interplay of region-specific factors, including baseline climate characteristics, the resilience of critical infrastructure (e.g., water and sanitation systems), and population behaviours (e.g., food handling practices, reliance on rainwater tanks) [Schramm et al., 2020]. Consequently, effective adaptation measures must be tailored to address these localised vulnerabilities. For instance, interventions in rural areas prone to strong rainfall- or heat-driven spikes might focus on fortifying water storage practices or enhancing agricultural hygiene, while urban strategies could prioritise the implementation of

effective heatwave alert systems and improvements to stormwater drainage to mitigate flood impacts [Ferrand, 2014, NSW Government, 2024].

### **Implications for surveillance and intervention**

These findings carry significant implications for public health surveillance and intervention, particularly in the context of projected increases in the frequency and intensity of extreme weather events under climate change [Semenza and Menne, 2012]. Our results underscore the potential for increased frequency and severity of salmonella outbreaks in susceptible regions. Public health agencies can leverage these findings by integrating climate metrics into disease early-warning systems, enabling the issuance of targeted alerts when forecasts indicate extreme heat or rainfall. This proactive approach enables the preemptive deployment of targeted interventions, including enhanced food safety inspections, rigorous water quality monitoring, and timely public advisories. Strengthening critical infrastructure, including sewer systems and stormwater drainage, as well as ensuring reliable refrigeration capacity, is especially vital in regions identified as highly vulnerable. Furthermore, public health education campaigns promoting safe food handling practices during heatwaves or floods (e.g., preventing cross-contamination, recommending boiling water in post-flood scenarios) can play a crucial role in mitigating the severity of outbreaks [Organization, 2018]. Ultimately, the development and implementation of regional adaptation strategies that specifically address the localised climate risks identified in this study, such as extreme heat in the Far West, flooding vulnerabilities in Illawarra, and combined risks in areas like Western Sydney, are likely to be the most effective.

### **Strengths and Limitations**

#### **Strengths**

This study leverages a long-term dataset and high-resolution climatic and health data to explore the relationship between environmental exposures and Salmonella incidence across multiple LHDs in NSW. The inclusion of distributed lag structures and spatial disaggregation allows for a robust investigation of temporal and regional variation in risk.

#### **Limitations**

We acknowledge the following limitations in this study. First, residual confounding by unmeasured variables such as air pollution, socioeconomic status, or individual-level comorbidities cannot be excluded. The reliance on aggregated data limits the ability to examine effect modification by demographic factors (e.g., age, sex) or behavioural exposures. Second, the analysis does not distinguish between sporadic and outbreak-associated cases, which may confound estimates of climate sensitivity, particularly during extreme weather events. Third, potential compound events were not explicitly modelled, limiting insight into more complex exposure scenarios. And lastly, we did not explore serotype-specific data may constrain understanding of transmission dynamics across different Salmonella strains under climate stress.

## 5 Conclusion

This study provides evidence that high ambient temperatures and elevated humidity levels are significant drivers of increased salmonella risk in NSW, with effects manifesting over short lags. While high rainfall tended to be associated with reduced risk in many areas, particularly coastal and temperate regions, suggesting disruption of transmission pathways, extreme rainfall and flood events showed a more complex or modest potential to elevate risk, albeit with notable spatial variability and associated uncertainty. Overall, temperature and humidity emerge as key meteorological factors associated with increased risk of salmonella, displaying regionally-varying effects and short-term associations. Understanding this climate-disease interplay is paramount for developing effective public health strategies and adaptation measures to safeguard food safety and prevent future salmonella outbreaks in a changing climate.

## References

- Luma Akil, H. Anwar Ahmad, and Remata S. Reddy. Effects of climate change on salmonella infections. *Foodborne Pathogens and Disease*, 11(12):974–980, 2014. doi: 10.1089/fpd.2014.1802. URL <https://doi.org/10.1089/fpd.2014.1802>. PMID: 25496072.
- Australian Government Department of Health and Aged Care. National notifiable diseases surveillance system (nndss) public dataset – salmonella, Oct 2024. URL <https://www.health.gov.au/resources/publications/national-notifiable-diseases-surveillance-system-nndss-public-dataset-salmonella?language=en>. Dataset.
- Jennifer R. Baker, Linnea Hardwick, and David W. Lane. Environmental conditions impacting survival of salmonella on surfaces. *Applied and Environmental Microbiology*, 85(6):e03124–18, 2019.
- Craig Bennett, CR MacIntyre, Rohan Stafford, et al. Assessment of the effect of a 41 °c heatwave on salmonella rates in australia. *International Journal of Environmental Research and Public Health*, 11(2):5212–5223, 2014.
- Julian Besag, Jeremy York, and Annie Mollié. Bayesian image restoration, with two applications in spatial statistics. *Annals of the Institute of Statistical Mathematics*, 43(1):1–59, 1991.
- Frank C. Curriero, Jonathan A. Patz, Joan B. Rose, and Lele Subhash. Temporal and environmental patterns of cryptosporidiosis and giardiasis in the chesapeake bay region. *American Journal of Epidemiology*, 156(3):288–296, 2001.
- Jonathan Darby and Harsha Sheorey. Searching for salmonella. *Australian Journal of General Practice*, 37(10):806, 2008.

Barbara P Davis, Janaki Amin, Petra L Graham, and Paul J Beggs. Climate variability and change are drivers of salmonellosis in australia: 1991 to 2019. *Science of The Total Environment*, 843:156980, 2022.

Perry de Valpine, Daniel Turek, Christopher Paciorek, Cliff Anderson-Bergman, Duncan Temple Lang, and Rado Bodik. Programming with models: writing statistical algorithms for general model structures with nimble. *Journal of Computational and Graphical Statistics*, 26(2):403–413, 2017.

Rennie M. D’Souza, Niels G. Becker, Gillian Hall, and Keith B. Moodie. Does ambient temperature affect foodborne disease? *Epidemiology*, 15(1):86–92, 2004.

Kristie L. Ebi, Ian Burton, and Glenn R. McGregor. Flooding and public health: a critical review of the evidence. *Health Effects of Flooding*, 367:1183–1189, 2006.

Ezgi Akpinar Ferrand. Rainwater harvesting as an effective climate change adaptation strategy in rural and urban settings. In *Managing Water Resources under Climate Uncertainty: Examples from Asia, Europe, Latin America, and Australia*, pages 405–420. Springer, 2014.

Laura Ford, Kathryn Glass, Mark Veitch, Robyn Wardell, Benjamin Polkinghorne, Tim Dobbins, Aparna Lal, and Martyn D. Kirk. Increasing incidence of salmonella in australia, 2000–2013. *PLOS ONE*, 11(10):e0163989, 2016. doi: 10.1371/journal.pone.0163989. URL <https://www.ncbi.nlm.nih.gov/pmc/articles/PMC5061413/>.

Antonio Gasparrini, Ben Armstrong, and Michael G. Kenward. Distributed lag non-linear models. *Statistics in Medicine*, 29(21):2224–2234, 2010.

Gillian V. Hall, Michael R. Raupach, et al. The heat–health watch/warning system in shanghai: A method for forecasting heat waves and heat stress–related mortality. *Environmental Health*, 11(3):23–31, 2012.

Kevin S Ikuta, Lucien R Swetschinski, Gisela Robles Aguilar, Fabrina Sharara, Tomislav Mestrovic, Authia P Gray, Nicole Davis Weaver, Eve E Wool, Chieh Han, Anna Gershberg Hayoon, Amiral Aali, Semagn Mekonnen Abate, Mohsen Abbasi-Kangevari, Zeinab Abbasi-Kangevari, Sherief Abd-Elsalam, Getachew Abebe, Aidin Abedi, Amir Parsa Abhari, Hassan Abidi, Richard Gyan Aboagye, Abdorrahim Absalan, Hiwa Abubaker Ali, Juan Manuel Acuna, Tigist Demssew Adane, Isaac Yeboah Addo, Oyelola A Adegbeye, Mohammad Adnan, Qorinah Estiningtyas Sakilah Adnani, Muhammad Sohail Afzal, Saira Afzal, Zahra Babaei Aghdam, Bright Opoku Ahinkorah, Aqeel Ahmad, Araz Ramazan Ahmad, Rizwan Ahmad, Sajjad Ahmad, Sohail Ahmad, Sepideh Ahmadi, Ali Ahmed, Haroon Ahmed, Jivan Qasim Ahmed, Tarik Ahmed Rashid, Marjan Ajami, Budi Aji, Mostafa Akbarzadeh-Khiavi, Chisom Joyqueen Akunna, Hanadi Al Hamad, Fares Alahdab, Ziyad Al-Aly, Mamoon A Aldeyab, Alicia V Aleman, Fadwa Alhalaiqa Naji Alhalaiqa, Robert Kaba Alhassan, Beriwan Abdulqadir Ali, Liaqat Ali, Syed Shujait Ali, Yousef Alimohamadi, Vahid Alipour, Atiye Alizadeh, Syed Mohamed Aljunid, Kasim Allel, Sami Almustanyir, Edward Kwabena Ameyaw, Arianna Maever L Amit, Nivedita Anandavelane, Robert Ancuceanu, Catalina Liliana Andrei, Tudorel Andrei,

Dewi Anggraini, Adnan Ansar, Anayochukwu Edward Anyasodor, Jalal Arabloo, Aleksandr Y Aravkin, Demelash Areda, Timur Aripov, Anton A Artamonov, Judie Arulappan, Raphael Taiwo Aruleba, Muhammad Asaduzzaman, Tahira Ashraf, Seyyed Sham-sadin Athari, Daniel Atlaw, Sameh Attia, Marcel Ausloos, Tewachew Awoke, Beatriz Paulina Ayala Quintanilla, Tegegn Mulatu Ayana, Sina Azadnajafabad, Amirhossein Azari Jafari, Darshan B B, Muhammad Badar, Ashish D Badiye, Nayereh Baghcheghi, Sara Bagherieh, Atif Amin Baig, Indrajit Banerjee, Aleksandra Barac, Mainak Bardhan, Francesco Barone-Adesi, Hiba Jawdat Barqawi, Amadou Barrow, Pritish Baskaran, Saurav Basu, Abdul-Monim Mohammad Batiha, Neeraj Bedi, Melaku Ashagrie Belete, Uzma Iqbal Belgaumi, Rose G Bender, Bharti Bhandari, Dinesh Bhandari, Pankaj Bhardwaj, Sonu Bhaskar, Krittika Bhattacharyya, Suraj Bhattarai, Saeid Bitaraf, Danilo Buonsenso, Zahid A Butt, Florentino Luciano Caetano dos Santos, Jiao Cai, Daniela Calina, Paulo Camargos, Luis Alberto Cámera, Rosario Cárdenas, Muge Cevik, Joshua Chadwick, Jaykaran Charan, Akhilanand Chaurasia, Patrick R Ching, Sonali Gajanan Choudhari, Enayet Karim Chowdhury, Fazle Rabbi Chowdhury, Dinh-Toi Chu, Isaac Sunday Chukwu, Omid Dadras, Fentaw Teshome Dagnaw, Xiaochen Dai, Saswati Das, Anna Dastiridou, Sisay Abebe Debela, Fitsum Wolde Demisse, Solomon Demissie, Diriba Dereje, Mrganaw Derese, Hardik Dineshbhai Desai, Fikadu Nugusu Dessalegn, Samuel Abebe A Dessalegni, Belay Desye, Kartik Dhaduk, Meghnath Dhimal, Sameer Dhingra, Nancy Diao, Daniel Diaz, Shirin Djalalinia, Milad Dodangeh, Deepa Dongarwar, Bezabih Terefe Dora, Fariba Dorostkar, Haneil Larson Dsouza, Eleonora Dubljanin, Susanna J Dunachie, Oyewole Christopher Durojaiye, Hisham Atan Edinur, Habtamu Bekele Ejigu, Michael Ekholueneiale, Temitope Cyrus Ekundayo, Hassan El-Abid, Muhammed Elhadi, Mohamed A Elmonem, Amir Emami, Luchuo Engelbert Bain, Daniel Berhanie Enyew, Ryenchindorj Erkhembayar, Babak Eshrati, Farshid Etaee, Adeniyi Francis Fagbamigbe, Shahab Falahi, Aida Fallahzadeh, Emerito Jose A Faraon, Ali Fatehizadeh, Ginenus Fekadu, João C Fernandes, Allegra Ferrari, Getahun Fetensa, Irina Filip, Florian Fischer, Masoud Foroutan, Peter Andras Gaal, Muktar A Gadanya, Abhay Motiramji Gaidhane, Balasankar Ganesan, Mesfin Gebrehiwot, Reza Ghanbari, Mohammad Ghasemi Nour, Ahmad Ghashghaee, Ali Gholamrezanezhad, Abdolmajid Gholizadeh, Mahaveer Golechha, Pouya Goleij, Davide Golinelli, Amador Goodridge, Damitha Asanga Gunawardane, Yuming Guo, Rajat Das Gupta, Sapna Gupta, Veer Bala Gupta, Vivek Kumar Gupta, Alemu Guta, Parham Habibzadeh, Atlas Haddadi Avval, Rabih Halwani, Asif Hanif, Md. Abdul Hannan, Harapan Harapan, Shoaib Hassan, Hadi Hassankhani, Khezar Hayat, Behzad Heibati, Golnaz Heidari, Mohammad Heidari, Reza Heidari-Soureshjani, Claudiu Herteliu, Demisu Zenbaba Heyi, Kamal Hezam, Praveen Hoogar, Nobuyuki Horita, Md Mahbub Hossain, Mehdi Hosseinzadeh, Mihaela Hostiuc, Sorin Hostiuc, Soodabeh Hoveidamanesh, Junjie Huang, Salman Hussain, Nawfal R Hussein, Segun Emmanuel Ibitoye, Olayinka Stephen Ilesanmi, Irena M Ilic, Milena D Ilic, Mohammad Tarique Imam, Mustapha Immurana, Leeberk Raja Inbaraj, Arnaud Iradukunda, Nahlah Elkudssiah Ismail, Chidozie C D Iwu, Chinwe Juliana Iwu, Linda Merin J, Mihajlo Jakovljevic, Elham Jamshidi, Tahereh Javaheri, Fatemeh Javanmardi, Javad Javidnia, Sathish Kumar Jayapal, Umesh Jayarajah, Rime Jebai, Ravi Prakash Jha, Tamas Joo, Nitin Joseph, Farahnaz Joukar, Jacek Jerzy Jozwiak, Salah Eddine Oussama Kacimi, Vidya Kadashetti, Laleh R Kalankesh, Rohollah Kalhor, Vineet Kumar

Kamal, Himal Kandel, Neeti Kapoor, Samad Karkhah, Bekalu Getnet Kassa, Nicholas J Kassebaum, Patrick DMC Katoto, Mohammad Keykhaei, Himanshu Khajuria, Abbas Khan, Imteyaz A Khan, Maseer Khan, Md Nuruzzaman Khan, Moien AB Khan, Moawiah Mohammad Khatatbeh, Mona M Khater, Hamid Reza Khayat Kashani, Jagdish Khubchandani, Hanna Kim, Min Seo Kim, Ruth W Kimokoti, Niranjan Kissoon, Sonali Kochhar, Farzad Kompani, Soewarta Kosen, Parvaiz A Koul, Sindhura Lakshmi Koulmane Laxminarayana, Fiorella Krapp Lopez, Kewal Krishan, Vijay Krishnamoorthy, Vishnutheertha Kulkarni, Naveen Kumar, Om P Kurmi, Ambily Kuttikkattu, Hmwe Hmwe Kyu, Dharmesh Kumar Lal, Judit Lám, Iván Landires, Savita Lasrado, Sang woong Lee, Jacopo Lenzi, Sonia Lewycka, Shanshan Li, Stephen S Lim, Wei Liu, Rakesh Lodha, Michael J Loftus, Ayush Lohiya, László Lorenzovici, Mojgan Lotfi, Ata Mahmoodpoor, Mansour Adam Mahmoud, Razzagh Mahmoudi, Azeem Majeed, Jamal Majidpoor, Alaa Makki, Galana Ayana Mamo, Yosef Manla, Miquel Martorell, Clara N Matei, Barney McManigal, Entezar Mehrabi Nasab, Ravi Mehrotra, Addisu Melese, Oliver Mendoza-Cano, Ritesh G Menezes, Alexios-Fotios A Mentis, Georgia Micha, Irmina Maria Michalek, Ana Carolina Micheletti Gomide Nogueira de Sá, Neda Milevska Kostova, Shabir Ahmad Mir, Mojgan Mirghafourvand, Seyyedmohammadsadeq Mirmoeeni, Erkin M Mirrakhimov, Mohammad Mirza-Aghazadeh-Attari, Abay Sisay Misganaw, Awoke Misganaw, Sanjeev Misra, Esmaeil Mohammadi, Mokhtar Mohammadi, Abdollah Mohammadian-Hafshejani, Shafiu Mohammed, Syam Mohan, Mohammad Mohseni, Ali H Mokdad, Sara Momtazmanesh, Lorenzo Monasta, Catrin E Moore, Maryam Moradi, Mostafa Moradi Sarabi, Shane Douglas Morrison, Majid Motaghinejad, Haleh Mousavi Isfahani, Amin Mousavi Khaneghah, Seyed Ali Mousavi-Aghdas, Sumaira Mubarik, Francesk Mulita, Getaneh Baye B Mulu, Sandra B Munro, Saravanan Muthupandian, Tapas Sadashivan Nair, Atta Abbas Naqvi, Himanshi Narang, Zuhair S Natto, Muhammad Naveed, Biswa Prakash Nayak, Shumaila Naz, Ionut Negoi, Seyed Aria Nejadghaderi, Sandhya Neupane Kandel, Che Henry Ngwa, Robina Khan Niazi, Antonio Tolentino Nogueira de Sá, Nafise Noroozi, Hasti Nouraei, Ali Nowroozi, Virginia Nuñez-Samudio, Jerry John Nutor, Chimezie Igwegbe Nzoputam, Ogochukwu Janet Nzoputam, Bogdan Oancea, Rahman Md Obaidur, Vivek Anand Ojha, Akinkunmi Paul Okekunle, Osaretin Christabel Okonji, Andrew T Olagunju, Bolajoko Olubukunola Olusanya, Ahmed Omar Bali, Emad Omer, Nikita Ottavnov, Bilcha Oumer, Mahesh P A, Jagadish Rao Padubidri, Keyvan Pakshir, Tamás Palicz, Adrian Pana, Shahina Pardhan, Jose L Paredes, Utsav Parekh, Eun-Cheol Park, Seoyeon Park, Ashish Pathak, Rajan Paudel, Uttam Paudel, Shrikant Pawar, Hamidreza Pazoki Toroudi, Minjin Peng, Umberto Pensato, Veincent Christian Filipino Pepito, Marcos Pereira, Mario F P Peres, Norberto Perico, Ionela-Roxana Petcu, Zahra Zahid Piracha, Indrashis Podder, Nayanum Pokhrel, Ramesh Poluru, Maarten J Postma, Naeimeh Pourtaheri, Akila Prashant, Ibrahim Qattea, Mohammad Rabiee, Navid Rabiee, Amir Radfar, Saber Raeghi, Sima Rafiei, Pankaja Raghav Raghav, Leila Rahbarnia, Vafa Rahimi-Movaghar, Mosiur Rahman, Muhammad Aziz Rahman, Amir Masoud Rahmani, Vahid Rahmanian, Pradhum Ram, Muhammad Modassar Ali Nawaz Ranjha, Sowmya J Rao, Mohammad-Mahdi Rashidi, Azad Rasul, Zubair Ahmed Ratan, Salman Rawaf, Reza Rawassizadeh, Mohammad Sadegh Razeghinia, Elrashdy Moustafa Mohamed Redwan, Misganu Teshoma Regasa, Giuseppe Remuzzi, Melese Abate Reta, Nazila Rezaei, Aziz Rezapour, Abanoub Riad, Rezaul Karim Ripon, Kristina E Rudd, Basema Saddik,

Saeid Sadeghian, Umar Saeed, Mohsen Safaei, Azam Safary, Sher Zaman Safi, Maryam Sahebazzamani, Amirhossein Sahebkar, Harihar Sahoo, Saina Salahi, Sarvenaz Salahi, Hedayat Salari, Sana Salehi, Hossein Samadi Kafil, Abdallah M Samy, Nima Sanadgol, Senthilkumar Sankararaman, Francesco Sanmarchi, Brijesh Sathian, Monika Sawhney, Ganesh Kumar Saya, Subramanian Senthilkumaran, Allen Seylani, Pritik A Shah, Masood Ali Shaikh, Elaheh Shaker, Murad Ziyaudinovich Shakhmardanov, Mequanent Melaku Sharew, Athena Sharifi-Razavi, Purva Sharma, Rahim Ali Sheikhi, Ali Sheikhy, Pavanchand H Shetty, Mika Shigematsu, Jae Il Shin, Hesamaddin Shirzad-Aski, K M Shivakumar, Parnian Shobeiri, Seyed Afshin Shorofi, Sunil Shrestha, Migbar Mekonnen Sibhat, Negussie Boti Sidemo, Mustafa Kamal Sikder, Luís Manuel Lopes Rodrigues Silva, Jasvinder A Singh, Paramdeep Singh, Surjit Singh, Md Shahjahan Siraj, Samarjeet Singh Siwal, Valentin Yurievich Skryabin, Anna Aleksandrovna Skryabina, Bogdan Socea, Damtew Damtew Solomon, Yimeng Song, Chandrashekhar T Sreeramareddy, Muhammad Suleman, Rizwan Suliankatchi Abdulkader, Saima Sultana, Miklós Szócska, Seyed-Amir Tabatabaeizadeh, Mohammad Tabish, Majid Taheri, Elahe Taki, Ker-Kan Tan, Sarmila Tandukar, Nathan Y Tat, Vivian Y Tat, Belay Negash Tefera, Yibekal Manaye Tefera, Gebremaryam Temesgen, Mohamad-Hani Temsah, Samar Tharwat, Arulmani Thiagarajan, Imad I Tleyjeh, Christopher E Troeger, Krishna Kishore Umapathi, Era Upadhyay, Sahel Valadan Tahbaz, Pascual R Valdez, Jef Van den Eynde, H. Rogier van Doorn, Siavash Vaziri, Georgios-Ioannis Verras, Harimadhav Viswanathan, Bay Vo, Abdul Waris, Gizachew Tadesse Wassie, Nuwan Darshana Wickramasinghe, Sajad Yaghoubi, Gahin Abdulraheem Tayib Yahya Yahya, Seyed Hossein Yahyazadeh Jabbari, Arzu Yigit, Vahit Yigit, Dong Keon Yon, Naohiro Yonemoto, Mazyar Zahir, Burhan Abdullah Zaman, Sojib Bin Zaman, Moein Zangiabadian, Iman Zare, Mikhail Sergeevich Zastrozhan, Zhi-Jiang Zhang, Peng Zheng, Chenwen Zhong, Mohammad Zoladl, Alimuddin Zumla, Simon I Hay, Christiane Dolecek, Benn Sartorius, Christopher J L Murray, and Mohsen Naghavi. Global mortality associated with 33 bacterial pathogens in 2019: a systematic analysis for the global burden of disease study 2019. *The Lancet*, 400(10369):2221–2248, 2022. ISSN 0140-6736. doi: [https://doi.org/10.1016/S0140-6736\(22\)02185-7](https://doi.org/10.1016/S0140-6736(22)02185-7). URL <https://www.sciencedirect.com/science/article/pii/S0140673622021857>.

Malcolm Maclure. The case-crossover design: a method for studying transient effects on the risk of acute events. *American Journal of Epidemiology*, 133(2):144–153, 1991.

Naveen Manchal, Megan K Young, Maria Eugenia Castellanos, Peter Leggat, and Oyelola Adegbeye. A systematic review and meta-analysis of ambient temperature and precipitation with infections from five food-borne bacterial pathogens. *Epidemiology & Infection*, 152:e98, 2024.

A Milazzo, LC Giles, Y Zhang, AP Koehler, JE Hiller, and P Bi. The effect of temperature on different salmonella serotypes during warm seasons in a mediterranean climate city, adelaide, australia. *Epidemiology & Infection*, 144(6):1231–1240, 2016.

Maria E. Morgado, Congrong Jiang, Juan Zambrana, et al. Climate change, extreme events, and increased risk of salmonellosis: foodborne diseases active surveillance network (food-

net), 2004–2014. *Environmental Health*, 20:105, 2021. doi: 10.1186/s12940-021-00787-y. URL <https://doi.org/10.1186/s12940-021-00787-y>.

NSW Department of Planning, Housing and Infrastructure. Population projections: Explore the data, 2024. URL <https://www.planning.nsw.gov.au/data-and-insights/population-projections/explore-the-data>.

NSW Government. Nsw climate change adaptation action plan 2025–2029. <https://www.climatechange.environment.nsw.gov.au/about-adaptnsw/nsw-government-action-climate-change/Adaptation-Action-Plan-2025-2029>, 2024. Accessed: 2025-06-26.

NSW Health. Salmonella fact sheet, 2024. URL <https://www.health.nsw.gov.au/Infectious/factsheets/Pages/salmonella.aspx>. Accessed: 2025-04-09.

World Health Organization. *Climate change and health: Key facts*. World Health Organization, 2018. Available at: <https://www.who.int/news-room/fact-sheets/detail/climate-change-and-health>.

Marcos Quijal-Zamorano, Miguel A Martinez-Beneito, Joan Ballester, and Marc Marí-Dell'Olmo. Spatial bayesian distributed lag non-linear models (sb-dlnm) for small-area exposure-lag-response epidemiological modelling. *International journal of epidemiology*, 53(3):dyae061, 2024.

HE Ratnayake, DP Eisen, OA Adegbeye, A Pak, and ES McBryde. Bacteraemia in tropical australia: A review. *Current Tropical Medicine Reports*, pages 1–12, 2024.

Elaine Scallan, Robert M. Hoekstra, Frederick J. Angulo, Robert V. Tauxe, Marc-Alain Widdowson, Sharon L. Roy, Jay Jones, and Patricia M. Griffin. Foodborne illness acquired in the united states—major pathogens. *Emerging Infectious Diseases*, 17(1):7–15, 2011.

Paul J Schramm, Munerah Ahmed, Hannah Siegel, Jamie Donatuto, Larry Campbell, Kristin Raab, and Erik Svendsen. Climate change and health: local solutions to local challenges. *Current environmental health reports*, 7:363–370, 2020.

Jan C. Semenza and Bettina Menne. Climate change impact assessment of food- and water-borne diseases. *Critical Reviews in Environmental Science and Technology*, 42(7):671–701, 2012.

Bieke Tack, Daniel Vita, Marie-France Phoba, Lisette Mbuiyi-Kalonji, Liselotte Hardy, Barbara Barbé, Jan Jacobs, Octavie Lunguya, and Liesbet Jacobs. Direct association between rainfall and non-typhoidal salmonella bloodstream infections in hospital-admitted children in the democratic republic of congo. *Scientific Reports*, 11(1):21617, 2021.

Deus Thindwa, Michael G Chipeta, Marc YR Henrion, and Melita A Gordon. Distinct climate influences on the risk of typhoid compared to invasive non-typhoid salmonella disease in blantyre, malawi. *Scientific reports*, 9(1):20310, 2019.

NSW Treasury. Intergenerational report treasury technical research paper series: An indicative assessment of four key areas of climate risk for the 2021 nsw intergenerational report, 2021. URL <https://www.treasury.nsw.gov.au/nsw-economy/nsw-intergenerational-report/nsw-intergenerational-report-treasury-technical-research>.

Lauren A. Williams, Jonathan D. Smith, Lisa A. Brown, and Harriet Wilson. Effects of ambient temperature on salmonella infections in temperate regions: a multi-region time-series analysis. *Environmental Research*, 182:109034, 2020.

World Health Organization. Salmonella (non-typoidal), 2018. URL [https://www.who.int/news-room/fact-sheets/detail/salmonella-\(non-typoidal\)](https://www.who.int/news-room/fact-sheets/detail/salmonella-(non-typoidal)). Accessed: 2025-04-09.

Patrick Zippenfenig. Open-meteo.com weather api, 2024. URL <https://zenodo.org/records/14582479>.

## A Supplementary Materials

## A.1 Exploratory (Spatial) Data Analysis

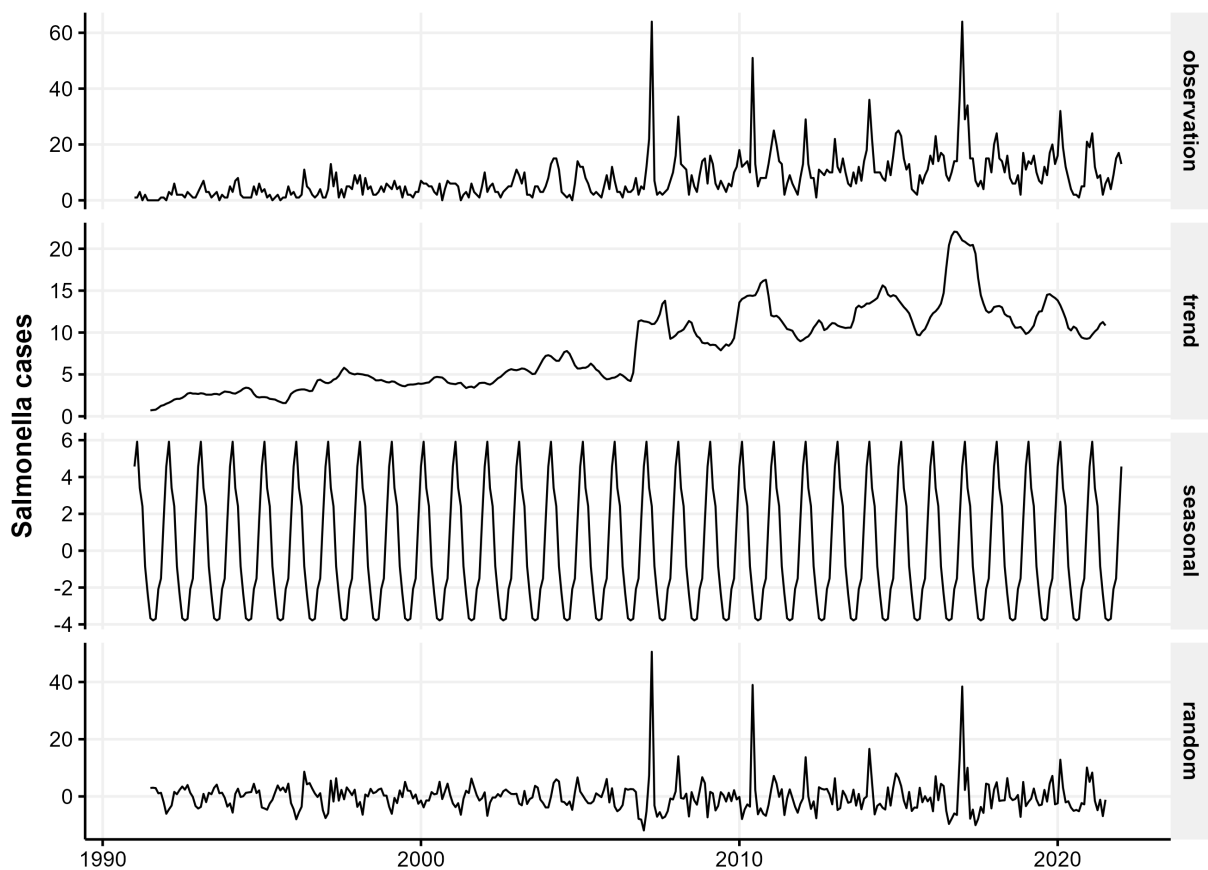


Figure 6: Decomposition of Salmonella time series data

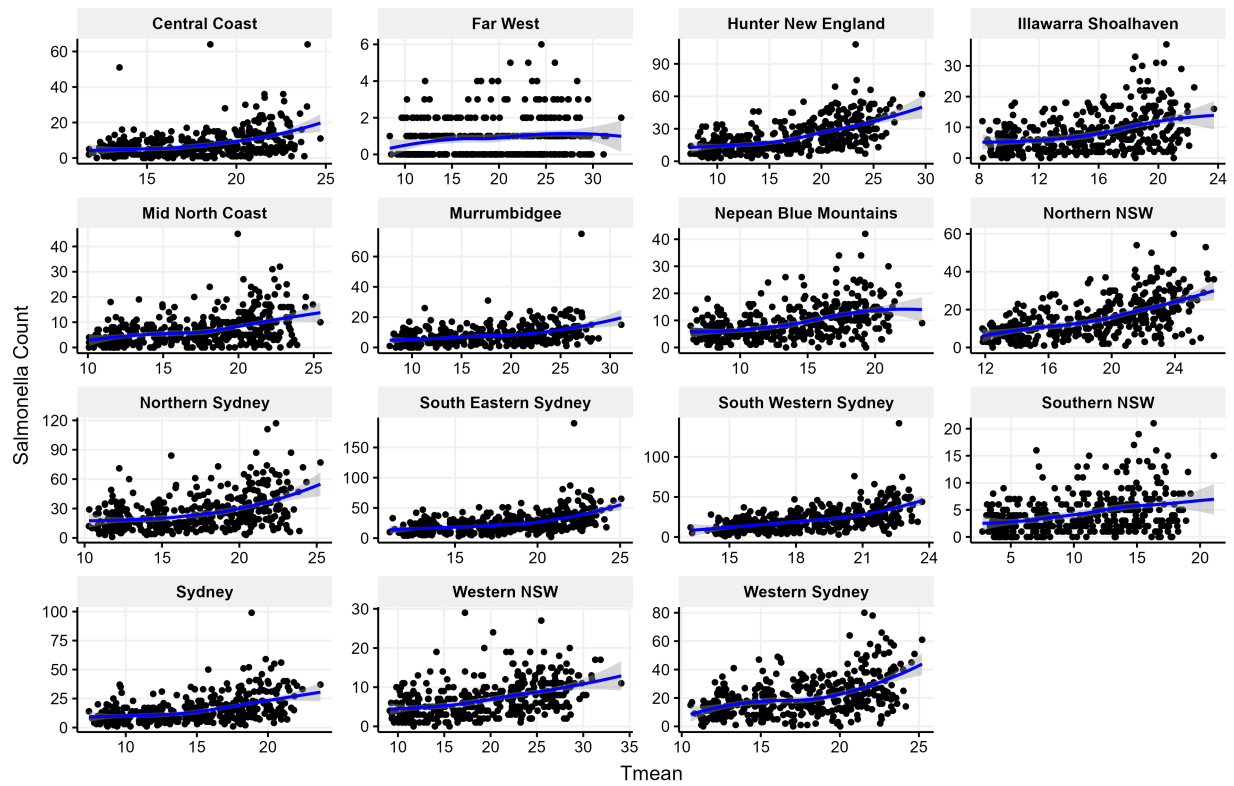


Figure 7: Salmonella cases vs monthly mean temperature across the LHDs

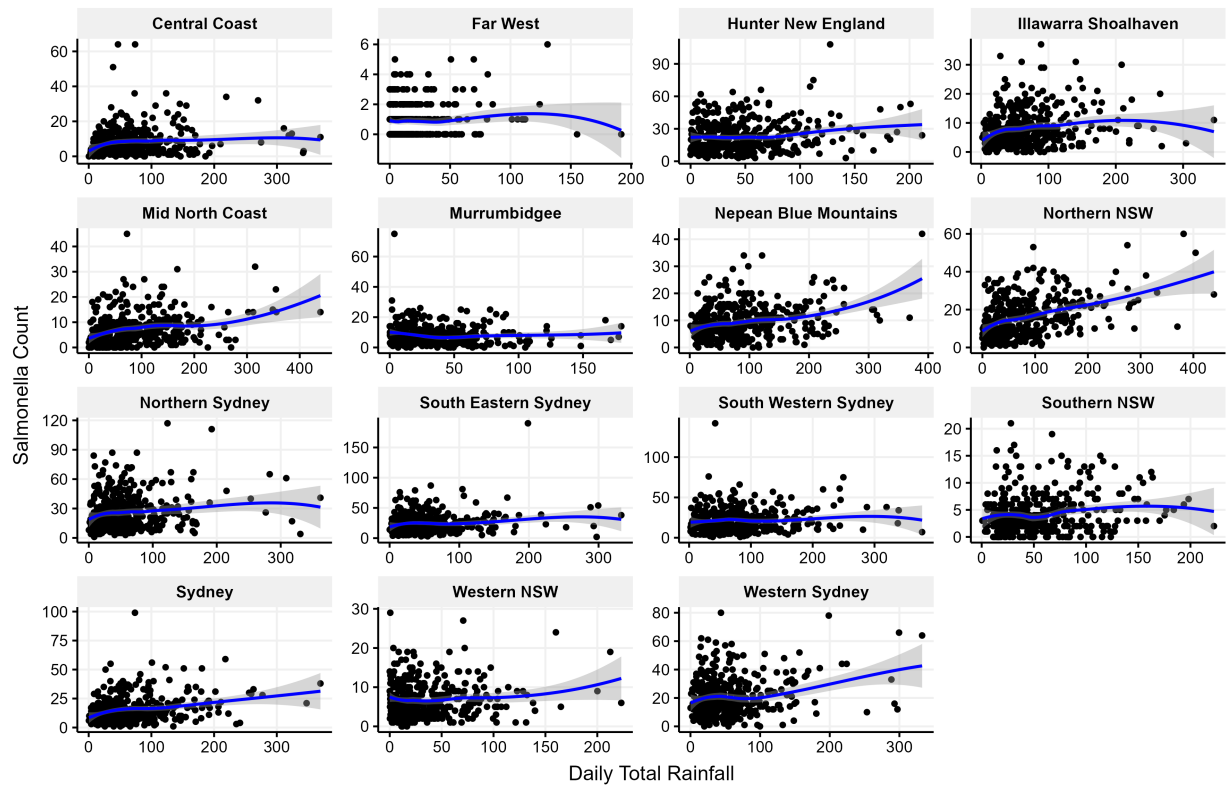


Figure 8: Salmonella cases vs rainfall across the LHDs

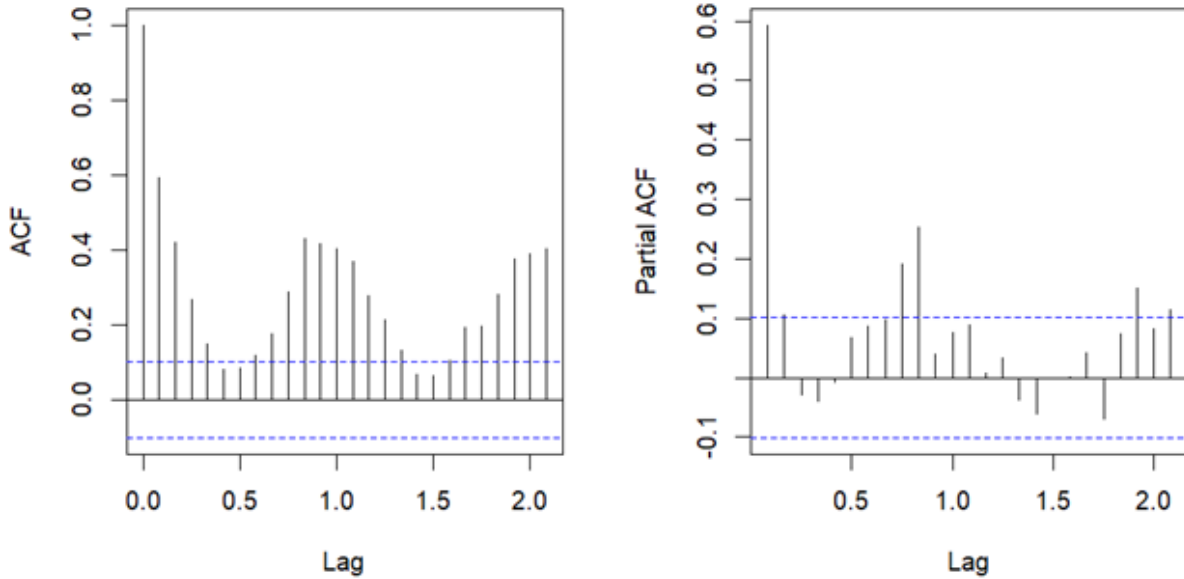


Figure 9: Autocorrelation function (ACF) and partial ACF of Salmonella incidence rate

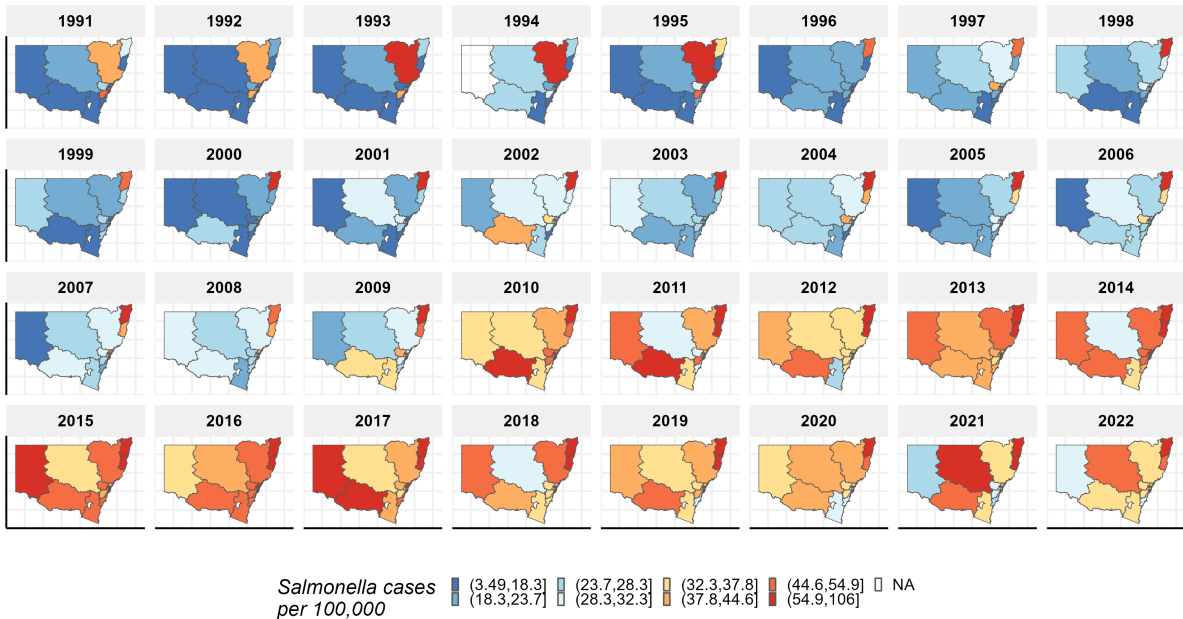
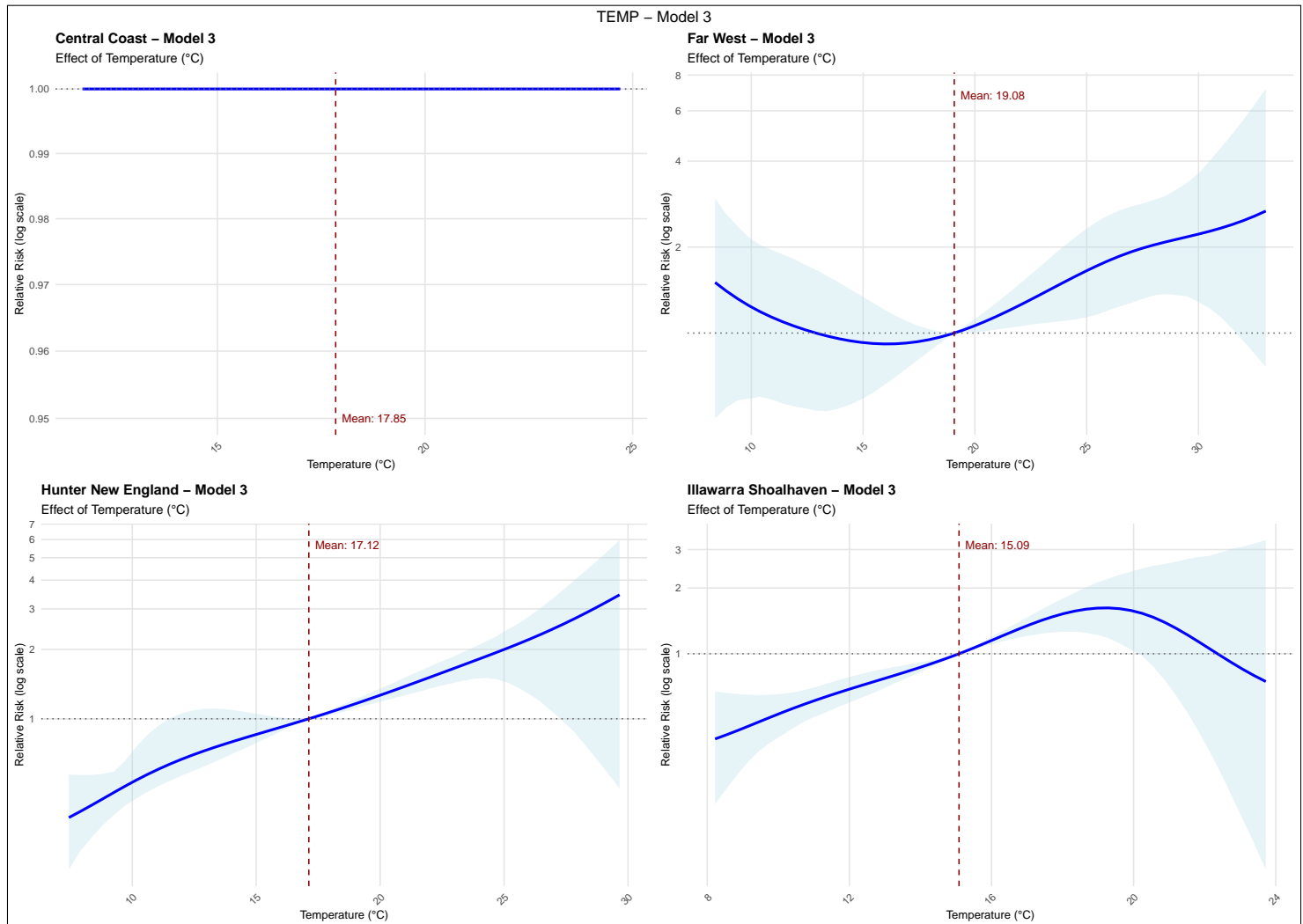
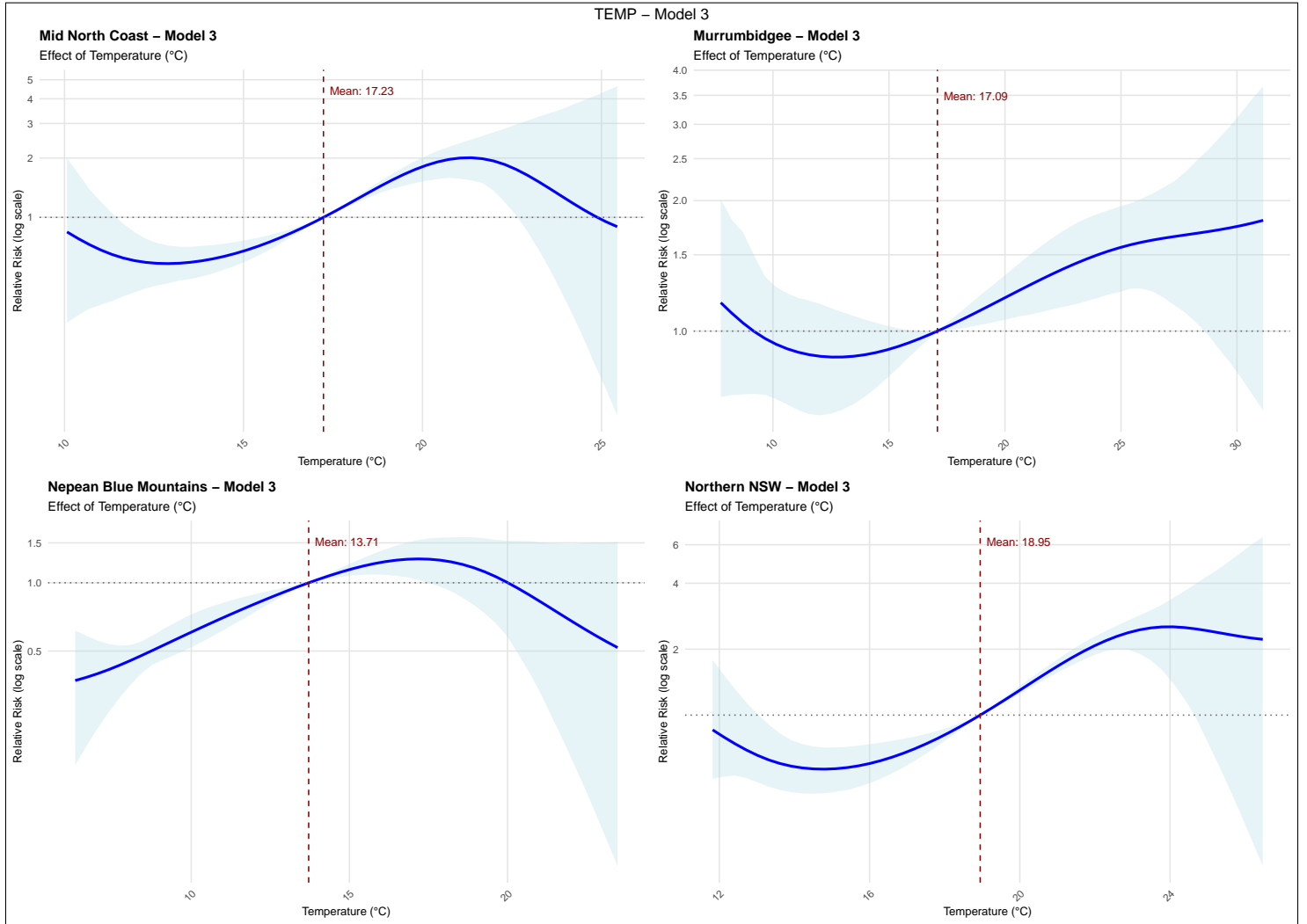
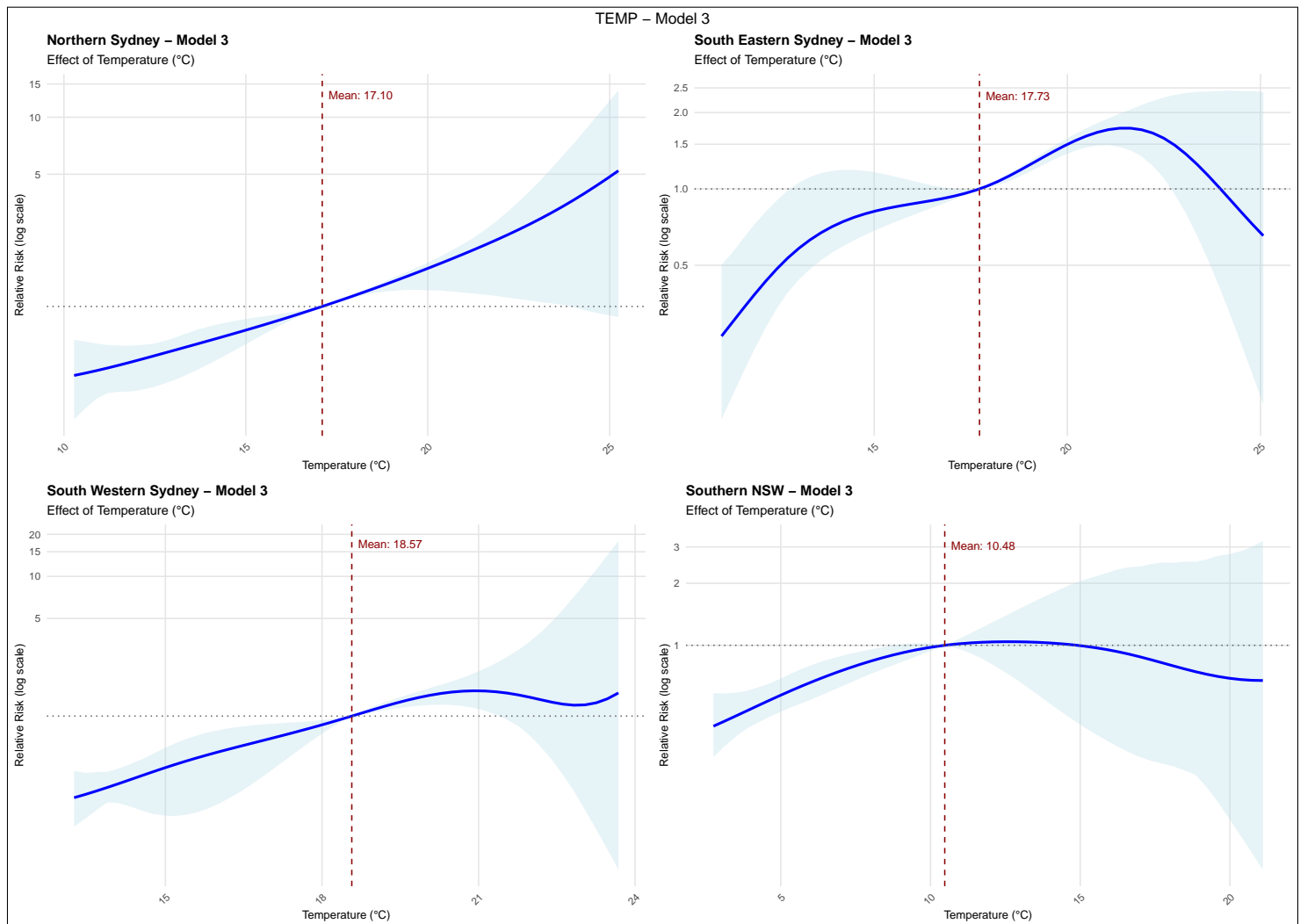


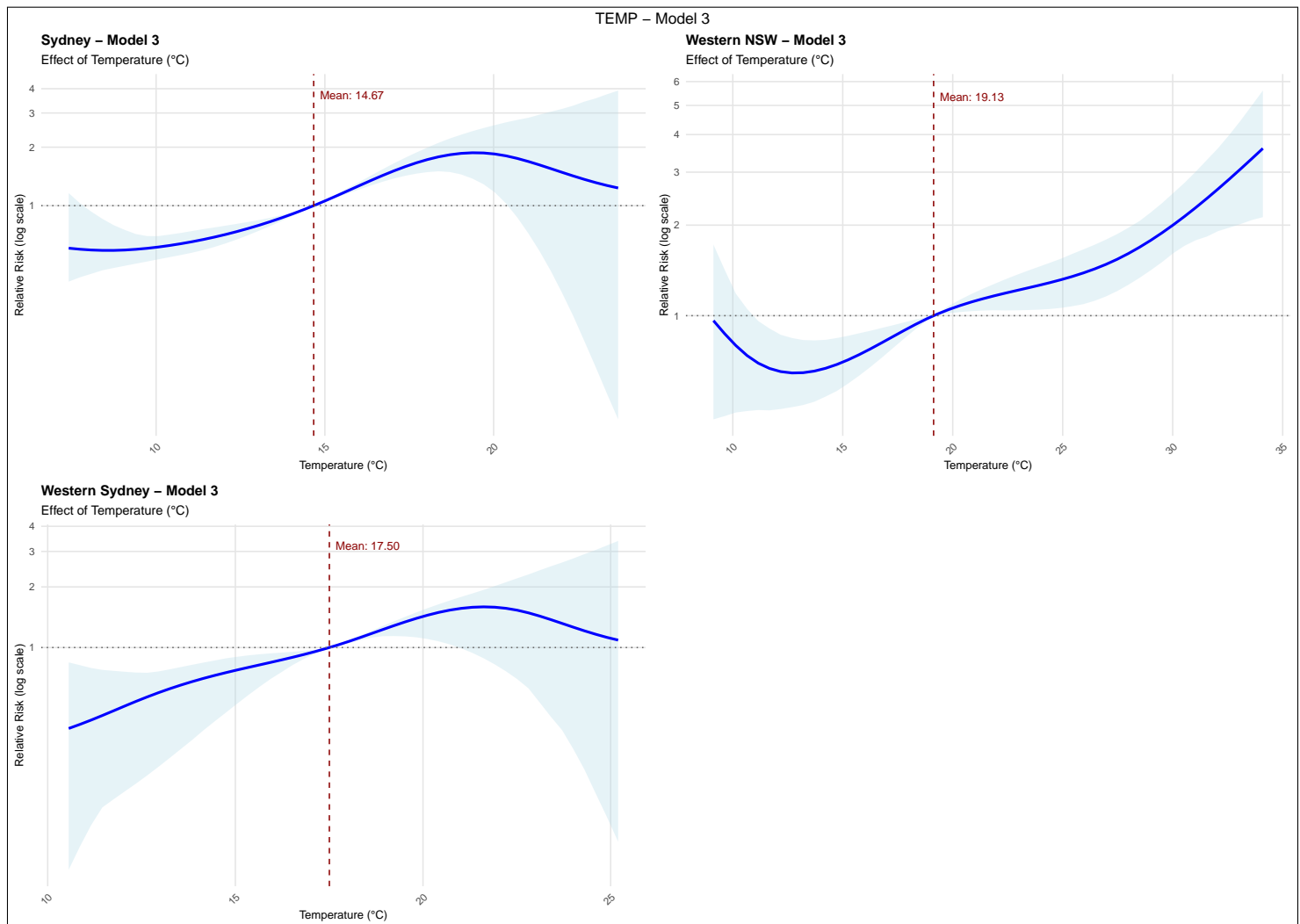
Figure 10: Spatiotemporal patterns of Salmonella cases per 100,000 population across the LHDs in New South Wales, Australia, from 1990 to 2022

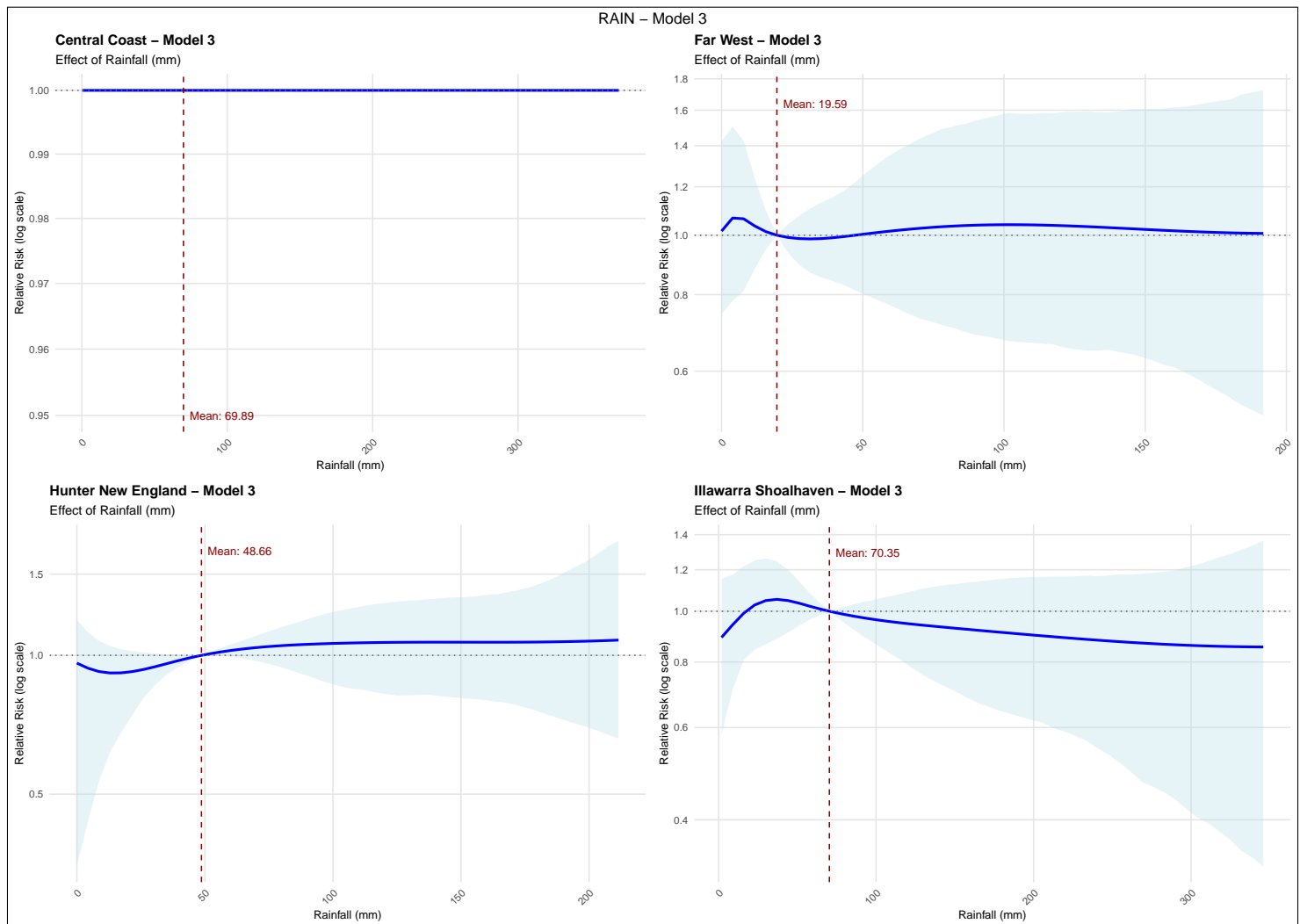
## A.2 Dose-response curves

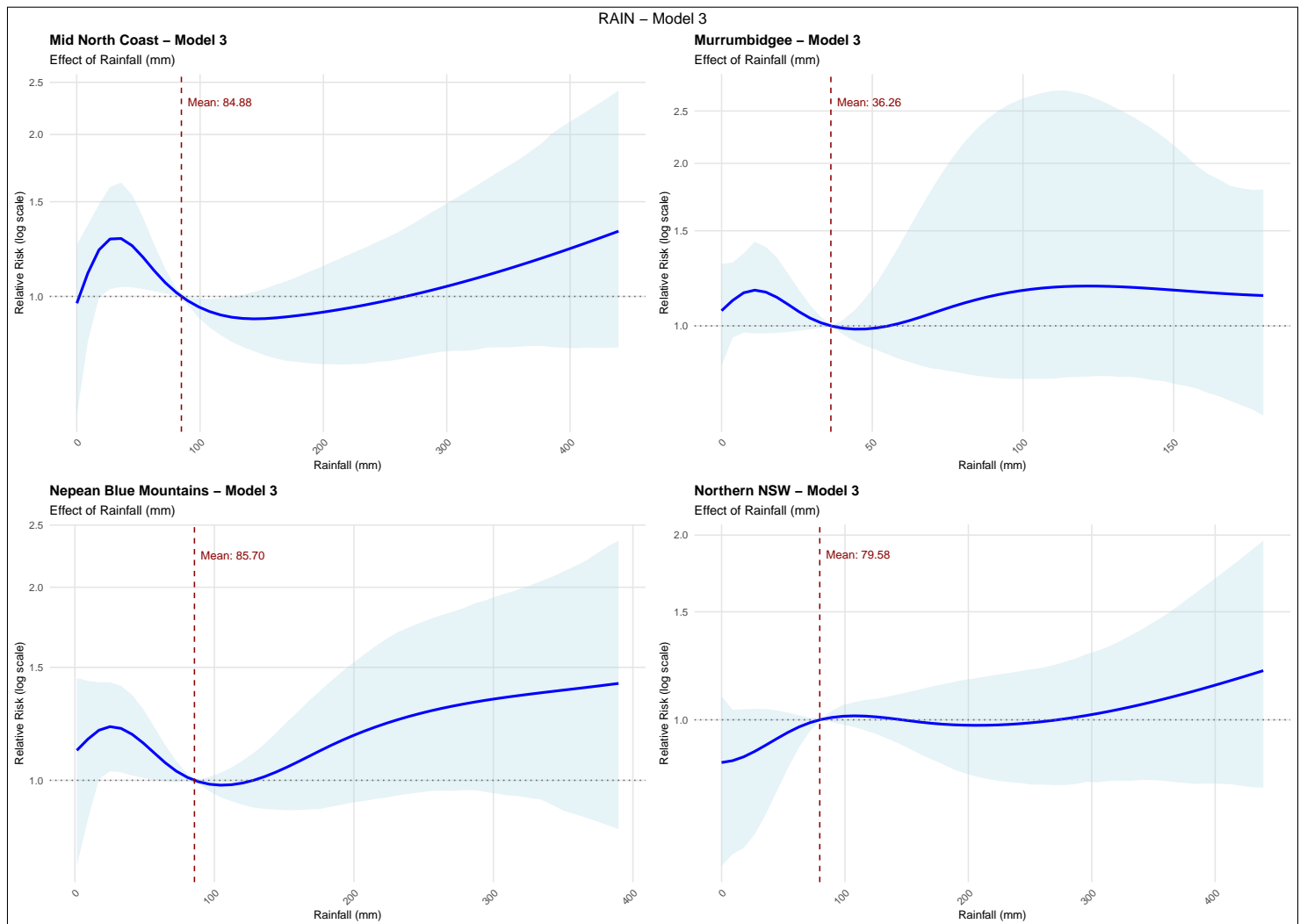


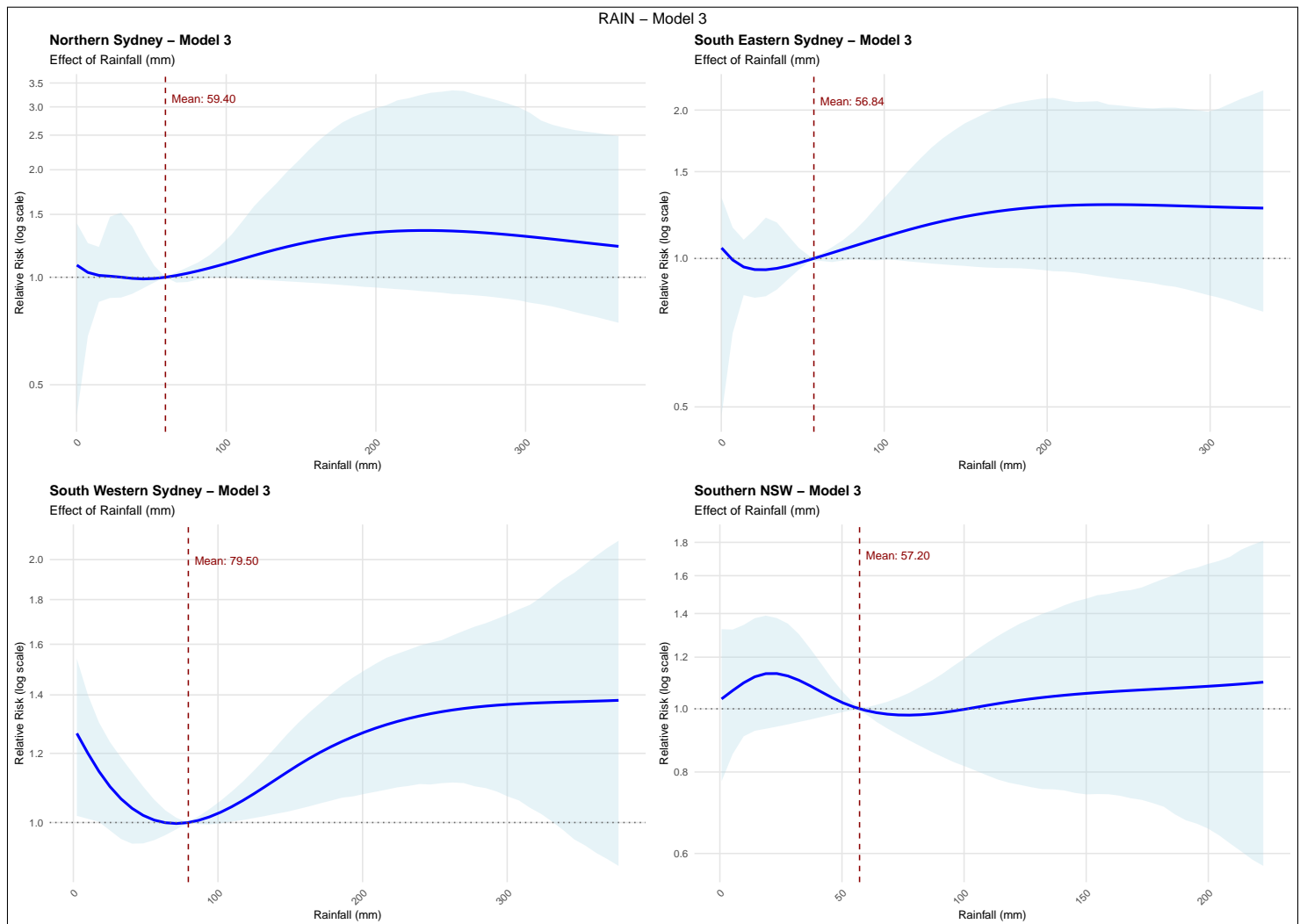


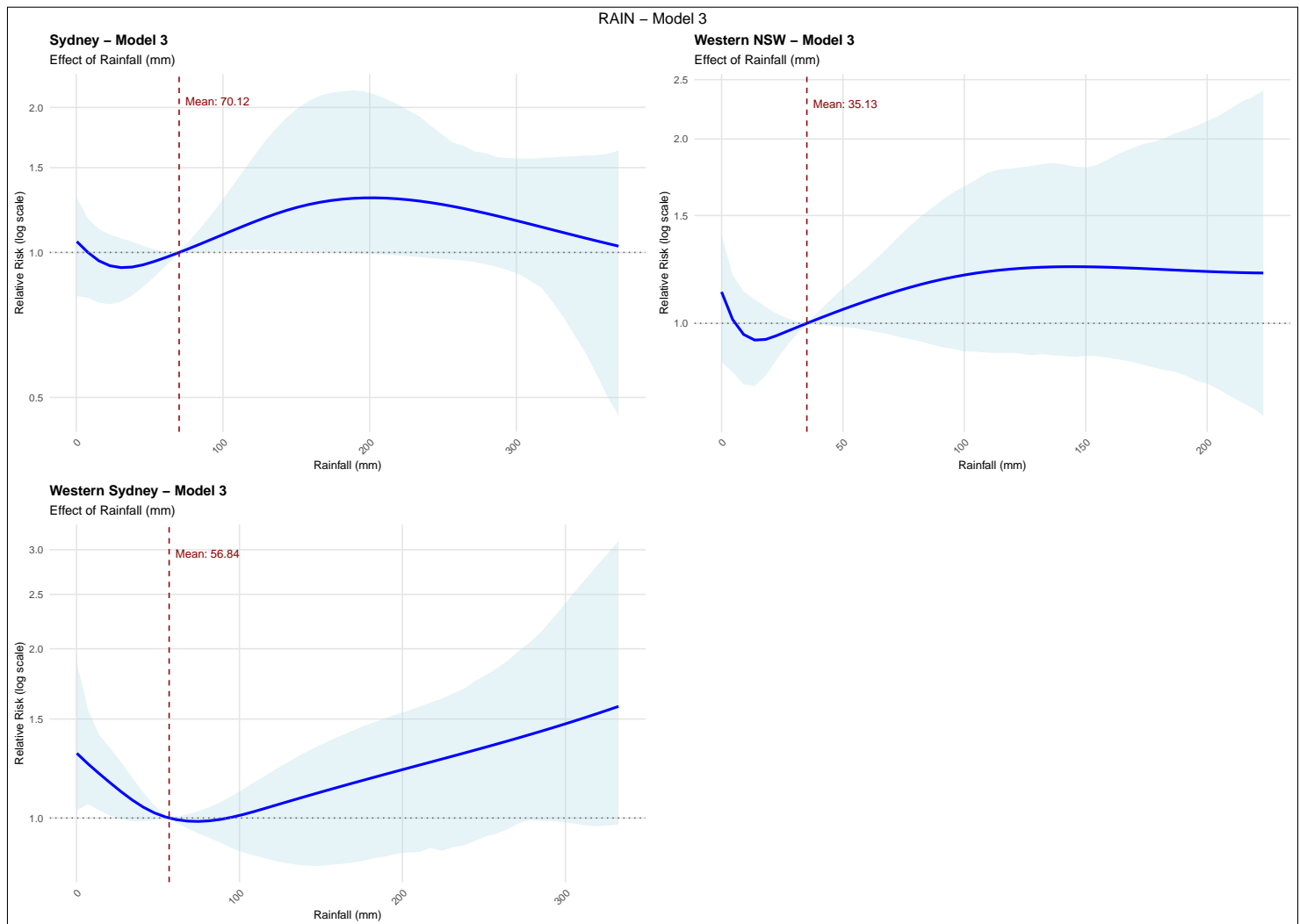


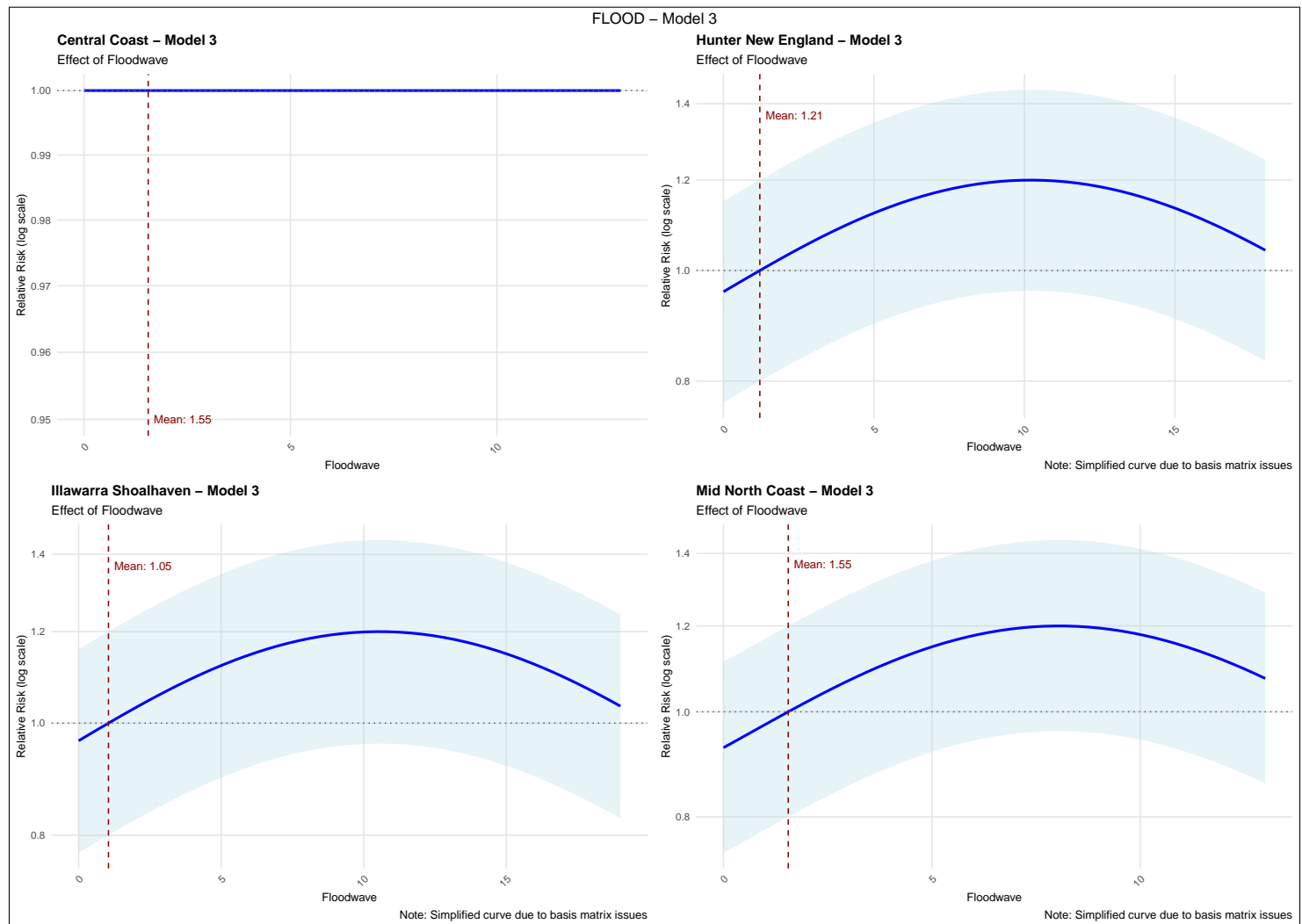


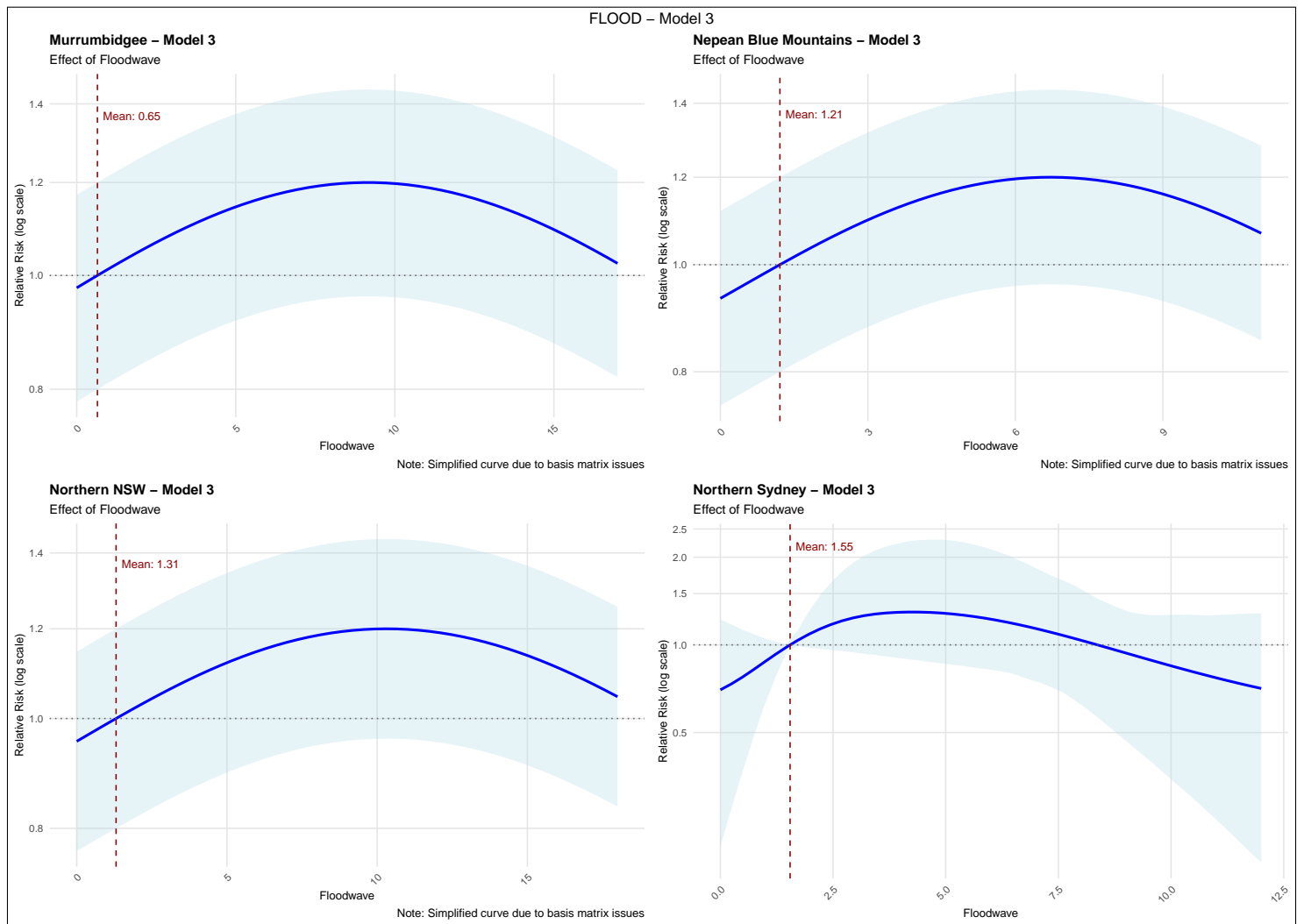


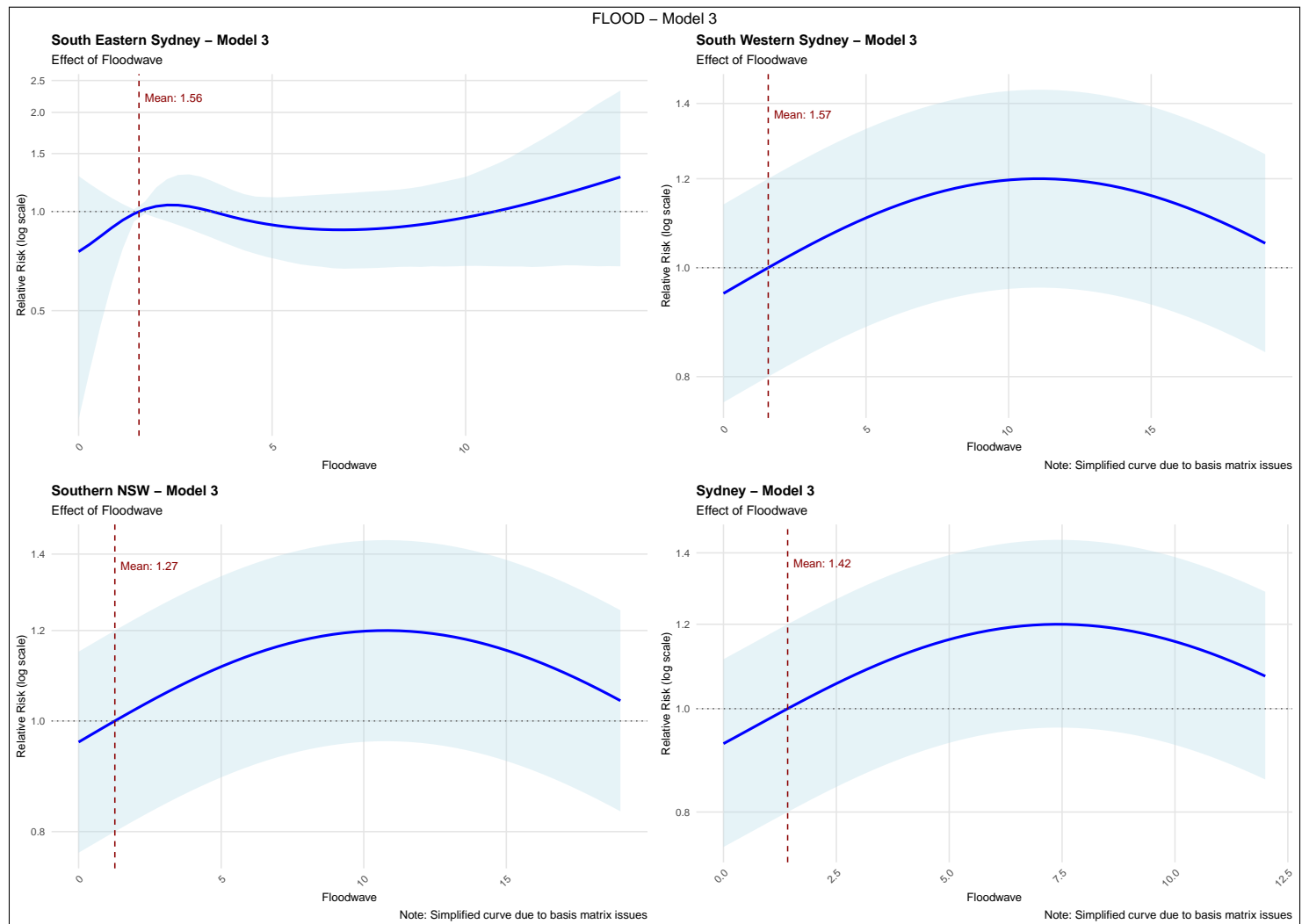


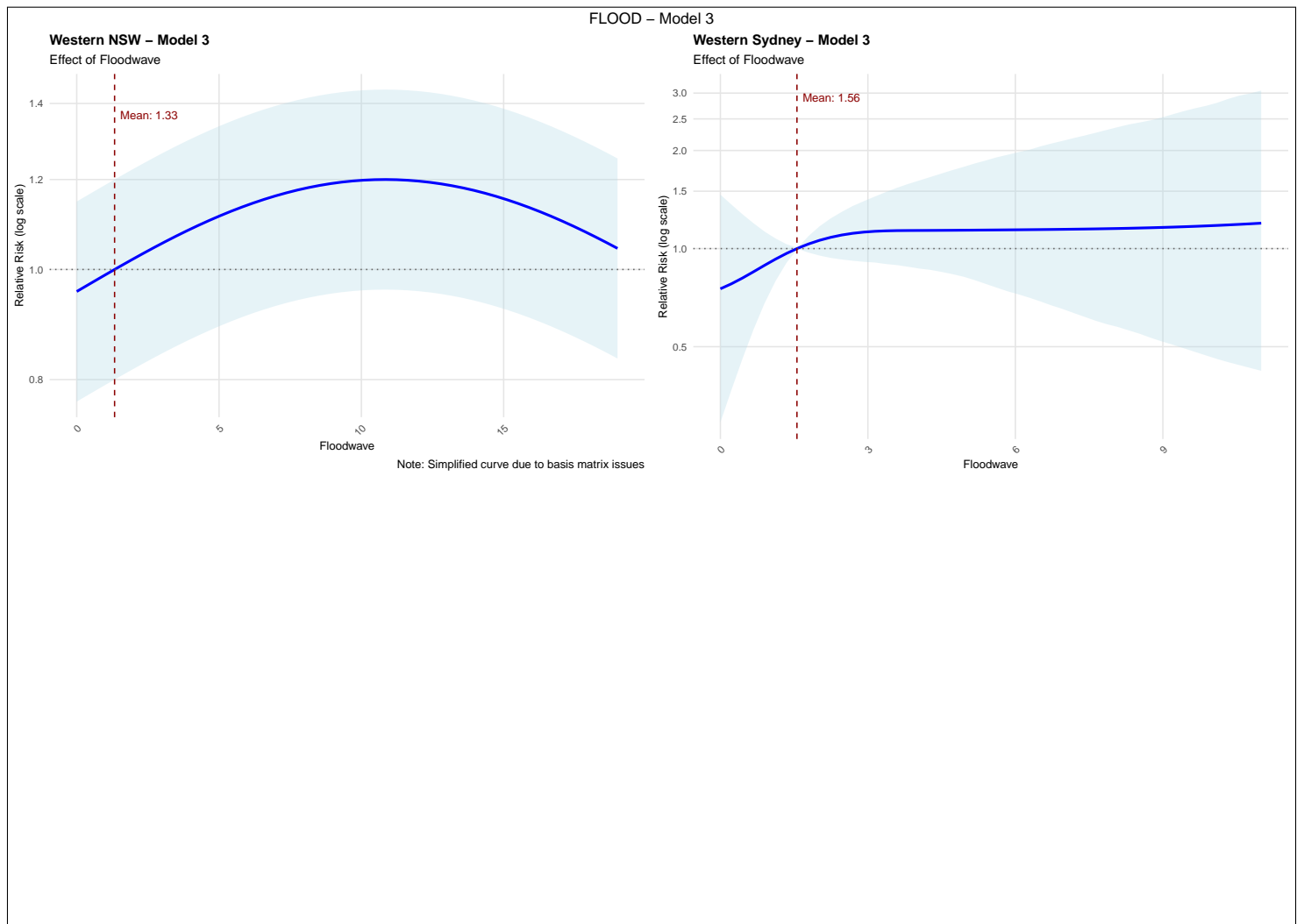


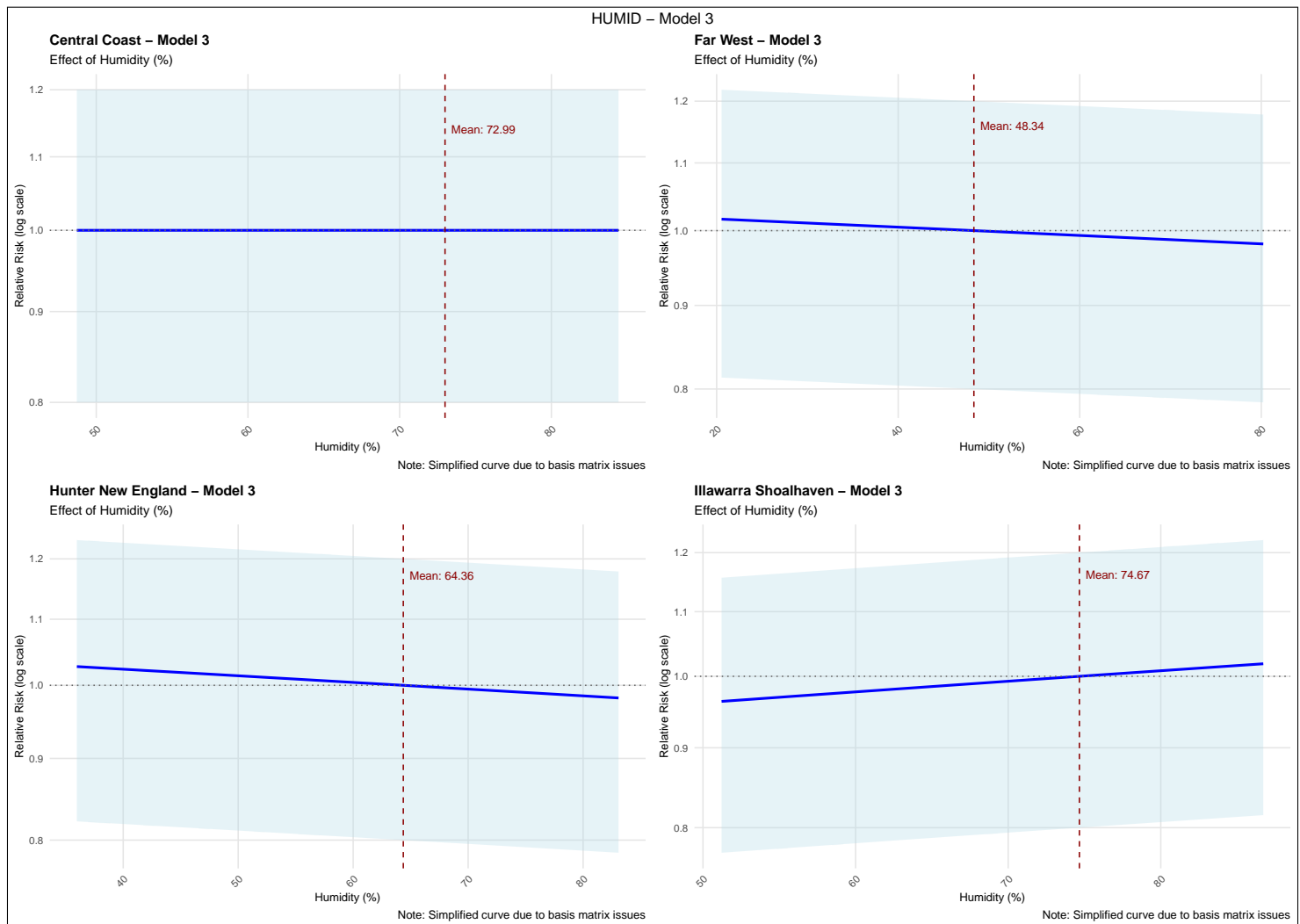


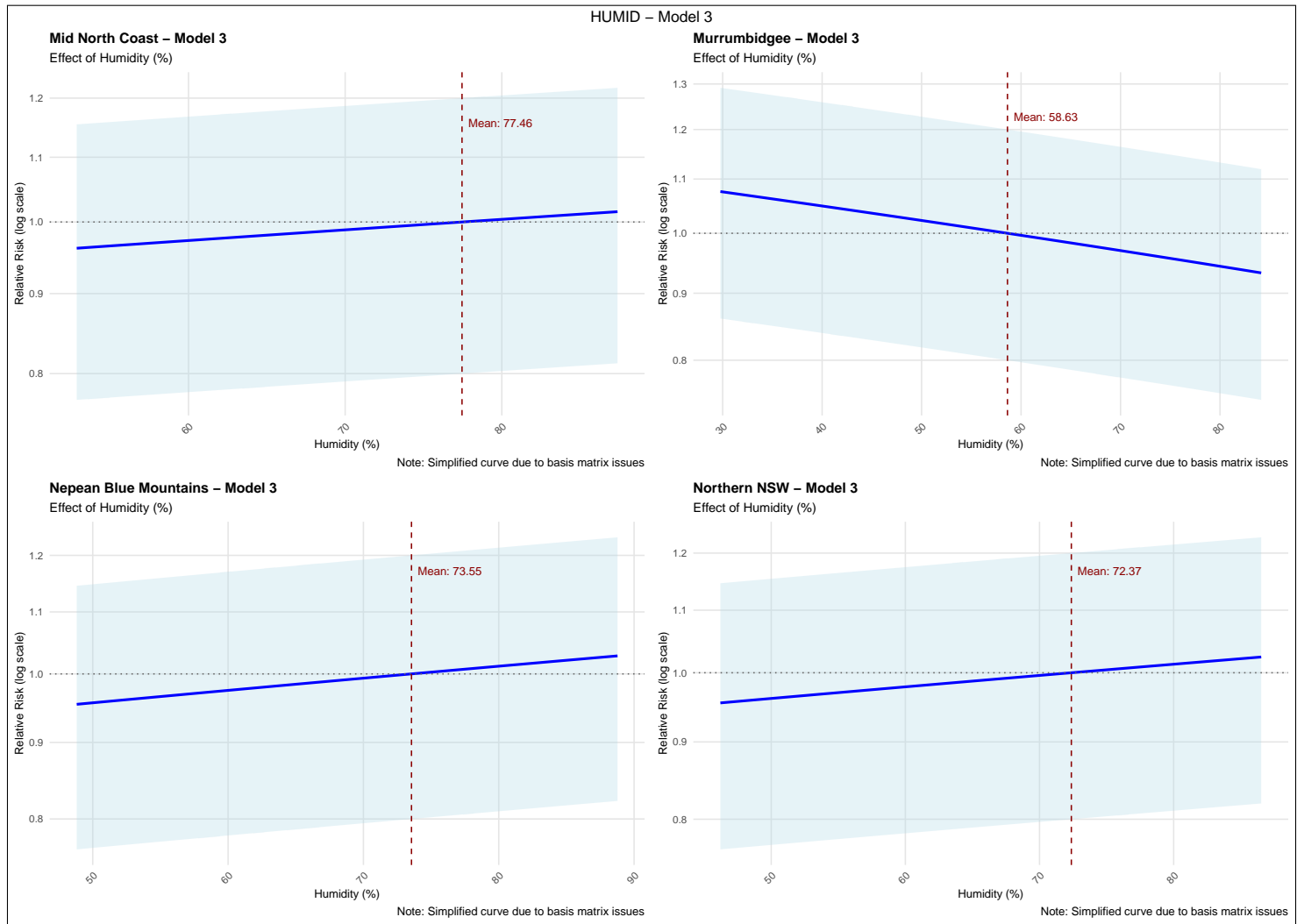


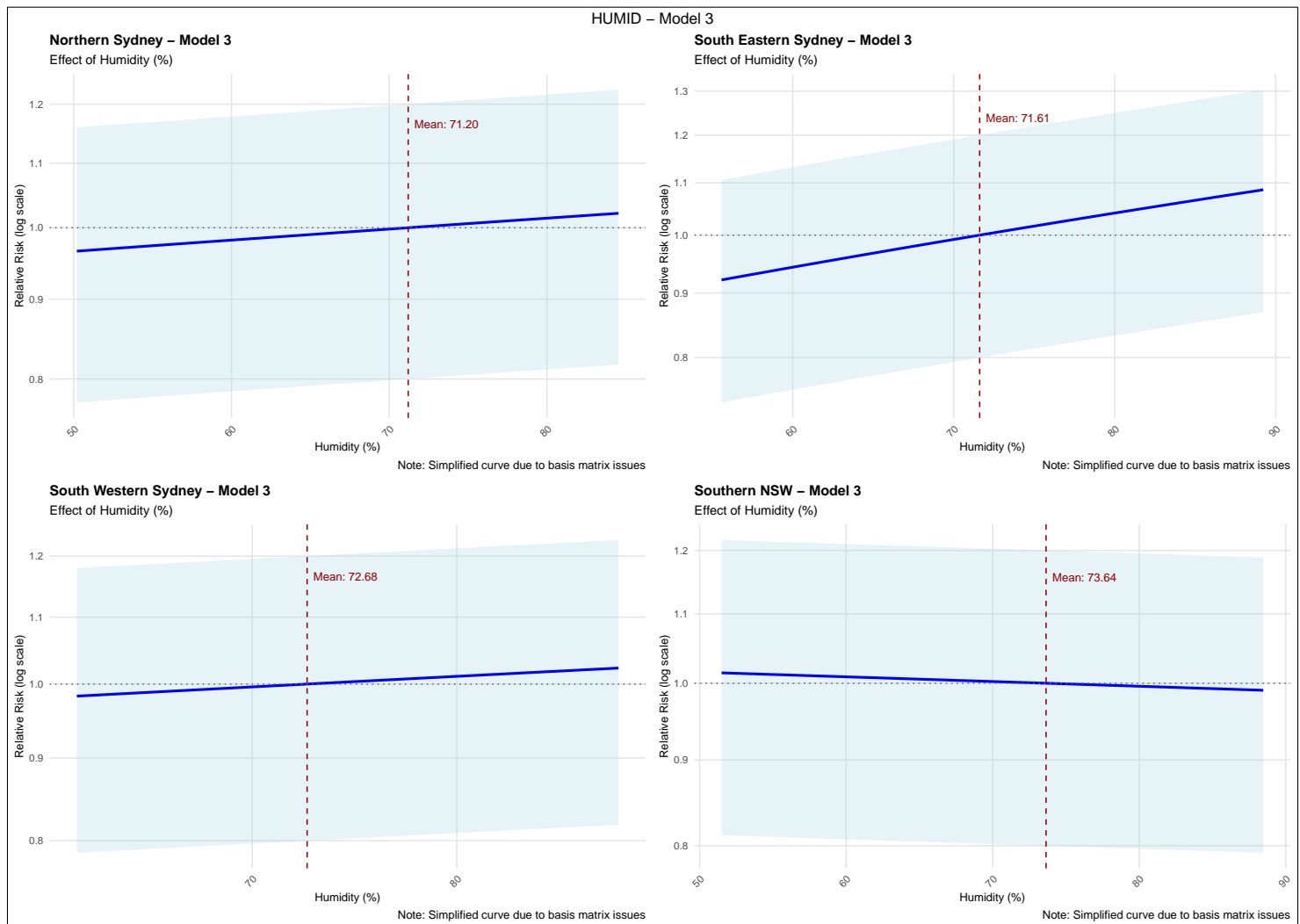


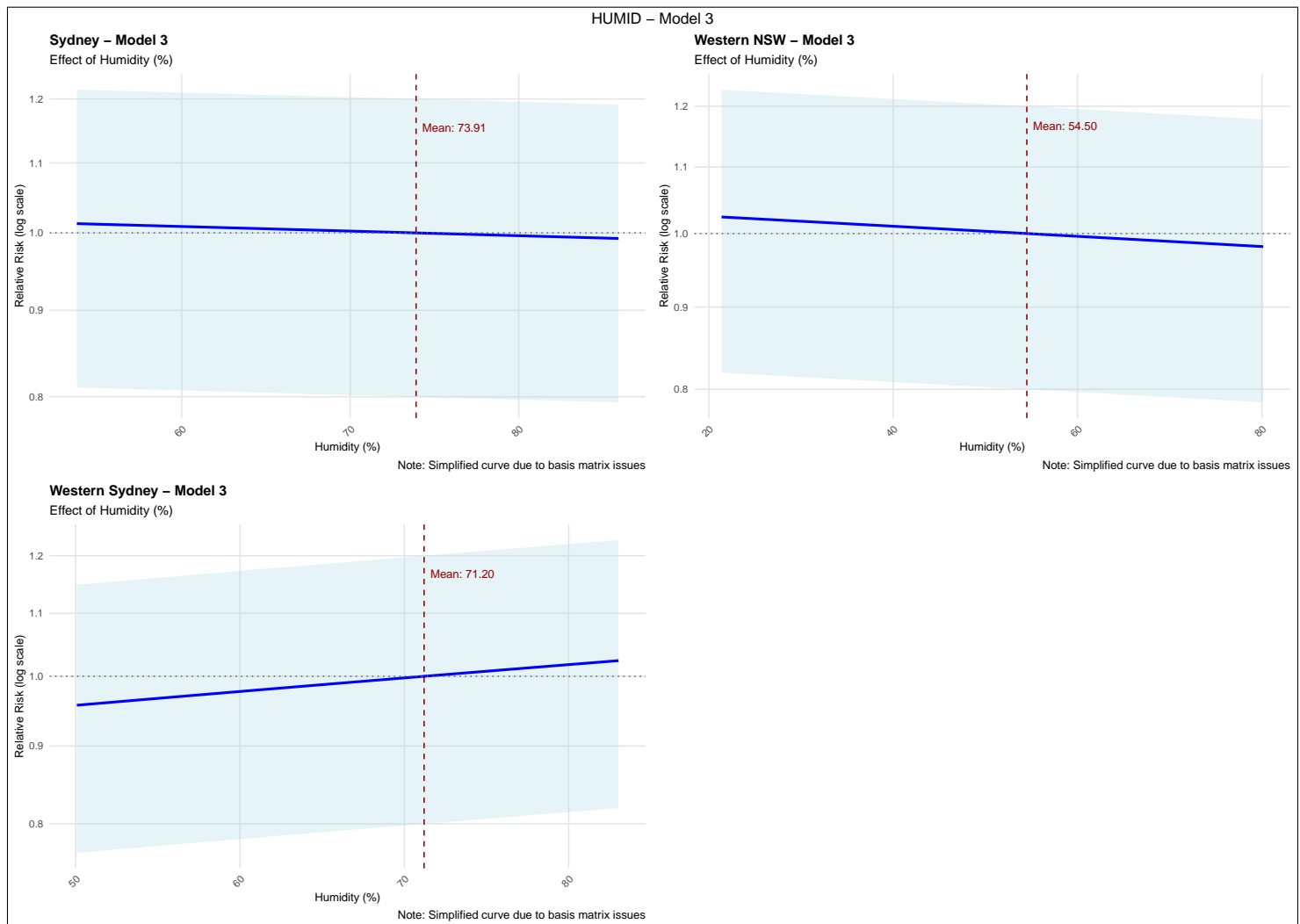


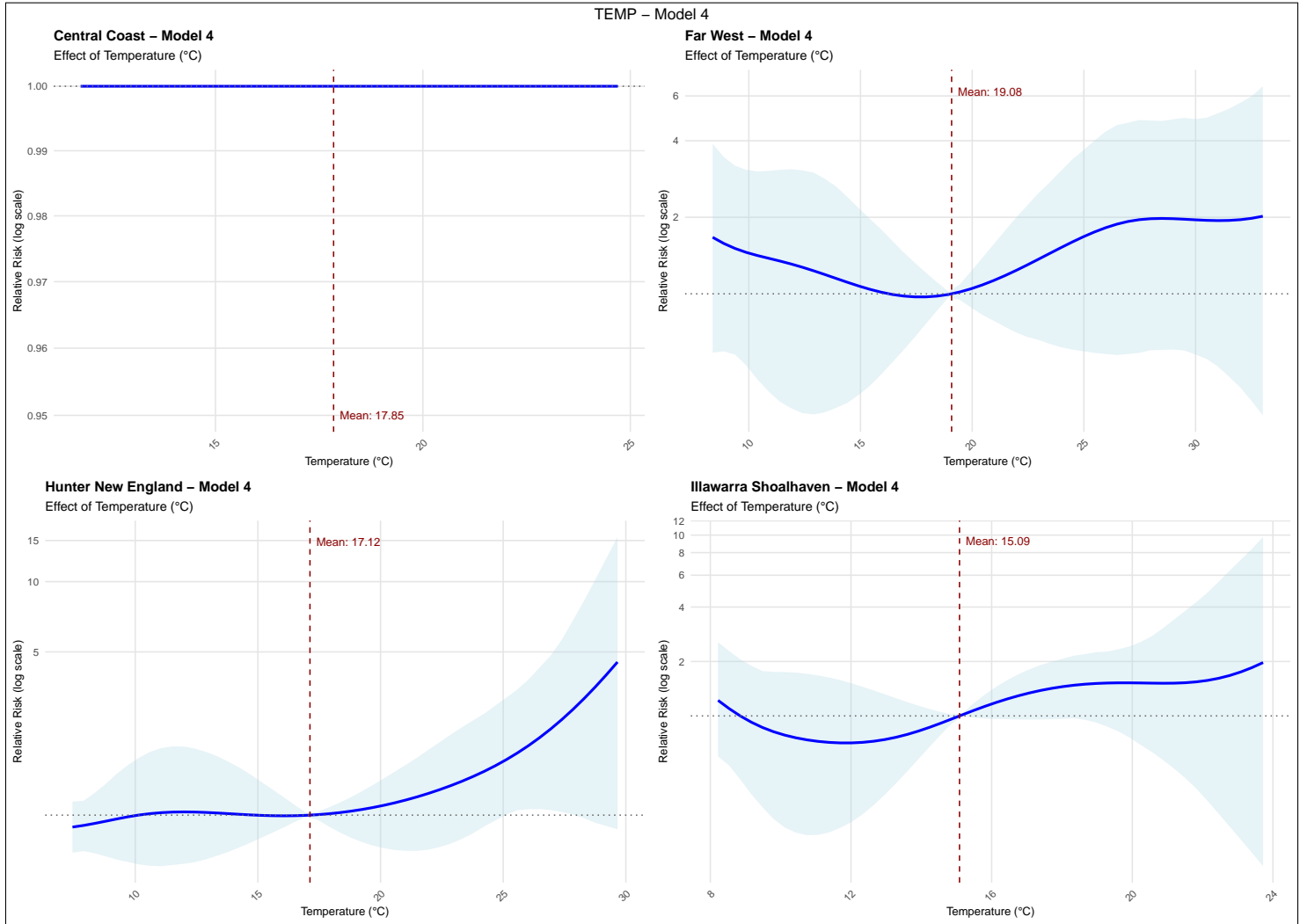


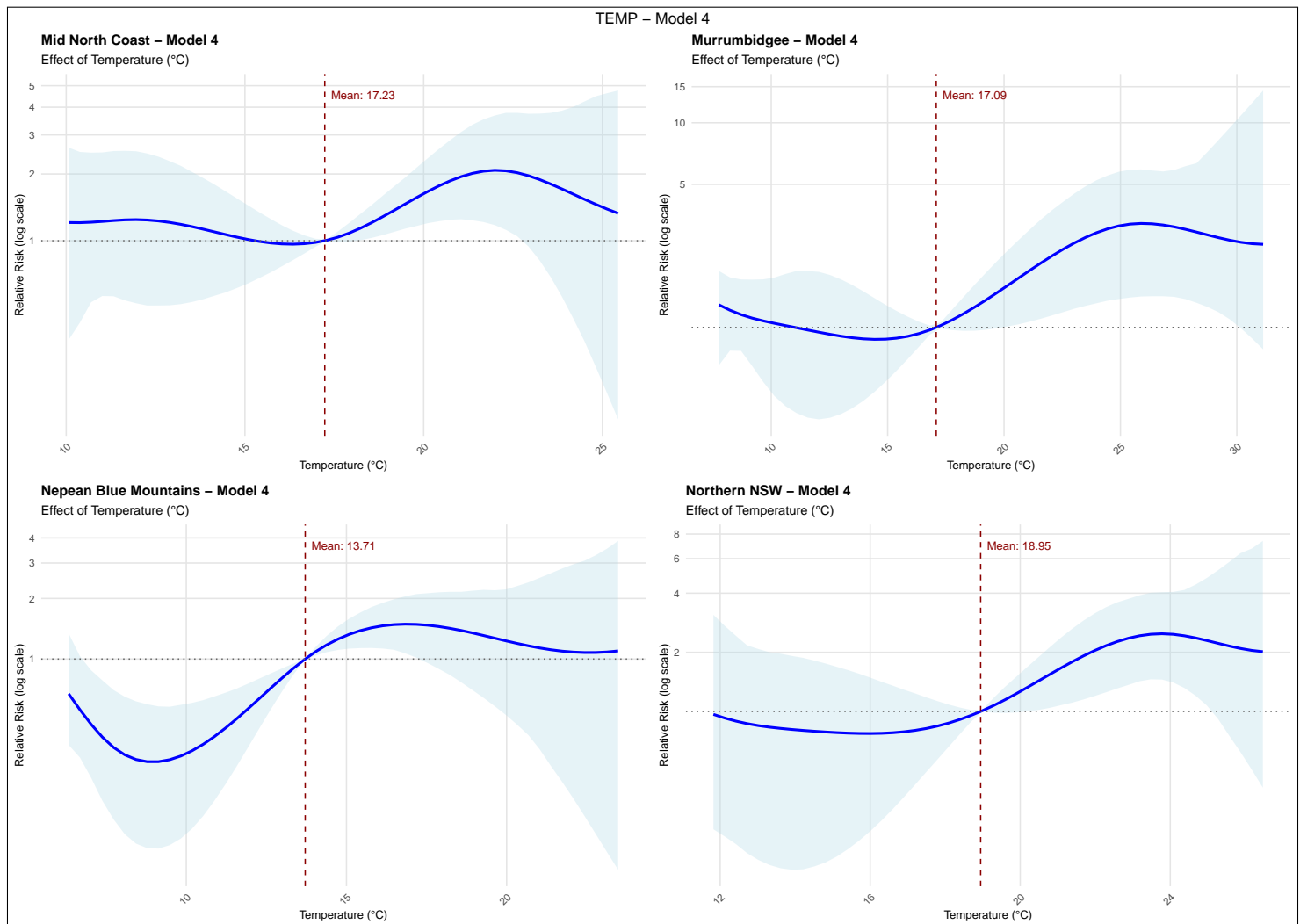


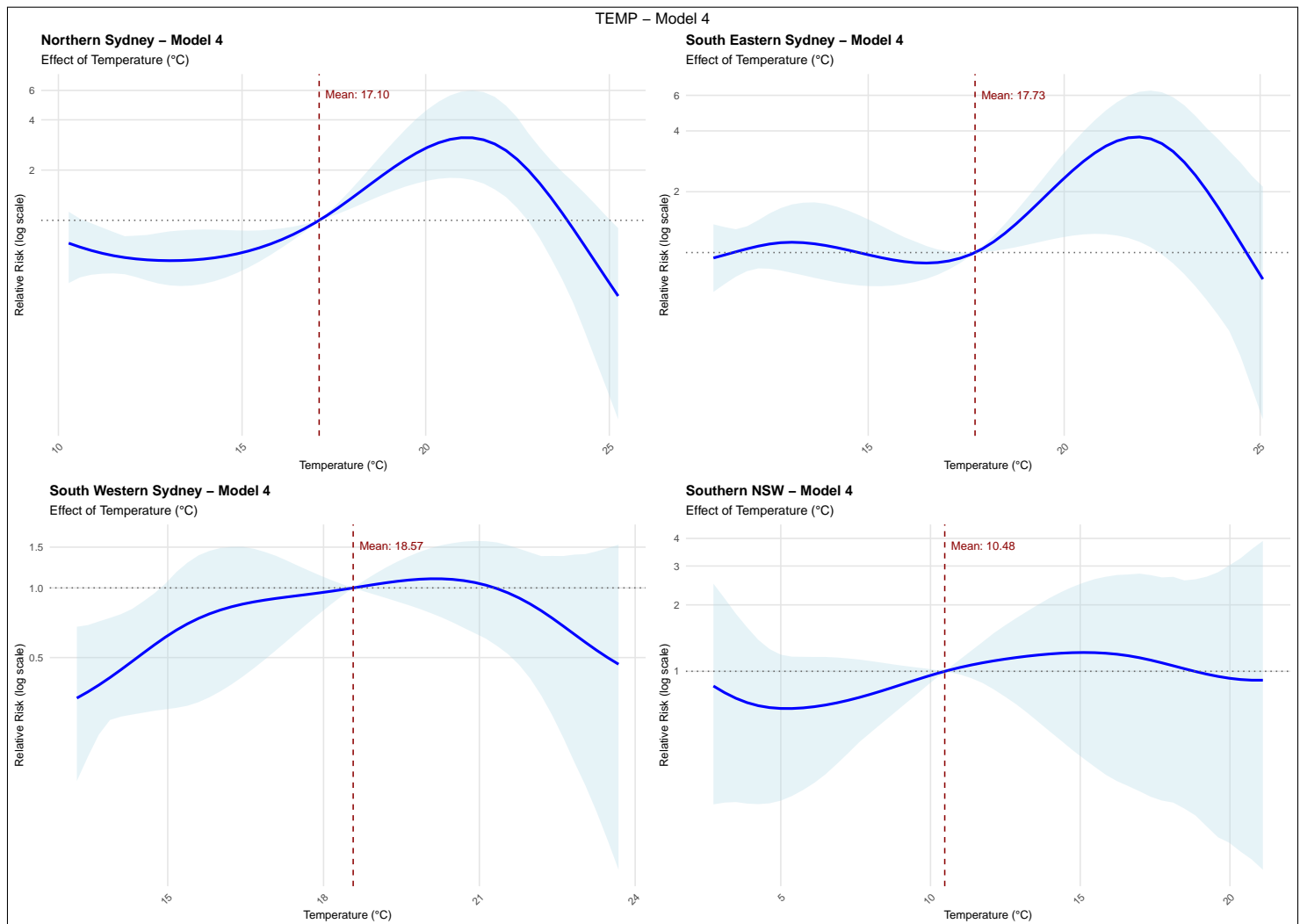


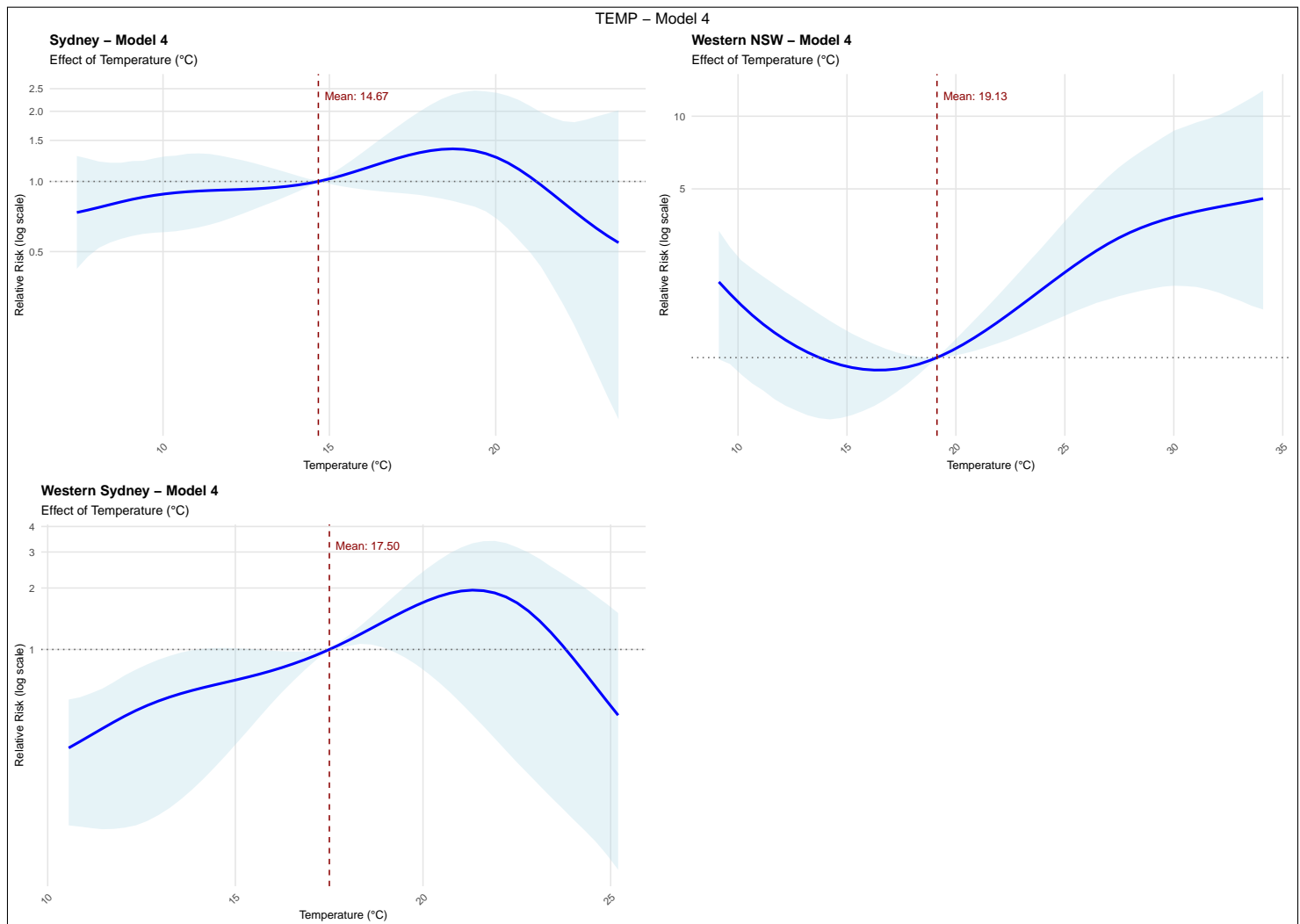


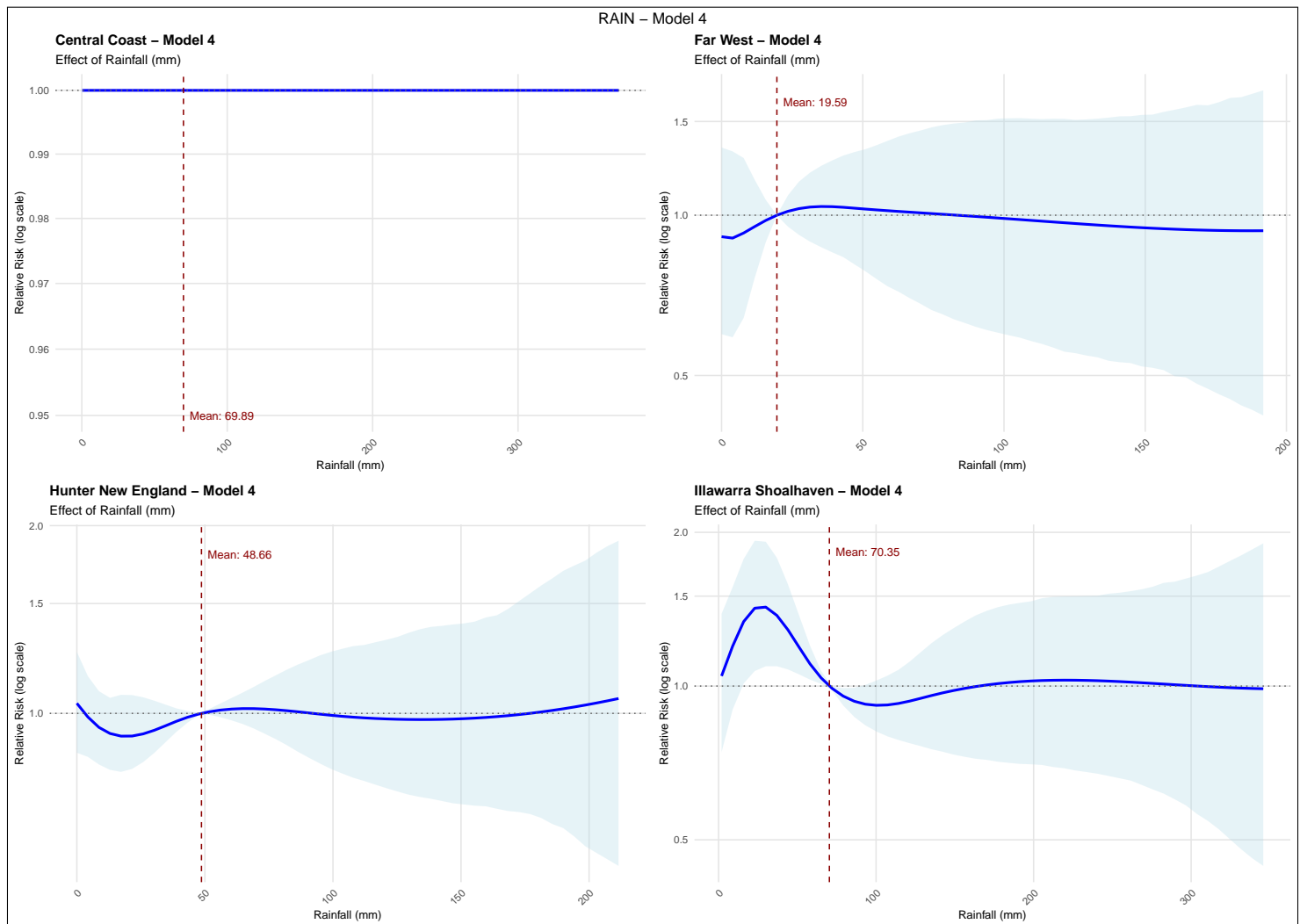


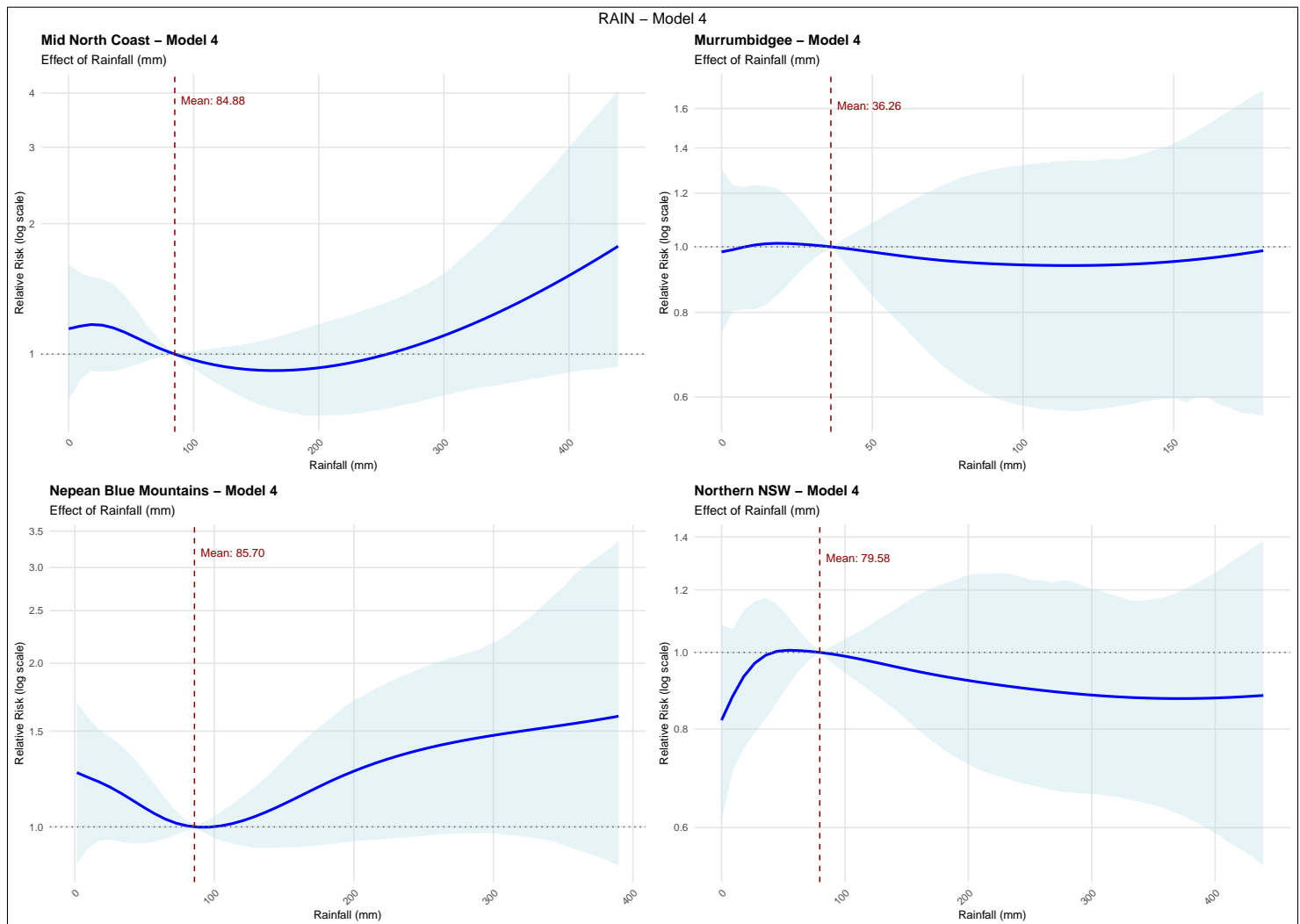


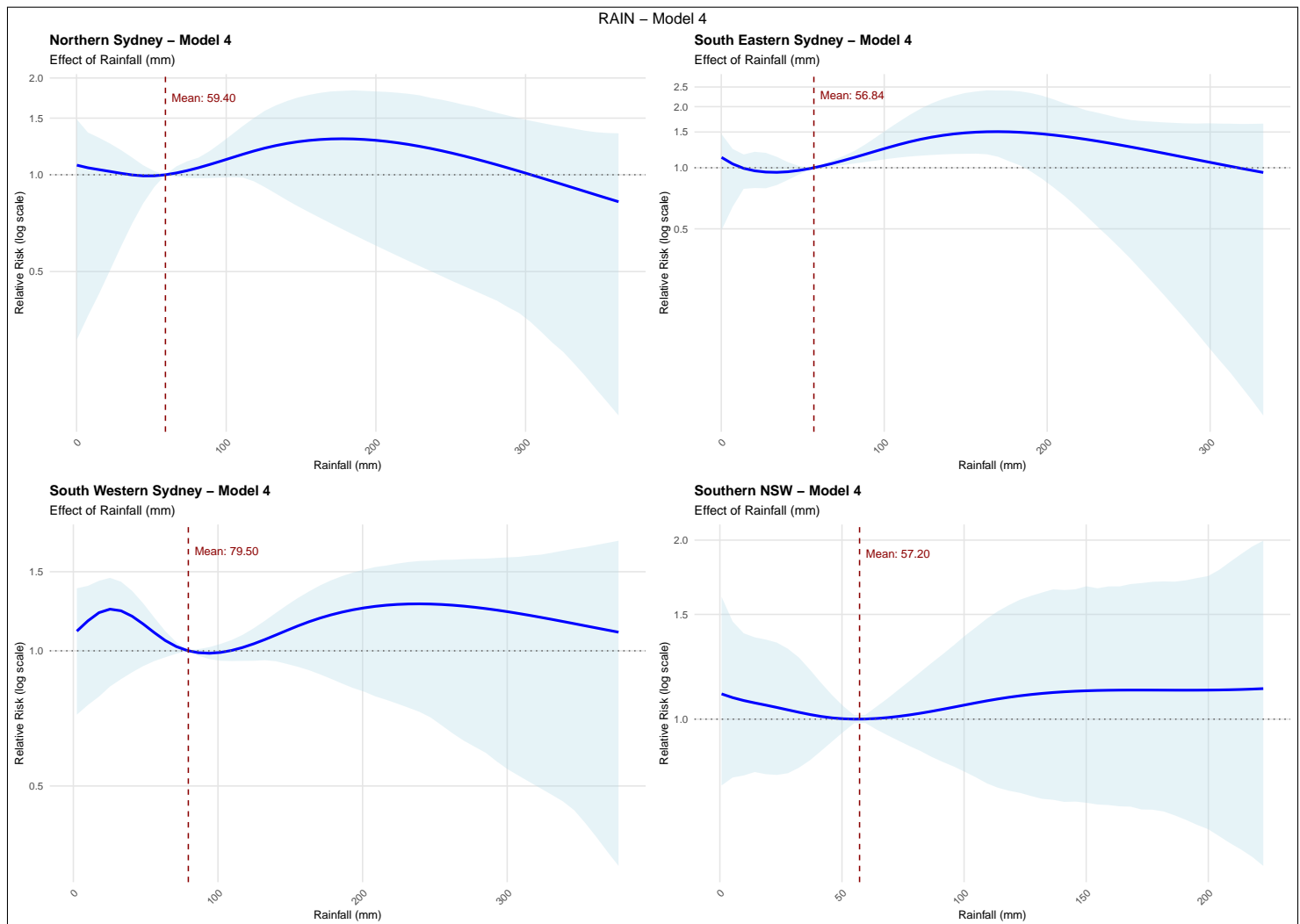


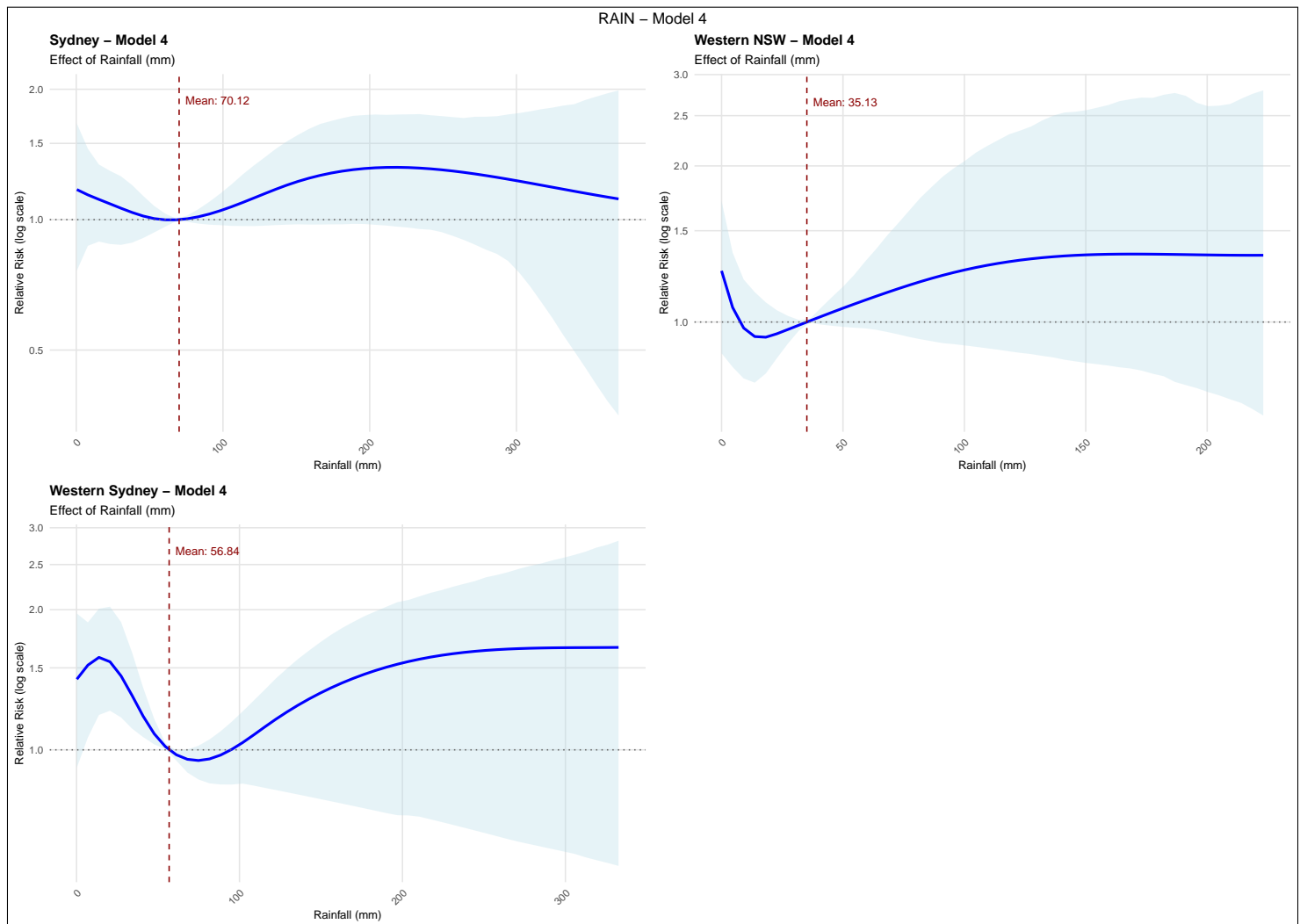


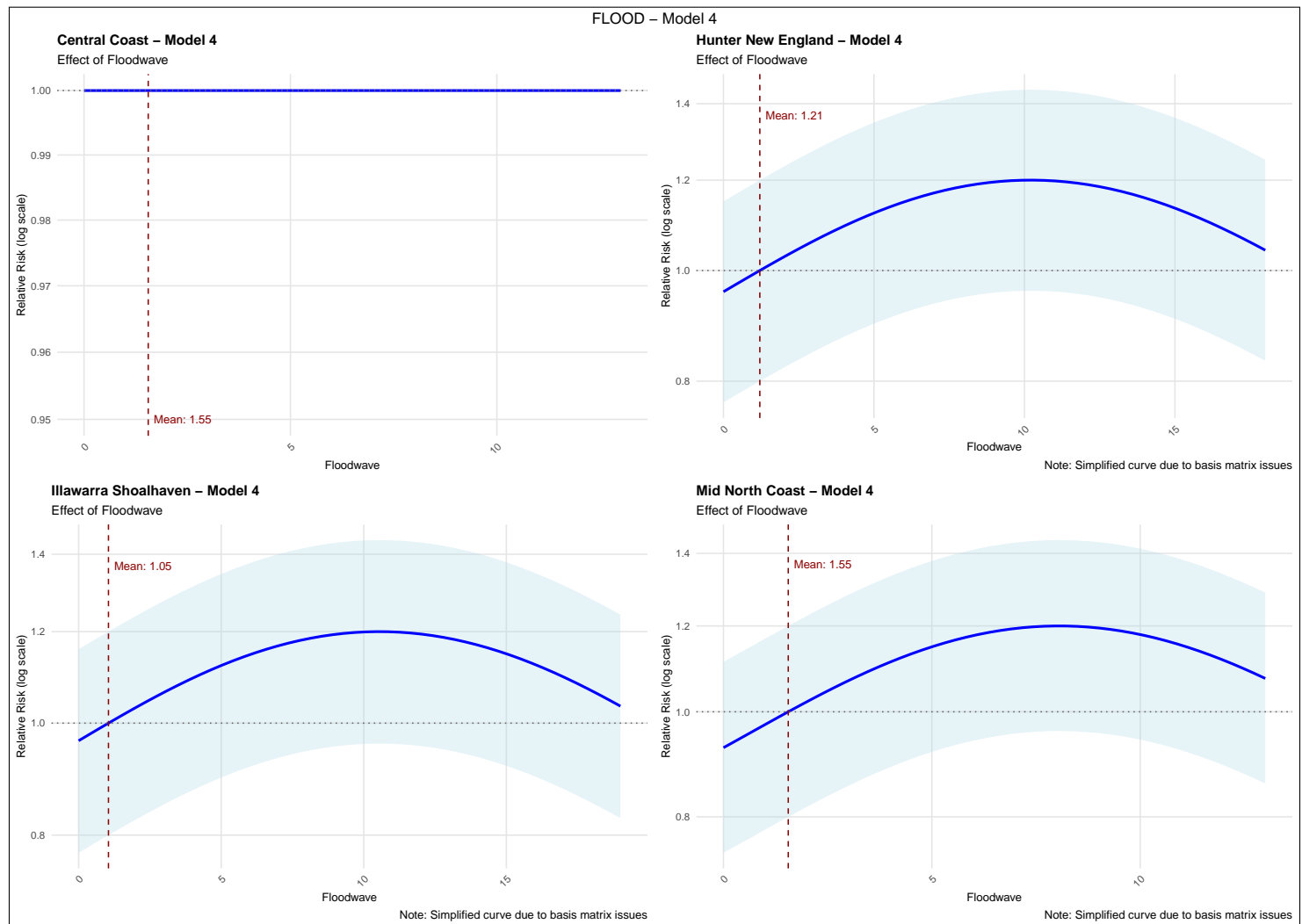


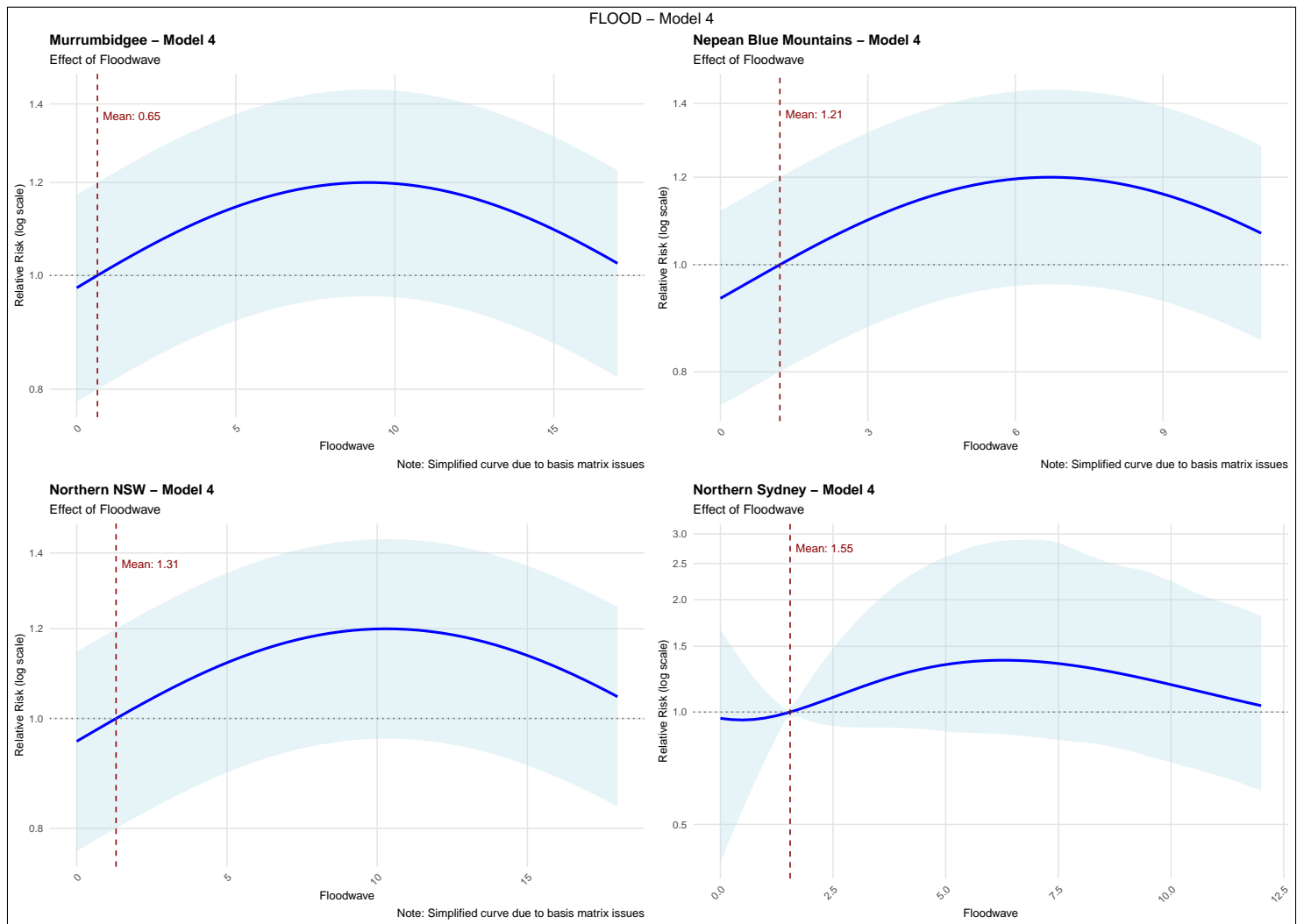


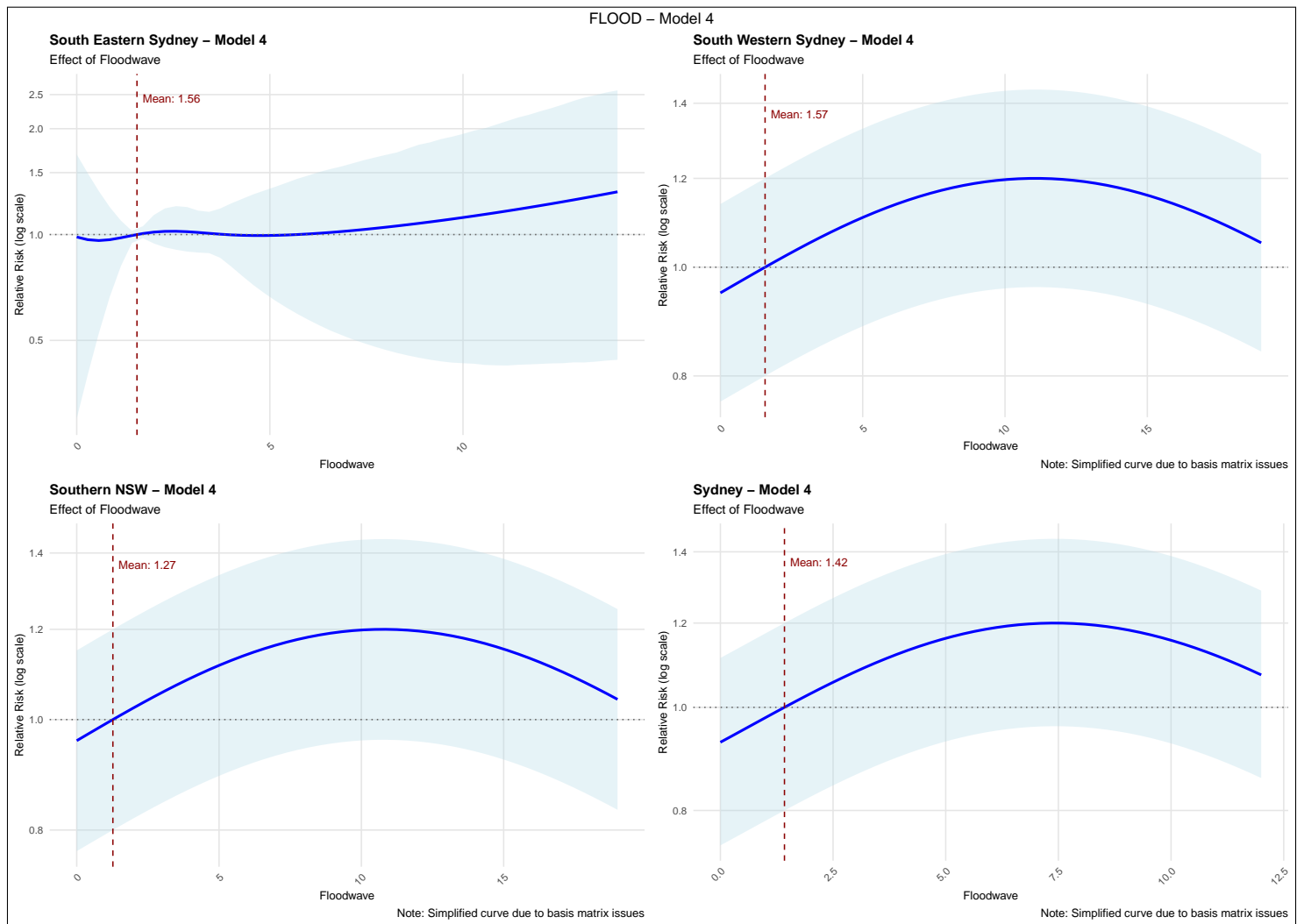


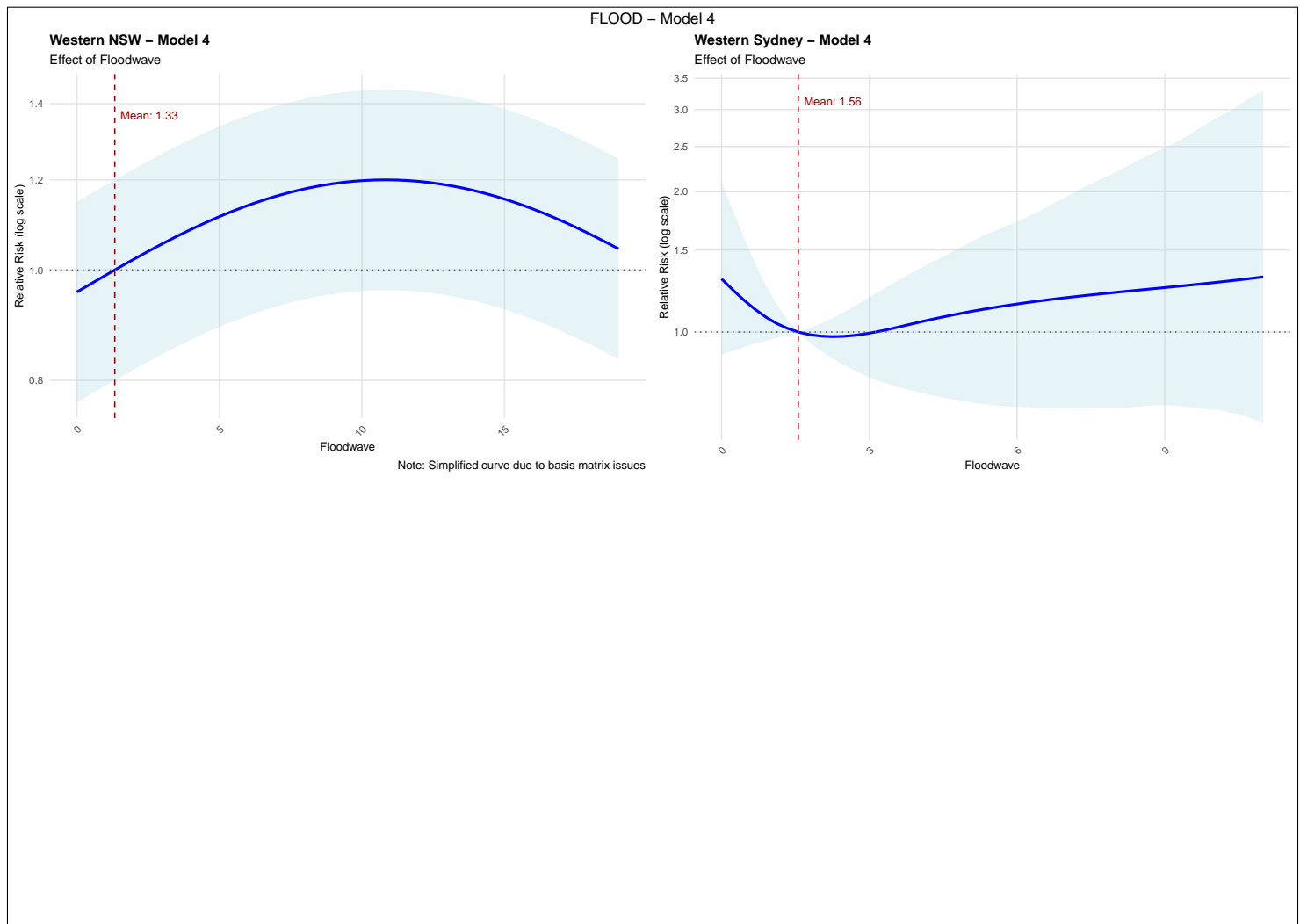


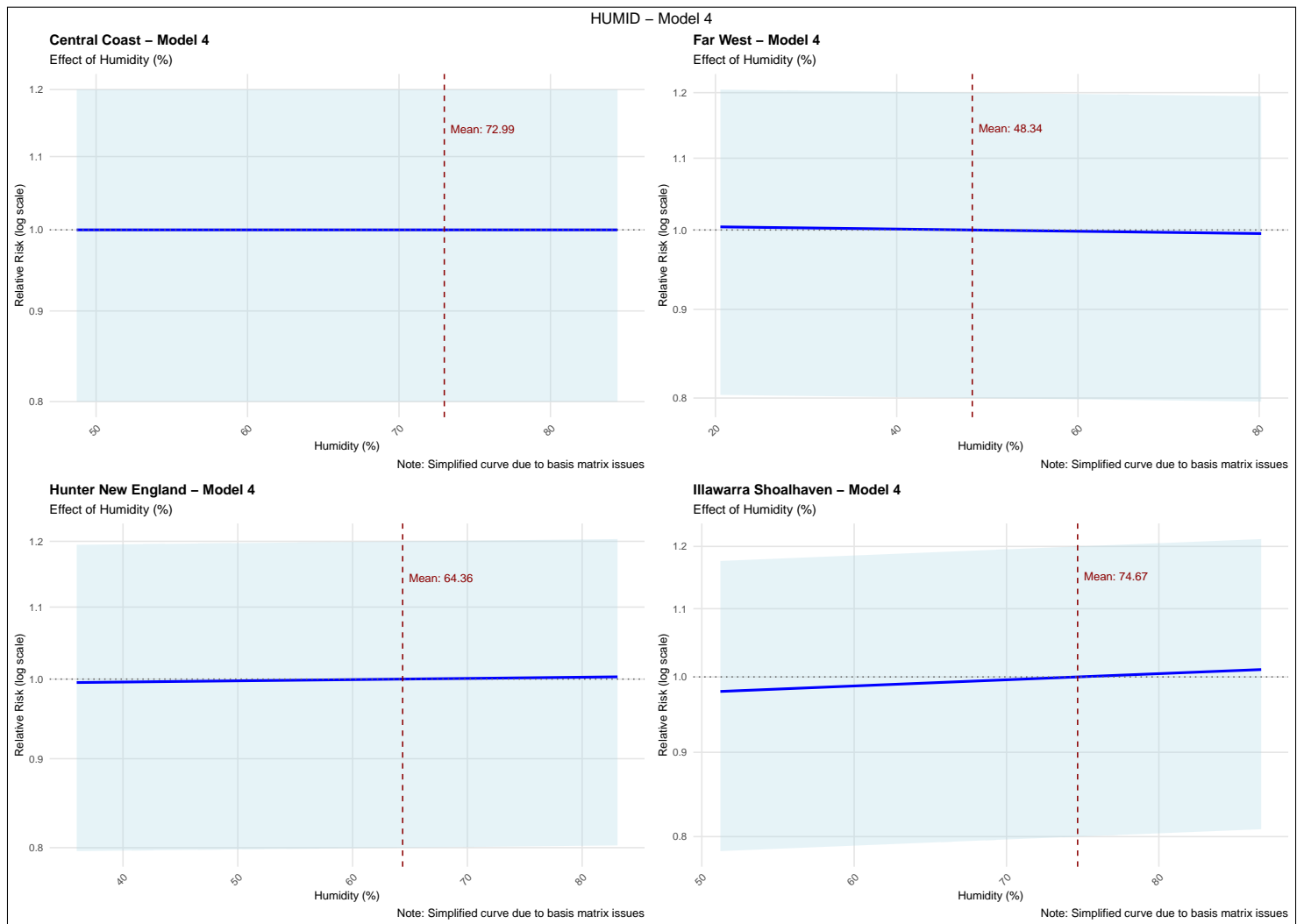


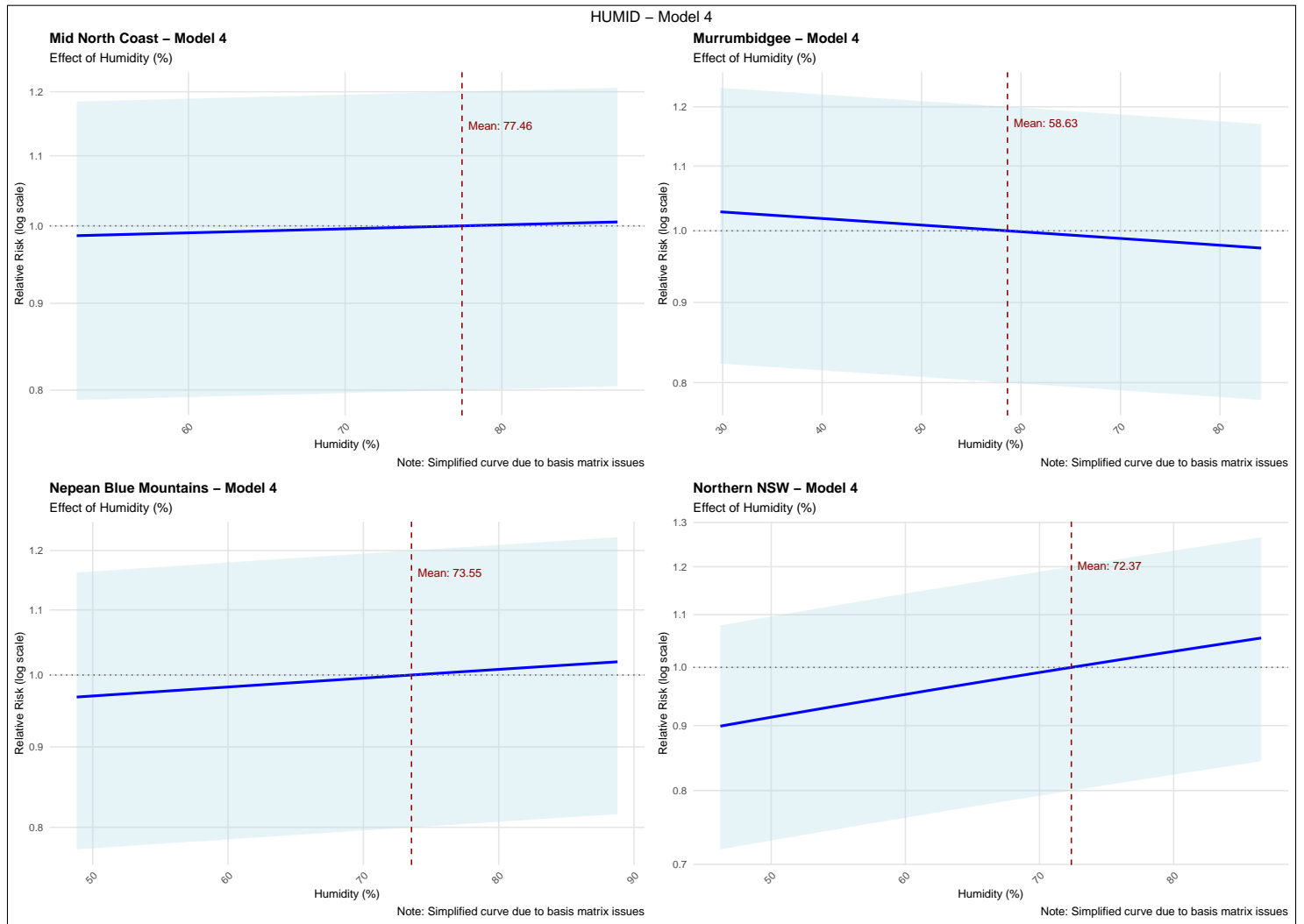


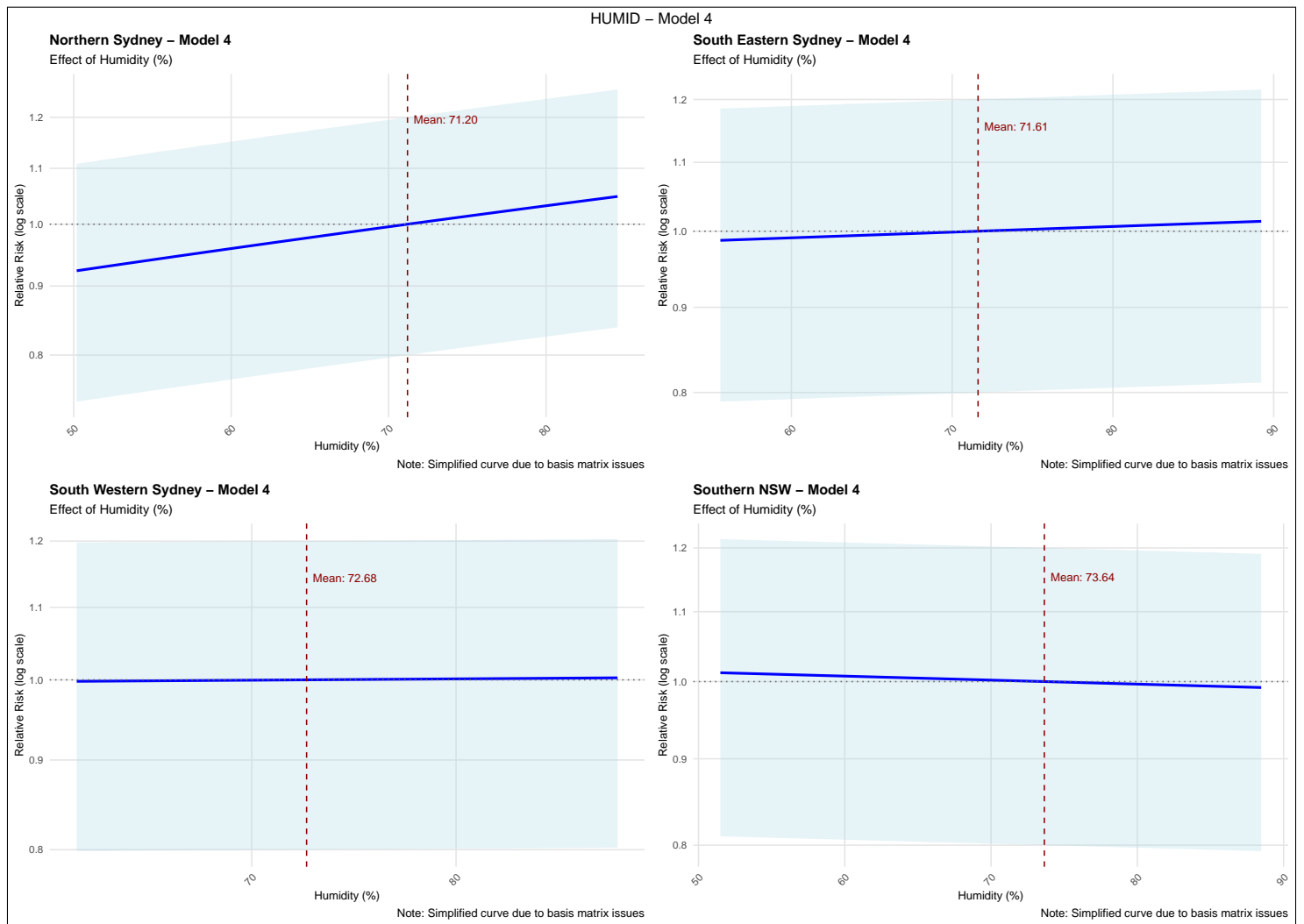


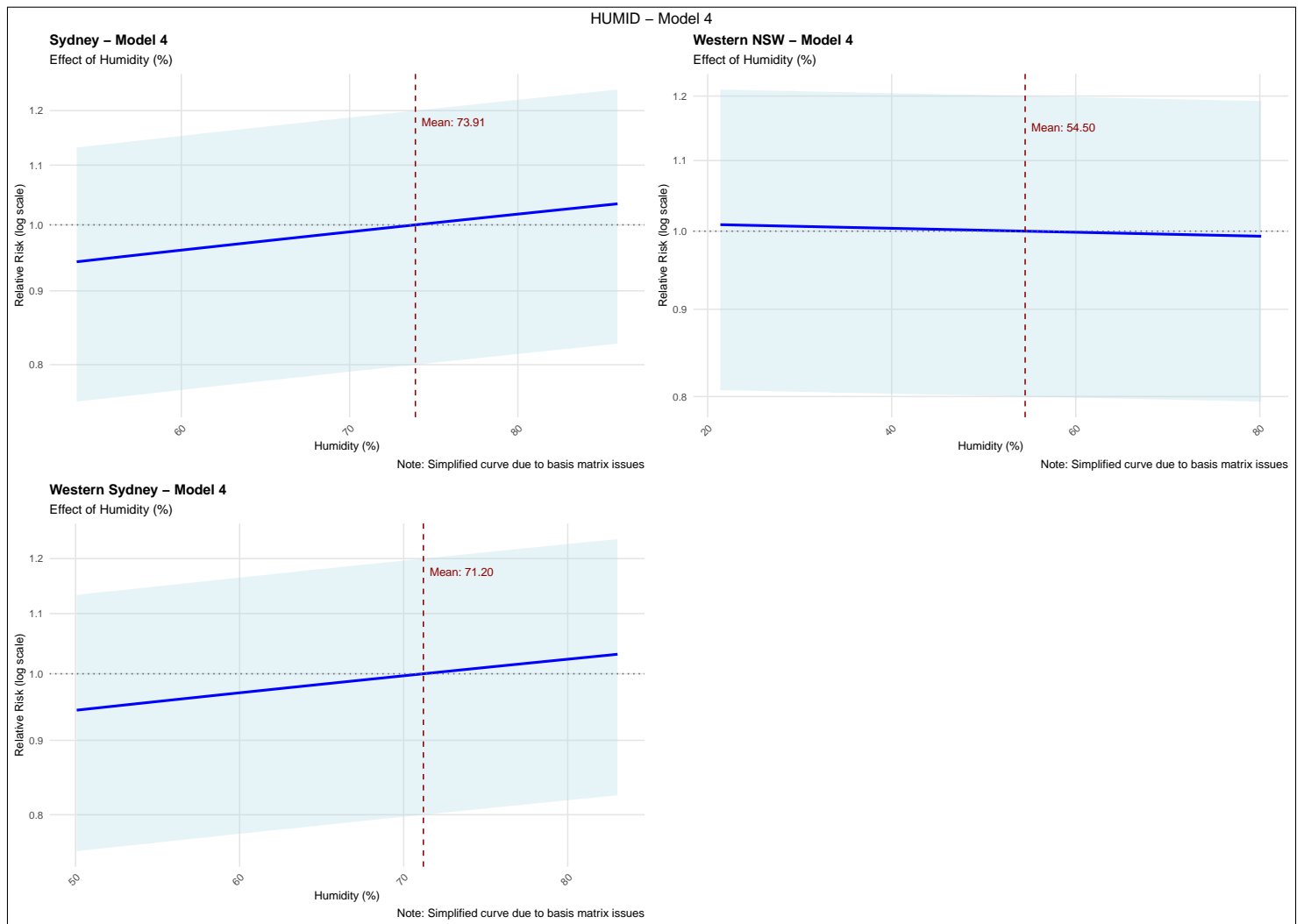












### A.3 Probability maps for case-crossover DLNM (CC)

Posterior probability that relative risk (RR) exceeds certain thresholds across NSW for Case-crossover DLNM.



Figure 11: Posterior probability map illustrating  $P(\text{RR} > 1.0, 1.2, 1.5)$  under CC DLNM for different climate exposures. Darker colors indicate higher confidence that the relative risk surpasses the chosen threshold. Some LHDs show distinct vulnerability to temperature, while others reflect rainfall or flooding concerns.

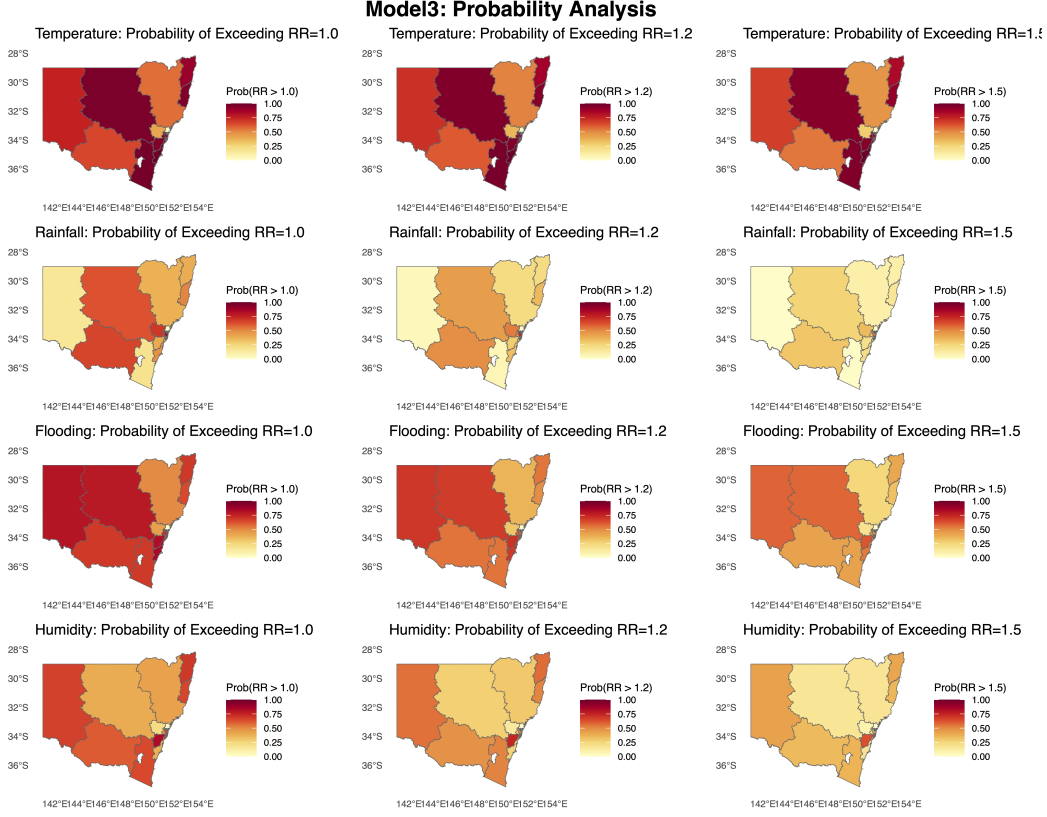


Figure 12: An alternative or complementary probability map under CC-DLN, possibly at different thresholds or for a different variable subset. These maps highlight localized patterns of exceedance risk, guiding targeted interventions in high-probability regions.

## Interpretation.

- **Heat and Humidity:** In many LHDs, the probability of exceeding RR=1.5 can be quite high during extreme temperature/humidity events.
- **Rainfall and Flooding:** Some areas remain near or below the threshold most of the time, while a few LHDs (e.g., Illawarra Shoalhaven) show substantial probability of exceedance in flood conditions.
- **Comparisons:** Contrasting these CC-DLN probability maps with time-series's spatiotemporal results (see main text) suggests that short-term fluctuations can yield slightly higher effect estimates but converge on the same climate drivers overall.